PROGRAM & ABSTRACTS

June 18-22, 2017, Vienna, Austria

EMN VIENNA MEETING & CCBP

CONTENTS

GENERAL INFORMATION

The 2017 EMN Vienna Meeting *(including EMN Meeting on Quantum and EMN Meeting on Soft Materials)* and Collaborative Conferences on Beam Physics will take place at ARCOTEL Wimberger Vienna Hotel, in Vienna, Austria from June 18 to 22, 2017.

Workshops on selected focus topics will include keynote, invited and poster presentations from Monday (June 19th) to Wednesday (June 21st).

Registration Desk Hours

The 2017 EMN Vienna & CC Beam Physics registration desk, located in the hotel, will be open during the following hours:

Sunday, June 18th ……………………………14:00pm -17:30pm

Monday, June 19th ……………………………7:45am -17:30pm

Tuesday, June 20th ……………………………7:45am -17:30pm

Wednesday, June 21st ……………………………7:45am -17:30pm

Publication Information

Authors of accepted presentations are encouraged but not required to submit their full manuscripts for publication reviewing as journal articles or book chapters. The following are possible publishing titles:

- **Nanoscale Research Letters (Springer)**

  Open access publishing is not without costs. For EMN submissions, Springer will provide 50% discount for each article accepted for publication. Fee to be paid by the author if the article is accepted for publication. In order to qualify for the 50% discount, please submit your article to the 'EMN Meeting' section during submission and mention the meeting in your waiver request".

- **Journal of Semiconductors (IOP)**

- **Journal of Electronic Science and Technology**

  JEST (International), Journal of Electronic Science and Technology (ISSN 1674-862X), is a peer-reviewed and open-access periodical, devoted to the purpose of providing rapid publication of original and significant contributions relating to state-of-the-art achievements in electronic science and technology. JEST sincerely invites original manuscripts (include original research articles as well as review articles) for 'Special Section on Energy, Materials, and Nanotechnology' and 'Special Section on Quantum Technology' in JEST. All the manuscripts will undergo the peer-review organized by EMN Conference publication committee. And the papers accepted by these two Special Sections will be freely open accessed.

- **OAHOST**

  OAHOST is a peer-reviewed, open access journal publishing quality research papers across all disciplines, which means that all published articles are made

freely available online without a subscription, and authors retain the copyright of their work. For EMN articles published the author publication fee will be waived, the EMN will pay to make the article open access as long as the manuscript can go through the peer-review organized by EMN publication committee. OAHOST is open to both original research articles as well as review articles.

General Chairs

Michael PROBST

Institute of Ion Physics, University of Innsbruck, Austria

Zhiming WANG

Institute of Fundamental and Frontier Sciences, UESTC, China

2017 EMN Europe Committee

Zlatan Aksamija, University of Massachusetts Amherst, USA

M. Isabel Alonso, ICMAB-CSIC, Spain

Willyanto Anggono, Petra Christian University, Indonesia

Supriyo Bandyopadhyay, Virginia Commonwealth University, USA

Ivan Bozovic, Brookhaven National Laboratory, USA

Ashok Chatterjee, University of Hyderabad, India

Po-Wen Chiu, National Tsing Hua University, Taiwan

Hans J. Fecht, University of Ulm, Germany

Jeff Th.M. De Hosson, University of Groningen, Netherlands

Vahid Jabbari, Department of Chemistry, Southern Methodist University, USA

José M. Kenny, University of Perugia, Italy

Lorenzo Pavesi, University of Trento, Italy

Fabio Pezzoli, LNESS and Universita' di Milano-Bicocca, Italy

Vladimir Privman, Clarkson University, USA

Michael Probst, University of Innsbruck, Austria

Luca Razzari, INRS University, Canada

Kuntal Roy, Purdue University, USA

Bin Tang, China Academy of Engineering Physics, China

Nihal Engin Vrana, PROTiP Medical, France

Zeev Weissman, Shenkar College of Engineering & Design, Israel

C. P. Wong, the Chinese University of Hong Kong, Hong Kong

Yang Yue, Juniper Networks, USA

Jialiang Xu, Tianjin University, China

Roberto Zivieri, University of Ferrara, Italy

Gary Chinga Carrasco, PFI, Focus area Biocomposites, Norway

Yu Chen, Beijing Institute of Technology, China

PROGRAM-AT-A-GLANCE

June 19, Monday   (Room A)

8:10-10:20	Quantum General I
10:35-12:15	Quantum General II
13:30-16:15	Quantum General III
16:15-17:55	Theoretical Aspects of Quantum

June 20, Tuesday   (Room A)

8:00-9:15	Quantum Engineering and Quantum Metrology
9:15-12:00	Quantum General IV
13:30-15:10	Quantum General V
15:10-15:40	Poster
15:40-17:45	Electronic Structure and Dynamics

June 20, Tuesday   (Room B)

8:00-10:05	Soft Magnetic Materials
10:20-12:00	Quantum Computation with Nanostructures and Dopants I
13:30-15:10	Soft Materials General
15:10-15:40	Poster
15:40-17:20	Quantum General VI

June 21, Wednesday   (Room A)

8:00-8:50	Quantum Computation with Nanostructures and Dopants II
8:50-11:40	Many Body Quantum Theory & Quantum General VII
13:40-14:55	Theory, Modelling, and Simulation
15:10-16:00	Beam Physics
16:00-17:15	Quantum General VIII

DETAILED MEETING PROGRAM

June 18, Sunday	
In the Hotel	
14:00-17:30	Onsite Registration & Sign up

June 19, Monday		
Room A		
8:00-8:10	*Opening*	
Session: Quantum General I		**Chair: Miroslav Pozek**
8:10-8:40	A01: Stimulated and Spontaneous Emission and the Laser Linewidth (Keynote)	**Markus Pollnau** University of Surrey, UK *P20*
8:40-9:05	A02: Topology-Driven Effects in Advanced Nanoarchitectures	**Vladimir Fomin** IFW Dresden, Germany *P21*
9:05-9:30	A03: Modelling of surface materials: Upwards from Quantum Chemistry	**Michael Probst** University of Innsbruck, Austria *P23*
9:30-9:55	A04: Quantum resistance standard device using epitaxial graphene on SiC	**Vladimir Falko** The University of Manchester, UK *P24*
9:55-10:20	A05: Laser Material Interactions for Flexible Applications	**Keon Jae Lee** Korea Advanced Institute of Science and Technology, Korea *P25*
10:20-10:35	*Session Break*	
Session: Quantum General II		**Chair: Vladimir Fomin**

10:35-11:00	A06: Ferromagnetism in Carbon Based Materials Probed by NMR	**Miroslav Pozek** University of Zagreb, Croatia *P26*
11:00-11:25	A07: Quantum Mechanical and Molecular Mechanical Studies of Chemical Reactions	**Hajime Hirao** City University of Hong Kong, Hong Kong *P27*
11:25-11:50	A08: Effective Theory of Non-Adiabatic Quantum Evolution Based on the Quantum Geometric Tensor	**Dmitry Solnyshkov** University Clermont Auvergne /CNRS, France *P28*
11:50-12:15	A09: Information entropies calculation using the J-matrix method	**Ibraheem M.A. Nasser** King Fahd University of Petroleum & Minerals, Saudi Arabia *P29*
12:15-13:30	*Lunch Break*	
Session: Quantum General III	**Chair: Michael Probst**	
13:30-13:55	A10: Nanoscale Spin Filters from Graphene Nanostructures	**Frank Hagelberg** East Tennessee State University, USA *P29*
13:55-14:20	A11: New perspective on the 2D metal-Insulator Transition	**Michael Osofsky** U.S. Naval Research Laboratory, USA *P31*
14:20-14:45	A12: Electron Spin at Work in Modern and Emerging Devices	**Viktor Sverdlov** Technische Universität Wien, Austria *P31*
14:45-15:10	A13: End states of rectangular armchair graphene ribbon	**Eric Yang** Korea University, Korea *P33*
15:10-15:25	*Session Break*	

15:25-15:50	A14: Fabrication and Optimization of Silver Nanowire Transparent conductive film via needle organic precursor by sonochemical process	**Yamato Hayashi** Tohoku University, Japan *P34*
15:50-16:15	A15: Colloidal Quantum Dot Optoelectric Applications	**Kyung-Sang Cho** Samsung Advanced Institute of Technology, Korea *P35*

Session: Theoretical Aspects of Quantum		**Chair: Frank Hagelberg**
16:15-16:40	A16: Geometric Images of Quantum Mechanical Functions and Objects	**Alexander P. Yefremov** People's Friendship University of Russia, Russia *P36*
16:40-17:05	A17: Harmonic Analysis of Quantum States and Observables	**Artur Sowa** University of Saskatchewan, Canada *P38*
17:05-17:30	A18: Stieltjes electrostatic model of quantum mechanics	**K.V.S. Shiv Chaitanya** BITS Pilani, India *P39*
17:30-17:55	A19: Twin physics - the concept of complementarity in the real world	**Anna Backerra** Independent theoretical physicist, the Netherlands *P40*

June 20, Tuesday **Room A**		
Session: Quantum Engineering and Quantum Metrology		**Chair: Evgeny Yu. Perlin**
8:00-8:25	A20: Quantized electrical conductance of thin metal nanowire	**Yoshifumi Oshima** Japan Advanced Institute of Science and Technology, Japan *P41*
8:25-8:50	A21: Quantum wave mixing and resolving photonic classical and non-classical coherent states	**Vladimir Antonov** Royal Holloway, University of London, UK *P42*
8:50-9:15	A22: Single carrier transport in graphene nanostructure	**Takuya Iwasaki** Japan Advanced Institute of Science and Technology, Japan *P43*
Session: Quantum General IV		**Chair: Markus Pollnau**
9:15-9:40	A23: Novel Transient Nonlinear Optical Processes in Bulk Solids and Nanostructures	**Evgeny Yu. Perlin** ITMO University, St. Petersburg, Russia. *P45*
9:40-10:05	A24: Spintronic applications of mono-axial chiral helimagnet	**Junichiro Kishine** The Open University of Japan, Japan *P46*
10:05-10:20	*Session Break*	
10:20-10:45	A25: Can Two-Way Direct Communication Protocols Be Considered Secure?	**Mladen Pavicic** Rudjer Boskovic Institute, Croatia *P48*
10:45-11:10	A26: Quantum Dynamics and Electronic Spectroscopy within the framework of Wavelets	**Mohamad Toutounji** United Arab Emirates University, UAE *P49*

11:10-11:35	A27: Quantum Vision in 3-D	**Yehuda Roth** Oranim Academic College, Israel *P50*
11:35-12:00	A28: Bosonization of open quasi-1D systems: Theory and applications	**Eugene Sukhorukov** University of Geneva, Switzerland *P50*
12:00-13:30	*Lunch Break*	
Session: Quantum General V		**Chair: Xiaozhong Zhang**
13:30-13:55	A29: How to make spin and lattice dynamical together?	**Jonas Fransson** Uppsala University, Sweden *P51*
13:55-14:20	A30: Effect of magnetic impurity on electronic spin levels in quantum ring	**Pinchas Dahan** Ruppin Academic Center, Israel *P52*
14:20-14:45	A31: Emissive ultra-small Au nanocluster for highly-efficient organic photovoltaics	**Dong Chan Lim** Korea Institute of Materials Science KIMS, Korea *P53*
14:45-15:10	A32: Geometrical contributions to the Exchange interactions: From Equilibrium to Nonequilibrium	**Frank Freimuth** Forschungszentrum Jülich, Germany *P54*
15:10-15:40	*Poster Session*	
Session: Electronic Structure and Dynamics		**Chair: Jonas Fransson**
15:40-16:05	A33: Semiconductor Based Magnetoresistance and Magnetic Logic	**Xiaozhong Zhang** Tsinghua University, China *P55*
16:05-16:30	A34: Electrical Transport Properties of Two-dimensional Electrons in InGaAsN/GaAsSb Type II Quantum Well	**Shuichi Kawamata** Osaka Prefecture University, Japan *P56*

16:30-16:55	A35: Density functional theory calculation for interface electronic structure of SiC power electronic devices	**Tomoya Ono** University of Tsukuba, Japan *P57*
16:55-17:20	A36: Dynamical mechanisms of biological macromolecular systems investigated by ab initio electronic structure calculations coupled to molecular dynamics	**Jiyoung Kang** University of Hyogo, Japan *P59*
17:20-17:45	A37: Experimental determination of the electronic structure of $CH_3NH_3PbI_3$ hybrid organic-inorganic perovskite	**Antonio Tejeda** CNRS, Université Paris Sud, France *P60*

	June 20, Tuesday	
	Room B	
	Session: Soft Magnetic Materials **Chair: Nikolai A. Usov**	
8:00-8:25	B01: A novel exchange spring magnet with an insulating nano-sized soft magnetic oxide exchange-coupled with micron-sized hard magnetic nitride	**Nobuyoshi Imaoka** National Institute of Advanced Industrial Science and Technology, Japan *P61*
8:25-8:50	B02: Tuning hysteresis in metamagnetic shape memory alloys for refrigeration applications	**Daniel Salazar** BCMaterials, Spain *P62*
8:50-9:15	B03: Abnormal growth of Goss grains in grain oriented silicon steel driven by distribution characteristics of VC nano-particles	**Ivan Petryshynets** The Institute of Materials Research, Slovak Academy of Sciences, Slovakia *P63*
9:15-9:40	B04: High frequency magnetoimpedance and magnetoelastic resonance in magnetic microwires for biological and tagging applications	**Pilar Marín** Complutense University of Madrid, Spain *P65*
9:40-10:05	B05: The behaviour of soft magnetic composite cores for Electrical Machines both in standard environmental conditions and in cryogenics	**Fabrizio Marignetti** University of Cassino and South Lazio, Italy *P65*
10:05-10:20	*Session Break*	
	Session: Quantum Computation with Nanostructures and Dopants I **Chair: Keith Runge**	
10:20-10:45	B06: Single dopants as stepping stones for inter-band tunneling in silicon tunnel diodes	**Manoharan Muruganathan** Japan Advanced Institute of Science and Technology, Japan *P67*

10:45-11:10	B07: Multi-scaled Simulations on Molecular-based Flash Memory	**Vihar Georgiev** University of Glasgow, UK *P68*
11:10-11:35	B08: Quantum tunneling microscope of an atomic scale device in silicon	**Benoit Voisin** The University of New South Wales, Australia *P70*
11:35-12:00	B09: Heavy-hole states in Ge hut wires	**Hannes Watzinger** Institute of Science and Technology Austria, Austria *P71*
12:00-13:30	*Lunch Break*	

Session: Soft Materials General		**Chair: Nobuyoshi Imaoka**
13:30-13:55	B10: Highly robust and low frictional double network ion gel	**Takaya Sato** National Institute of Technology, Japan *P72*
13:55-14:20	B11: Recent advances in unusual optical coatings for flexible optoelectronic device applications	**Young Min Song** Gwangju Institute of Science and Technology, Korea *P73*
14:20-14:45	B12: Characterization of Wavelength Effect on Photovoltaic Property of poly-Si Solar Cell by Using Photoconductive Atomic Force Microscopy(PC-AFM)	**Jinhee Heo** Korea Institute of Materials Science, Korea *P74*
14:45-15:10	B13: Organoclay nanocomposites for sustainable management of toxic waste compounds	**Esperanza Pavón** Instituto de Ciencia de Materiales de Sevilla, Spain *P75*
15:10-15:40	*Poster Session*	

Session: Quantum General VI		**Chair: Mladen Pavicic**
15:40-16:05	B14: Quantum Analogue Computing with Phi-Bits	**Keith Runge** University of Arizona, USA *P77*

16:05-16:30	B15: Quantum Computation: From Laboratory Demonstrations to state-of-the-art Algorithms for Quantum image Processing	**Abdullah M. Iliyasu** Prince Sattam Bin Abdulaziz University, Saudi Arabia Tokyo Institute of Technology, Japan *P78*
16:30-16:55	B16: The foundation of Biothermology from the point of view of nano/microscale thermophysical properties of biopolymers	**Noriko Hiroi** Keio University, Japan *P79*
16:55-17:20	B17: Dynamics of quantum mechanical systems in the area of quark physics	**Shashank Bhatnagar** Chandigarh University, India *P80*

June 21, Wednesday
Room A

Session: Quantum Computation with Nanostructures and Dopants II
Chair: Manoharan Muruganathan

8:00-8:25	A38: Hybrid Quantum Systems: Spin qubits coupled to electromagnetic fields	**Guido Burkard** University of Konstanz, Germany *P82*
8:25-8:50	A39: Electronic structure of zigzag nanoribbons in an uniform magnetic field	**Jan Smotlacha** Bogoliubov Laboratory of Theoretical Physics, Russia *P83*

Session: Many Body Quantum Theory & Quantum General VII
Chair: Vlasta Bonacic-Koutecky

8:50-9:20	A40: The ladder physics in the Spin Fermion model (Keynote)	**Alexei Tsvelik** Brookhaven National Laboratory, USA *P84*
9:20-9:45	A41: Strange metal state near a heavy-fermion quantum critical point	**Chung-Hou Chung** National Chiao Tung University, Taiwan *P84*
9:45-10:00	*Session Break*	
10:00-10:25	A42: An effective potential theory for time-dependent multi-configuration wave function	**Tsuyoshi Kato** The University of Tokyo, Japan *P85*
10:25-10:50	A43: Typical and untypical states for non-equilibrium quantum dynamics	**Robin Steinigeweg** University Osnabrück, Germany *P87*
10:50-11:15	A44: Dynamics of a Mobile Impurity in a One-Dimensional Bose Liquid	**Aleksandra Petkovic** Université de Toulouse, CNRS, France *P87*

11:15-11:40	A45: The upper security bound for subcarrier wave quantum key distribution	**Anton Kozubov** ITMO University, St. Petersburg, Russia *P88*
11:40-13:40	*Lunch Break*	

Session: Theory, Modelling, and Simulation		**Chair: Fabrizio Marignetti**
13:40-14:05	A46: New insights from mesoscopic simulations of electrolyte transport under confinement	**Vincent Dahirel** UMR 8234 CNRS / UPMC Univ Paris 6, France *P90*
14:05-14:30	A47: Magnetization Reversal Process in Thin Amorphous Ferromagnetic Film with Surface Anisotropy	**Nikolai A. Usov** National University of Science and Technology MISiS, Russia *P91*
14:30-14:55	A48: Granular Matter in Extraterrestrial Environments – Modeling and Simulation of Regolith in Planetary Exploration	**Roy Lichtenheldt** German Aerospace Center DLR, Germany *P92*
14:55-15:10	*Session Break*	

Session: Beam Physics		**Chair: Mohamad Toutounji**
15:10-15:35	A49: Experimental and modelling studies of interaction of e- beam (10-345 MeV) with materials designed for radiation shielding for the MCP detector on JUICE mission to Jupiter	**Marek Tulej** Physics Institute, University Bern, Switzerland *P94*
15:35-16:00	A50: Emittance Reduction by increasing the ion source extraction field: comparing data with simulations	**Martin P. Stockli** Oak Ridge National Laboratory, USA *P95*

Session: Quantum General VIII	**Chair: Mohamad Toutounji**

16:00-16:25	A51: Tuning optical and catalytical properties of ligated metallic nanoclusters for bio-imaging application and hydrogen storage	**Vlasta Bonacic-Koutecky** Humboldt Universitat zu Berlin, Germany *P97*
16:25-16:50	A52: Nonlinear Plasmonics and Extremely Accurate Sensing	**Sergey Ponomarenko** Dalhousie University, Canada *P97*
16:50-17:15	A53: To be presented	**Hardy Schloer** Schloer Consulting Group, Germany *P99*

June 20, Tuesday Afternoon 15:10-15:40	
Poster Session	
P01: Construction of diabatic states and evaluation of non-adiabatic coupling terms by using adiabatic potential energies only	**Kyoung Koo Baeck** Gangneung-Wonju National University, Korea *P99*
P02: Microstructural Evolution of Electroless Ni deposited Electrospun Hollow Metal Nanotube for Electrolytic Cell SOEC and Bio-Sensing Applications	**Sung Gyu Pyo** Chung-Ang University, Korea *P100*
P03: Theoretical identification of frontier orbitals that are possibly responsible for electron transfer in hydrogenases with oxygen-tolerance	**Jaehyun Kim** University of Hyogo, Japan *P102*

ABSTRACT SESSION

A01: Stimulated and Spontaneous Emission and the Laser Linewidth (Keynote)

Markus Pollnau[1]

[1]*Department of Electrical and Electronic Engineering, Faculty of Engineering and Physical Sciences, University of Surrey, Guildford, United Kingdom*
Email: pollnau@kth.se

The processes of absorption and stimulated emission [1] are investigated via (i) energy conservation in a Fabry-Perot resonator [2], (ii) the Lorentz-oscillator model, and (iii) the Kramers-Kronig relations [3,4]. Vacuum fluctuations are taken into account, the duration of spontaneous emission into a resonator mode is considered [5], and the relation between stimulated and spontaneous emission is clarified. It is shown that previous models about the laser linewidth [6,7,8,9] start from incorrect assumptions about the physical foundations of spontaneous emission. Based on these results, a semi-classical approach to the laser linewidth below, around, and above the laser threshold which is consistent with resonator theory is presented [10]. These results also shed new light on the usually considered linewidth-narrowing and -broadening factors.

Experimentally the linewidth is investigated in an Al_2O_3:Yb^{3+} distributed-feedback resonator below laser threshold [11,12]. The linewidth is measured versus launched pump power and losses or gain, demonstrating that neither the usual model of a Fabry-Perot resonator nor the previous models of the laser linewidth can explain the measured results.
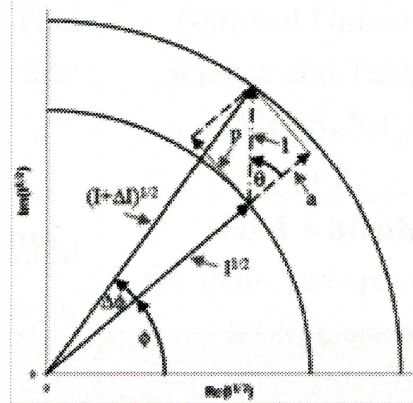
Fig1. Amplitude-phase diagram visualizing the previous interpretation of quantum noise and laser linewidth [7,8,9]. Quantum noise in a laser is induced by adding with an arbitrary phase difference θ a spontaneously emitted photon (dashed-dotted arrow) of intensity 1 to the intra-cavity laser field (short solid arrow) of intensity I and phase ϕ, resulting in an intra-cavity laser field of intensity $I + \Delta I$ (long solid arrow) and inducing a phase shift $\Delta\phi$.

References

[1] A. Einstein, *Phys. Z.* **18**, 121 (1917).
[2] N. Ismail, C. C. Kores, D. Geskus, and M. Pollnau, *Opt. Express* **24**, 16366 (2016).
[3] R. de L. Kronig, *J. Opt. Soc. Am.* **12**, 547 (1926).

[4] H. A. Kramers, *Atti Cong. Intern. Fisica* (Transactions of Volta Centenary Congress) Como **2**, 545 (1927).

[5] M. Eichhorn and M. Pollnau, *IEEE J. Sel. Top. Quantum Electron.* **21**, 9000216 (2015).

[6] A. L. Schawlow and C. H. Townes, *Phys. Rev.* **112**, 1940 (1958).

[7] M. Lax, *Phys. Rev.* **160**, 290 (1967).

[8] H. Haken, Laser theory, in *Encyclopedia of Physics* (Springer, Berlin, Heidelberg, 1970), vol. XXV/ 2c.

[9] C. H. Henry, *IEEE J. Quantum Electron.* **18**, 259 (1982).

[10] M. Eichhorn and M. Pollnau are preparing a manuscript titled „Laser linewidth, spectral coherence, and the laser eigenvalue".

[11] E. H. Bernhardi, H. A. G. M. van Wolferen, L. Agazzi, M. R. H. Khan, C. G. H. Roeloffzen, K. Wörhoff, M. Pollnau, and R. M. de Ridder, *Opt. Lett.* **35**, 2394 (2010).

[12] E. H. Bernhardi, H. A. G. M. van Wolferen, K. Wörhoff, R. M. de Ridder, and M. Pollnau, *Opt. Lett.* **36**, 603 (2011).

A02:   Topology-Driven   Effects   in Advanced Nanoarchitectures

Vladimir M. Fomin

[1]*Institute for Integrative Nanosciences (IIN), Leibniz Institute for Solid State and Materials Research (IFW) Dresden, D-01069 Dresden, Germany*

Email: v.fomin@ifw-dresden.de

Analysis of topologically nontrivial manifolds at the nanoscale is of immense importance for semiconductor, superconductor and graphene physics as well as for electronics, magnetism, optics, optoelectronics, thermoelectrics and quantum computing. Advances of high-tech nanostructure fabrication techniques have allowed for generating topologically nontrivial manifolds at the nanoscale with man-made space metrics, which determine electronic, optical, magnetic and transport properties of such objects and novel potentialities of nanodevices due to their unique topology.

The physics of quantum rings is overviewed from basic concepts rooted in the quantum-mechanical paradigm—via unprecedented challenges brilliantly overcome by both theory and experiment—to promising application perspectives. [1] Self-assembled quantum volcanos, which are singly connected, surprisingly exhibit the Aharonov-Bohm behavior in experiment. This is explained by the fact that the electron wave functions in a quantum volcano are topologically identical to the electron wave functions in a quantum ring. Symbiosis of the geometric potential and an inhomogeneous twist renders an observation of the topology effect on the electron ground-state energy in microscale Möbius strips into the realm of experimental verification. A delocalization-to-localization transition for

the electron ground state is unveiled in inhomogeneous Möbius strips. [2]

An Abrikosov vortex (antivortex) is a topological defect with winding number $n = 1$ ($n = -1$) and a vanishing order parameter at $r = 0$. The pattern of superconductor vortices in a micro- or nanoarchitecture represents therefore an important study case for arranging topological defects in confined geometries. The pattern of superconductor vortices in a micro- or nanoarchitecture represents therefore an important study case for arranging topological defects in confined geometries. The rolling-up fabrication methods have provided qualitatively novel curved superconductor micro- and nanoarchitectures, e.g., nanotubes [3] and nanohelices [4]. Vortex dynamics in open superconductor microtubes in the presence of a transport current are influenced by the interplay between the scalar potential and the inhomogeneous magnetic field component normal to the surface. Using the inhomogeneous transport current allows one to control the branching and to reduce the average number of vortices occurring in the tube per nanosecond. [5]

A Möbius ring resonator [6] and a rolled-up asymmetric microcavity [7] are representative examples, which give rise to fascinating topological effects by virtue of Möbiosity, spin-orbit coupling and non-Abelianism. The cone-like rolled-up asymmetric microcavities provide a platform to realize spin–orbit coupling of light for the examination of non-trivial topological effects in the context of a non-Abelian evolution [6]. In asymmetric microcavities, the geometric phase is directly measured by monitoring the polarization tilt angles, while the eccentricities indicate the mode conversion between the right and left circular bases. Those findings imply promising applications by manipulating photons in on-chip quantum devices.

References

[1] V. M. Fomin (Ed.), *Physics of Quantum Rings*, Springer, Berlin-Heidelberg, 2014, 487 p.

[2] V. M. Fomin, S. Kiravittaya, and O. G. Schmidt, *Phys. Rev. B* **86**, 195421 (2012).

[3] V. M. Fomin, R. O. Rezaev, and O. G. Schmidt, *Nano Letters* **12**, 1282 (2012).

[4] V. M. Fomin, R. O. Rezaev, E. A. Levchenko, D. Grimm, and O. G. Schmidt, *arXiv*: 1703.08530 [supr-con, mes-hall] (2017).

[5] R. O. Rezaev, E. A. Levchenko, and V. M. Fomin, *Sup. Sci. and Technology* **29**, 045014 (2016).

[6] S. L. Li, L. B. Ma, V. M. Fomin, S. Böttner, M. R. Jorgensen, and O. G. Schmidt, *arXiv*: 1311.7158 [physics.optics] (2013).

[7] L. B. Ma, S. L. Li, V. M. Fomin, M. Hentschel, J. B. Götte, Y. Yin, M. R.

Jorgensen, and O. G. Schmidt, *Nature Commun.* **7**, 10983 (2016).

A03: Modelling of surface materials: Upwards from Quantum Chemistry

Lei Chen[1], Alexander Kaiser[1], Michael Gyoeroek[1], Ivan Sukuba[12] and <u>Michael Probst</u>[1]

[1]Institute of Ion Physics and Applied Physics, University of Innsbruck, 6020 Innsbruck, Austria

[2]Department of Nuclear Physics and Biophysics, Faculty of Mathematics, Physics and Informatics, Comenius University, SK-84248, Bratislava, Slovakia

Metal surfaces of beryllium and tungsten feature in important parts of nuclear fusion devices currently being build (ITER) and planned (DEMO). They can undergo various transformation and alloys of these metals can form upon operation of the devices. It is therefore of interest to look at these materials from the perspective of theoretical atomistic materials science. This starts with quantum chemical calculation and can go up the multiscale ladder to differential equation codes [1] or kinetic Monte Carlo [2] and other higher-level treatments that incorporate realistic geometries and environments.

Binding energies of surface atoms are related to materials stability. Quantum chemical calculations give values of 4.08-5.63 eV for beryllium and 6.81-10.04 eV for tungsten were obtained [3] from large scale calculations using plane-wave DFT calculations with the VASP code. An analytical force field of the bond order potential type [4] agrees with these values for beryllium, but some of the tungsten surface atoms are too strongly bound. Alloys are naturally more complicated. Be and W atoms on the (001) surface of $Be_{12}W$ are slightly less bound than on the pure Be and W surfaces, respectively. For higher tungsten content, i.e. for Be_2W (figure 1) the situation different surface terminations with several sites each are possible. For some surface sites of this alloy the surface binding energies are enhanced while for others they are diminished, compared to the pure metal surfaces. The cohesive energy of the material is the equivalent of these energies inside the bulk. It is found that its dependency on the mole fraction follows an almost linear relationship.

The complexity of these systems is discussed by giving examples from experimental data and a brief overview of modelling efforts taking place at many laboratories is given.
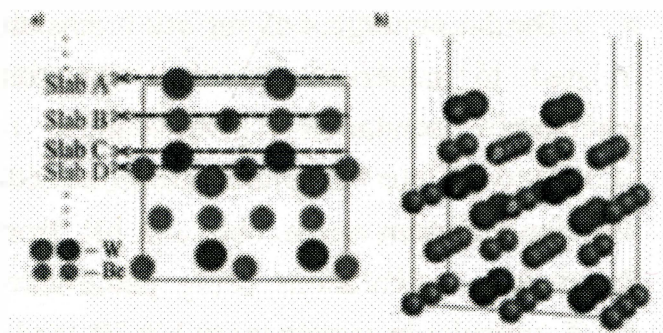
Figure 1: Schematic view of two unit cells of Be$_2$W

References

[1] "Modelling of Impurity Transport and Plasma-Wall Interaction in Fusion Devices with the ERO Code: Basics of the Code and Examples of Application", Kirschner, A.; Tskhakaya, D.; Kawamura, G.; Borodin, D.; Brezinsek, S.; Ding, R.; Linsmeier, Ch.; Romazanov, J. *Contributions to Plasma Physics (2016), 56(6-8), 622-627.*

[2] "Temperature dependence of underdense nanostructure formation in tungsten under helium irradiation Valles", G.; Martin-Bragado, I.; Nordlund, K.; Lasa, A.; Bjorkas, C.; Safi, E.; Perlado, J. M.; Rivera, A. *Journal of Nuclear Materials (2017), 490, 108-114.*

[3] "Surface binding energies of beryllium/tungsten alloys", Gyoeroek, M.; Kaiser, A.; Sukuba, I.; Urban, J.; Hermansson, K.; Probst, M. *Journal of Nuclear Materials (2016), 472, 76-81.*

[4] "Atomistic simulations of the effect of reactor-relevant parameters on Be sputtering", Safi, E.; Bjorkas, C.; Lasa, A.; Nordlund, K.; Sukuba, I.; Probst, M. *Journal of Nuclear Materials (2015), 463, 805-809*

A04: Quantum resistance standard device using epitaxial graphene on SiC

Vladimir Falko
National Graphene Institute, the University of Manchester

Standardisation of electronics components requires the availability of standards for their parameters, such as resistance, for their comparative tests to the products. Currently, the chain of resistance standards involves comparison to metallic bars kept under constantly maintained special conditions in few metrology institutes in the world. The alternative trend for maintaining the resistance standard is based on the fundamental phenomenon of the Quantum Hall effect, which consists in the precise quantisation of Hall resistance in two-dimensional electron systems in units of h/e^2, determined by the fundamental constants of nature: electron charge and Planck's constant. This sets the trend in developing the quantum resistance standard (QRS) which value and precision are set by the nature rather than a historical choice. Due to specific spectrum of electrons in graphene, this two-dimensional material is the best platform for realising the quantum

resistance standard. Here, we report that epitaxial graphene synthesised on Si-terminated surface of SiC provides the best conditions for robust quantisation of Hall resistance, 10^{-11} accuracy at 15T and 10^{-6} at 5T. The performance of this system is determined by the peculiar charge transfer between graphene and SiC surface. Also, we analyse the cooling of edge state electrons in graphene by acoustic phonon emission, and propose a design of G/SiC the QRS device where the influence of the hot spot near current contacts on the quantum Hall effect on the actively measured part is reduced by the sample geometry.

A05: Laser Material Interactions for Flexible Applications

Keon Jae Lee[1],*

[1]*Associate Professor, Department of Materials Science and Engineering, KAIST, 305-701, Korea, E-mail address: keonlee@kaist.ac.kr*

This seminar introduces recent progresses of laser material interactions that can extend the application of self-powered flexible electronics and two-dimensional materials. Laser technology is extremely important for future flexible electronics since it can adopt high temperature process on plastics, which is essential for high performance electronics, due to ultra-short pulse duration. (e.g. LTPS process over 1000 °C. The first part will introduce self-powered flexible piezoelectric energy harvesting via inorganic based laser lift off (ILLO). Energy harvesting technologies converting external sources (such as vibration and bio-mechanical energy) into electrical energy is recently a highly demanding issue. The high performance flexible thin film nanogenerator was transferred by ILLO from bulk substrates for self-powered biomedical devices such as pacemaker and brain stimulation. The second part will introduce flexible large scale integration (LSI) and high density 1S1R memristor devices via ILLO. Flexible memory is an essential part of electronics for data processing, storage, and radio frequency (RF) communication. To fabricate flexible memristor arrays, we adopted innovative transfer protocol of high density 1S1R memory using ILLO technology. The third part will discuss the laser material interaction for two-dimensional materials. We observed a melt-mediated phase separation into two thin layers from SiC wafers via excimer laser. This technology is very useful to make new two dimensional materials.

References *(from Keon's group as corresponding authors)*

[1] Nano Letters 11, 5438, 2011.
[2] Nano Letters 10, 4939, 2010.
[3] Nano Letters 12, 4810, 2012.
[4] Nano Letters 14, 7031, 2014

[5] Adv. Mater, 26, 2514, 2014.
[6] Adv. Mater. 26, 4880, 2014
[7] Adv. Mater, 26, 7480, 2014
[8] Adv. Mater. 24, 2999, 2012.
[9] Adv. Mater. 27, 3982, 2015
[10] Adv. Mater. 27, 2866, 2015
[11] Energy Environ. Sci. 8, 2677, 2015
[12] Energy Environ. Sci., 7, 4035, 2014
[13] ACS Nano 7, 11016, 2013
[14] ACS Nano 9, 4120, 2015
[15] ACS Nano 7, 4545, 2013
[16] ACS Nano 7, 2651, 2013.
[17] ACS Nano 8, 9492, 2014
[18] ACS Nano 8, 7671, 2014
[19] ACS Nano, 9, 6587, 2015
[20] Adv. Energy Mater. 3, 1539, 2013
[21] Adv. Energy Mater. 5, 1500051, 2015
[22] Adv. Func. Mater. 24, 2620, 2014
[23] Adv. Func. Mater. 24, 6914, 2014
[24] Nano Energy, 14, 111, 2015
[25] Nano Energy, 1, 145, 2012

Keon Jae Lee is an associate professor in Dept. of MSE at KAIST. He earned the Ph.D degree from University of Illinois Urbana Champaign, in 2006. His current research interests are self-powered flexible electronic system for bio, energy and electronic devices. He has coauthored over 60 SCI papers in journal including Science, Nature Materials, Nano Letters, Adv. Mater, Energy Environ. Sci, ACS Nano, Adv. Energy Mater., Adv. Func. Mater., Nano Energy. He has filed ~150 patents and more than 40 of these are licensed.

A06: Ferromagnetism in Carbon Based Materials Probed by NMR

M. Požek,[1] D. Pelc,[1] I. Marković,[1] T. Cvitanić,[1] J. C. C. Freitas,[2] W. L. Scopel,[3] W. S. Paz,[2] L. V. Bernardes,[4] F. E. Cunha-Filho,[4] C. Speglich,[4] F. M. Araújo-Moreira[4]

[1]Department of Physics, Faculty of Science, University of Zagreb, Zagreb, Croatia.
Email: mpozek@phy.hr
[2]Department of Physics, Federal University of Espírito Santo, Vitória, ES, Brazil
[3]Department of Exact Sciences, Federal Fluminense University, Volta Redonda, RJ, Brazil
[4]Department of Physics, Federal University of São Carlos, São Carlos, SP, Brazil.

We present an investigation of local magnetic fields in ferromagnetic graphite, using nuclear magnetic resonance (NMR) of carbon nuclei. Guided by ab initio calculations, we detect a ^{13}C NMR signal in chemically modified graphite without external magnetic fields, conclusively demonstrating the intrinsic ferromagnetic character of the material. Our work is the first detection of internal fields in carbon-based ferromagnets, and the values of the fields suggest that the magnetism is induced by defects in the material structure.[1] The zero-field NMR signal survives up to temperatures above 200 K, in agreement with previous macroscopic magnetization measurements, providing perspectives for the application of this

unique material at room temperature. Furthermore, we investigate the dynamics of domain walls, through measurements of nuclear relaxation times and the ferromagnetic enhancement of the ^{13}C NMR signal. Two dynamically distinct carbon sites are found, and we discuss their origin and the consequences for the microscopic structure of the material.
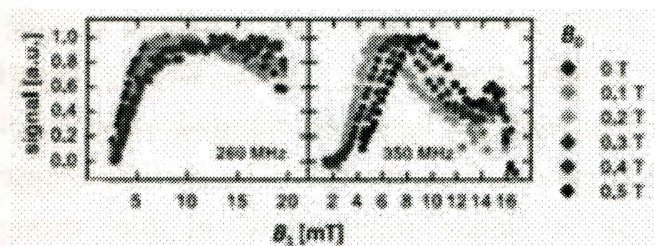

Fig1. The dependence of signal intensity on external field B_0 and excitation field B_1 for two dynamically distinct carbon sites.

Reference

[1] J. C. C. Freitas et al., *Scientific Reports* **5**, 14761 (2015).

A07: Quantum Mechanical and Molecular Mechanical Studies of Chemical Reactions

Hajime Hirao[1]
[1]*Department of Biology and Chemistry, City University of Hong Kong, Hong Kong, China Email:hhirao@cityu.edu.hk, web site: personal.cityu.edu.hk/~hhirao*

Computational chemistry offers extremely green techniques for conducting research into molecules and materials. In addition, the physical principles used in computational chemistry underlie all branches of chemistry; as such, computational chemistry has unlimited potential to contribute to the advancement of fundamental chemistry in every different subdiscipline as well as to finding solutions to critical challenges that humankind faces today. With this in mind, our computational exploration of chemistry applies quantum chemistry, multiscale QM/MM and and many other advanced computational chemistry techniques to porous coordination polymers (PCPs, or metal-organic frameworks, MOFs) and nanomaterials. In particular, using computational approaches and often with experimental collaborators, we seek to derive information about chemical reaction mechanisms and bonding patterns of these complex molecules.

References

[1] Kazuki Doitomi, Kai Xu, and Hajime Hirao, "Mechanism of an Asymmetric Ring-Opening Reaction of Epoxide with Amine Catalyzed by a Metal-Organic Framework: Insights from Combined Quantum Mechanics and Molecular Mechanics Calculations", Dalton Trans. 2017, 46, 3470-3481.

[2] Ramana Singuru, Quang Thang Trinh, Biplab Banerjee, Bolla Govinda Rao, Linyi Bai, Asim Bhaumik, Benjaram Mahipal Reddy, Hajime Hirao, and John Mondal, "Integrated Experimental and Theoretical

Study of Shape-Controlled Catalytic Oxidative Coupling of Aromatic Amines over CuO Nanostructures", ACS Omega 2016, 1, 1121-1138.

[3] Adhitya Mangala Putra Moeljadi, Rochus Schmid, and Hajime Hirao, "Dioxygen Binding to Fe-MOF-74: Microscopic Insights from Periodic QM/MM Calculations", Can. J. Chem. 2016, 94, 1144-1150 (special issue dedicated to Professors Russell Boyd and Arvi Rauk).

[4] Hajime Hirao, Wilson Kwok Hung Ng, Adhitya Mangala Putra Moeljadi, and Sareeya Bureekaew, "Multiscale Model for a Metal-Organic Framework: High-Spin Rebound Mechanism in the Reaction of the Oxoiron(IV) Species of Fe-MOF-74", ACS Catal. 2015, 5, 3287-3291.

A08: Effective Theory of Non-Adiabatic Quantum Evolution Based on the Quantum Geometric Tensor

D. Solnyshkov[1], O. Bleu[1], and G. Malpuech[1]

[1]*Institut Pascal, University Clermont Auvergne/CNRS, Clermont-Ferrand, France*

Email:dmitry.solnyshkov@uca.fr

We study the role of the quantum geometric tensor [1] in the evolution of quantum systems. We show that all its components play an important role on the extra phase acquired by a spinor and on the trajectory of an accelerated wavepacket in any realistic finite-duration experiment. While the adiabatic phase is determined by the Berry curvature (the imaginary part of the tensor), the non-adiabaticity is determined by the quantum metric (the real part of the tensor) and allows to determine corrections in the regimes where Landau-Zener approach is inapplicable. We find a correction to the anomalous velocity which appears in the semi-classical equations [2] for an accelerated wavepacket at geodesic trajectories. The particular case of a planar microcavity in the strong coupling regime allows to extract the quantum geometric tensor components by direct light polarization measurements and to check their effects on the quantum evolution.

Figure 1 shows the effect of the non-adiabaticity on the Berry phase in the simplest case of a spinor in a rotating magnetic field (a), with a mechanical analogy: a rotating wheel on a shaft (b). When the duration of the experiment (1 single turn) is increased, the phase converges to the adiabatic value of π (c), and the correction is linear in field's rotation frequency ω (d).
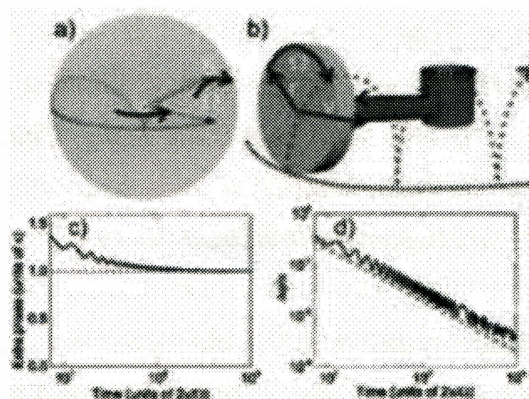
Fig1. (a) Bloch sphere with the spin (red arrow) and the magnetic field Ω (blue arrow), adiabatic trajectory (blue) and real trajectory (red dashed line); (b) Mechanical analog: "adiabatic" trajectory of an infinitely small wheel (blue), cycloid trajectory of a point on a wheel (red). Ω - wheel rotation frequency, v - wheel velocity, ω - shaft center rotation; (c) Total extra phase for one full spinor rotation as a function of the rotation time; (d) Deviation from the adiabatic Berry phase: numerical calculation (black) and analytical correction exhibiting $1/T$ decay (red dashed).

References

[1] J. P. Provost and G. Vallee, Commun. Math. Phys. 76, 289 (1980).
[2] M.-C. Chang and Q. Niu, *Phys. Rev. Lett.* **75**, 1348 (1995).

A09: Information entropies calculation using the J-matrix method

I.Nasser[1], Afaf Abdel-Hady[2]
¹Department of Physics, King Fahd University of Petroleum & Minerals, Dhahran 31261, Saudi Arabia
Email: imnasser@kfupm.edu.sa, web site: http://faculty.kfupm.edu.sa/PHYS/imnasser/
²Department of basic Science, Faculty of Engineering, Egyptian Chinese University, Cairo, Egypt

Using the J-matrix method [1], the scaling laws are given for the entropies in the information theory. The method has been applied using the modified Hulthén potential (MHP) [2]. The scaling laws are specified in the position and momentum spaces as a function of $|\mu-\mu_{c,n\ell}|^{\delta}$, where δ is the critical exponent, μ is the screening parameter and $\mu_{c,n\ell}$ its critical value for the specific quantum numbers n and l. Scaling laws for other physical quantities, such as energy eigenvalues, the moments, static polarizability, transition probabilities, etc. are also given. Some of these are reported for the first time. The 2-dimension visualization of the Shannon charge density will be explained and discussed as we approach the ionization limit. The outcome is compared with the available literatures' results.

References

[1] M. S. Abdelmonem, Afaf Abdel-Hady and I. Nasser, Mol. Phys., Manuscript DOI: 10.1080/00268976.2017.1299887 (2017).
[2] S. H. Patil and K. D. Sen, Int. J. Quantum Chem. **107**, 1864 (2007).

A10: Nanoscale Spin Filters from Graphene Nanostructures

Frank Hagelberg[1], Alexander Kaiser[2], Ivan Sukuba[2], Michael Probst[2]

[1]*Department of Physics and Astronomy, East Tennessee State University, Johnson City, TN, USA*
Email:hagelber@etsu.edu, web site: http://faculty.etsu.edu/HAGELBER/comp_chem.html
[2]*Institut für Ionenphysik und Angewandte Physik, University of Innsbruck, Innsbruck, Austria*

Graphene nanoribbons (GNRs) are well-known candidates for conductors in nanoelectronic circuits,[1] since they are chemically inert and mechanically stable, and thus can be easily handled and exposed to relatively high operating temperatures. Recently, it has been predicted that H-terminated single-walled carbon nanotubes of the zigzag type (zSWCNTs) can be used as gates in a spin valve or spin filter circuit due to the antiferromagnetic nature of their electronic ground state, characterized by unpaired electrons with opposite spin orientation at either end of the tube.[2,3]

In this contribution, we present investigations on the spin filter properties of various carbon nanostructures by use of a non-equilibrium Green's function (NEGF) procedure.[4] In particular, several configurations involving armchair graphene nanoribbons (aGNRs) of the type nFe-aGNR, with n =1, 2, will be discussed in terms of the magnetocurrent ratio (MCR) as a function of the bias. For both single and double substitution, the results are seen to vary sensitively with the number and the substitutional sites of the atomic impurities. A further parameter of relevance for the case of double substitution is the relative orientation of the magnetic moments of the two impurities. MCR values exceeding 80 percent were recorded for both single and double substitution. In particular, high spin polarization efficieny is found for an arrangement involving two Fe atoms substituted at bulk sites along the aGNR length coordinate. This effect is seen to diminish with increasing distance between the impuritiy atoms. For adequate description of the current-voltage profiles, taking into account the bias dependence of the transmission function proves to be imperative.
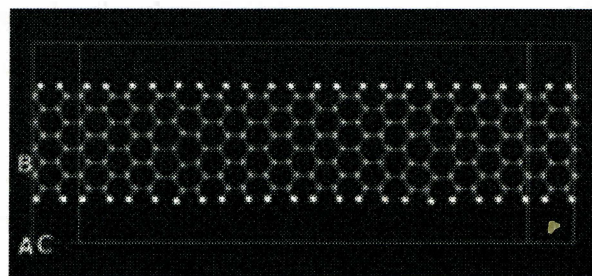
Fig1. An armchair graphene nanoribbon of the (0,8) type with two substitutional Fe atoms.

References

[1] L.Liu, W.Ma, Z. Zhang, *Small*, 2011, *7*, 1504–1520.
[2] J.Wu, F.Hagelberg, *Phys. Rev. B*, **2009**, *79*, 115436.
[3] O.V. Khavryuchenko, G. H. Peslherbe, F. Hagelberg, *J. Phys. Chem. C* **2015** *119*, 3740.
[4] Atomistix ToolKit version 2015.1, QuantumWise A/S (www.quantumwise.com)

A11: New perspective on the 2D metal-Insulator Transition

M. S. Osofsky[1], J. Prestigiacomo[1], S. C. Hernández-Hangarter[1], A. Nath[2], V. Wheeler[1], S. G. Walton[1], R. L. Myers-Ward[1], C. M. Krowne[1], D. K. Gaskill[1], K. Bussmann[1], K. M. Charipar[1], and D. R. Rolison[1]

[1]*U.S. Naval Research Laboratory, Washington, DC 20375, USA*
Email:Michael.osofsky@nrl.navy.mil, web site: http://www.mxu.edu/jdoe.htm
[2]*George Mason University, Fairfax, VA 22030, USA*

The discovery of low-dimensional metallic systems such as high-mobility metal oxide field-effect transistors, the cuprate superconductors, and graphene, silicene, phosphorene, conducting oxide interfaces (*e.g.*, $LaAlO_3/SrTiO_3$), and a large variety of transition metal chalcogenide and dichalcogenide systems contradicts the seminal theory for transport in disordered metals that predicts that the metallic state cannot exist in two dimensions (2D).[1] A key issue in such studies is the nature of the metal insulator transition (MIT) in 2D. Since the MIT is a quantum phase transition (one that occurs at T=0K) the transport properties should be independent of the chemical and structural details of the system. In this presentation, we will demonstrate that a generic phase diagram for the 2D MIT can be constructed for two very different systems: 1) highly disordered RuO_2 nanoskins and 2) plasma-functionalized graphene. This phase diagram consists of three regions: metallic, weakly localized insulator with conductivity, $\sigma \sim logT$, and strongly localized insulator. We will present details of the transport properties of the disordered RuO_2 nanoskins and plasma-functionalized graphene near their respective MITs.

Reference

[1] Abrahams, E., Anderson, P.W., Licciardello, D.C., & Ramakrishnan, T.V. Scaling theory of localization: Absence of quantum diffusion in two dimensions. *Phys. Rev. Lett.* **42**, 673–676 (1979).

A12: Electron Spin at Work in Modern and Emerging Devices

Viktor Sverdlov[1], Josef Weinbub[2], Siegfried Selberherr[1]

[1]*Institute for Microelectronics, TU Wien, Gußhausstraße 27-29, 1040 Wien, Austria*
[2]*Christian Doppler Laboratory for High Performance TCAD at the Institute for Microelectronics, TU Wien, Gußhausstraße 27-29, 1040 Wien, Austria*
Email :{sverdlov|weinbub|selberherr}@iue.tuwien.ac.at, web site: http://www.iue.tuwien.ac.at

The continuous increase in performance of modern integrated circuits has been constantly supported by the

miniaturization of electronic components and interconnects. Although the feasibility of the 7nm technology node was recently demonstrated [1], fabrication costs, control, and integration combined with reliability issues will gradually bring the metal-oxide-semiconductor field-effect transistor (MOSFET) scaling to an end. The MOSFET operation is fundamentally based on the charge of an electron interacting with the gate potential, which allows controling the current flow in the channel between source and drain, which makes it a charge-based approach (i.e. electrical current) and thus ultimately consumes electrical power. To reduce power consumption, the electron spin is considered as a potential candidate for building innovative devices complementing or even replacing the conventional charge-based electronics as it allows to introduce non-volatility in the device operation and opens a way to reduce the dependence on charge transport, i.e., to significantly reduce power consumption. The spectacular experimental demonstration of a SpinFET [2] - predicted 25 years ago [3] - brings semiconductor spintronics closer to applications.

In order to realize a SpinFET, three fundamental ingredients are required: efficient spin injection/detection, spin propagation, and spin manipulation by purely electrical means [3,4]. In silicon, however, the gate voltage-dependent spin manipulation is overshadowed by a weak spin-orbit interaction [4,5]. Regardless of the weak interaction, it results in a finite probability for a spin flip at every electron scattering event, which leads to the injected spin relaxing to its equilibrium zero value. Because in thin silicon films the spin relaxation is mostly determined by scattering between the equivalent valleys, the spin lifetime is significantly enhanced by uniaxial stress [6] as it efficiently lifts the degeneracy between these valleys. Since the spin-orbit field acts in-plane, the spin lifetime can be further boosted by a factor of two for in-plane injection as compared to the injection orthogonally to the film [7]. The spin lifetime in silicon films can be engineered to guarantee the spin propagation at distances (about a micrometer), which is sufficient for practical applications. For spin injection in silicon within the three-terminal injection scheme the respective signal appeared to be orders of magnitude larger than the theory predicts [8]. Although magnetoresistance due to spin-dependent resonant tunneling [9] is likely responsible for the large signal, the reason for the discrepancy is under scrutiny [10]. To add to the controversy, a different expression for magnetoresistance was recently suggested [11]. To resolve the discrepancy, a numerical Monte Carlo approach for the spin- dependent trap-assisted tunneling in tunnel junctions was developed [12]. We demonstrate that the spin-dependent tunneling rates are determined by the two spin-up/spin-down levels considered in [11] only if the magnetic field is parallel to the

magnetization. In a general case all four eigenvalues of a 4×4 transition matrix must be considered, which explains the controversy [12].

References

[1] S.-Y.Wu et al., IEDM 2016, p.43-46; R.Xie et al., IEDM 2016, p.4750.

[2] P. Chuang et al., Nat.Nanotechnol. 10, 35 (2015).

[3] S.Datta and S.Das, Appl.Phys.Lett. 56, 665 (1990).

[4] T.Tahara et al., Appl.Phys.Express, 8, 113004 (2015).

[5] D.Osintsev et al., Solid-State Electron. 71, 25 (2012).

[6] V.Sverdlov and S.Selberherr, Phys.Rep. 585, 1 (2015).

[7] J.Ghosh et al., J.Nano Res., 39, 34 (2016).

[8] R.Jansen, Nat.Mater. 11, 400 (2012).

[9] Y.Song and H.Dery, Phys.Rev.Lett. 113, 047205 (2014).

[10] F. Rortais et al., Phys.Rev.B 94, 174426 (2016); A.Spiesser et al., Appl.Phys.Express 9, 103001 (2016).

[11] Z.Yue al., Phys.Rev.B 91, 195316 (2015).

[12] V.Sverdlov et al., IWCN 2017, accepted.

A13: End states of rectangular armchair graphene ribbon

Y. H. Jeong, S. -R. Eric Yang[1]

[1]*Department of Physics, Korea University, Seoul, Korea*

Email:eyang812@gmail.com

We consider the end states of a half-filled rectangular armchair graphene ribbon (RAGR) in a staggered potential (see Fig.1). Taking electron-electron interactions into account we find that, as the strength of the staggered potential varies, three types of couplings between the end states can occur: antiferromagnetic without or with spin splitting, and paramagnetic without spin-splitting. We find that a spin-splitting is present only in the staggered potential region $0 < \Delta < \Delta_c$. The transition from the antiferromagnetic state at $\Delta = 0$ to the paramagnetic state goes through an intermediate spin-split antiferromagnetic state, and this spin-splitting disappears suddenly at Δ_c. For small and large values of Δ the end charge can be connected to the Zak phase of the periodic armchair graphene ribbon (PARG) with the same width, and it varies continuously as the strength of the potential changes.
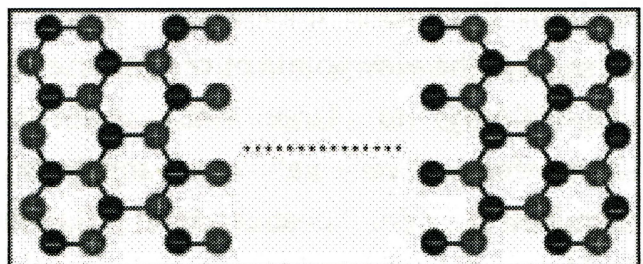
Fig1. RAGR has two long armchair edges and two short zigzag edges. The lengths of the armchair and zigzag edges are, respectively, L_{arm} and L_{zig} (ribbon width W is equal to L_{zig}). The staggered potential energy is $\epsilon_i = \Delta/2$ on sublattice A (red circles) and $\epsilon_i = -\Delta/2$ on sublattice B (blue circles). Left (right) end is made of A (B)-type sites.

A14: Fabrication and Optimization of Silver Nanowire Transparent conductive film via needle organic precursor by sonochemical process

Yamato Hayashi

Department of Applied Chemistry, School of Engineering, Tohoku University, Sendai, Miyagi, JAPAN

Email:hayashi@aim.che.tohoku.ac.jp, web site: http://www.che.tohoku.ac.jp/~aim

Silver nanowire transparent conductive film, which is prepared by depositing silver nanowires onto a substrate, shows both high optical transparency and high electrical conductivity. The film can be easily prepared *via* liquid suspension, so it is said to have advantages as compared to Indium Tin Oxide transparent conductive film from the viewpoints of cost saving and applicability to large area substrate. Moreover, silver nanowire transparent conductive film coated onto flexible polymer substrate shows good bending tolerance, it can be used in flexible devices, such as flexible display, lighting equipment, and so on. Generally, polyol method, which is performed in liquid phase, is used as a synthetic method of silver nanowires. Although silver nanowires with high aspect ratio and nanometer-sized diameter can be synthesized by this method, there are some problems on synthetic conditions, processes, and waste emission. Furthermore, silver nanowires obtained by polyol method are single-crystalline solid wires. In general, it is necessary to apply silver nanowires to complicated high temperature and high pressure annealing process to make connections among wires when transparent conductive film is prepared. Consequently, the overall process requires high cost and emits much waste. To improve these problems, a novel method, painting and subsequent reduction of organic precursor, is proposed in this study. In this method, needle-shaped organic precursor was fabricated by sonochemical process, and then silver nanowire is simply obtained by splaying and reducing them to metallic silver with retaining their needle-shaped morphology. Ultrasound indicates many chemical and physical effects such as microstreaming, microjet in sonochemical process [1]. By optimizing ultrasonic synthetic and reducing conditions of the precursor, preparation of highly transparent and conductive silver nanowire transparent conductive film could be expected [2-4]. Nanowire are not single crystal nanowire

but connected many polycrystal structure. Transparent conductive film fabricated by using these materials showed about 10 Ohm/sq. of resistivity and over 70 % of transparency, relative high performance. In addition, it doesn't require high temperature condition when reducing the precursor, that is, it can be applicable to low heat resistance materials, such as PET, PC, and so on. From these reasons, this material is expected to be a novel material for flexible transparent conductive film.
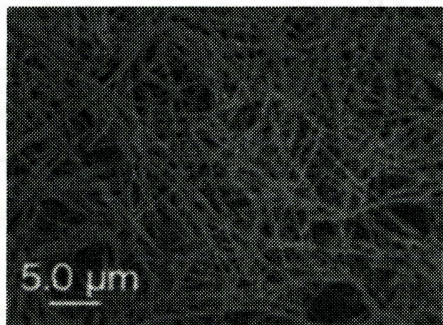

Fig.1. Image of Silver Nanowire by sonochemical process

References

[1] K. S. Suslick, *Science*, 247, (1990) 1439.

[2] K. Sugawara, Y. Hayashi, J. Fukushima H. Takizawa, Mat. Sci. Forum.. 804 (2014) 115.

[3] K. Sugawara, Y. Hayashi, J. Fukushima H. Takizawa, Cryst. Res. Technol.. 50 (2015) 319.

[4] Y. Hayashi, K. Fujita, I. Narita, M. Inoue, H. Takizawa, *IEEE NANO 2016*, Article number 7751502, (2016) 257.

A15: Colloidal Quantum Dot Optoelectric Applications

Kyung-Sang Cho[1], Chan-Wook Baik[1], Jun-Hee Choi[1]
[1]*Device Lab., Samsung Advanced Institute of Technology, Suwon, Gyeong-gi, South Korea*
Email:k-s.cho@samsung.com

Colloidal quantum-dots (QDs) have received considerable attention in the past two decades. Especially they were considered as a promising candidate as a new material for electroluminescent (EL) light-emitting devices with many technological advantages, such as high quantum yields, extremely narrow emission, spectral tunability, good solution processability, and a higher stability than organic lumophores [1-4]. The use of QDs in the light-emitting diodes was first proposed by Alivisatos et al. [1] and various approaches have been followed to improve the performance of devices, including the design of novel device structures, the development of novel QD and transport materials, and the optimization of carrier injection [2-4]. Recently a functioning monochromatic-QD display and full-color RGB QD display was demonstrated by our group [2,3].

In this report, various issues of QD-LED fabrication and enhancement of the device performance on QD-LED and QD-display are discussed including the design of QD materials, device structure, interface control, charge/energy transfer of

QD layer and QD-patterning. Studies of the QD-monolayer assembled structure and their application into the QD white-light-emitting devices are also shown [5]. Besides QD-LEDs, some recent research for the optoelectronic device applications of colloidal QDs (i.e. QD lasers and high performance QD phototransistors) will be presented.

References

[1] V. L. Colvin, M. C. Schlamp and A. P. Alivisatos, *Nature* **370,** 354 (1994).

[2] K. S. Cho, E. K. Lee, W. J. Joo, E. J. Jang, T. H. Kim, S. J. Lee, S. J. Kwon, J. Y. Han, B. K. Kim, B. L. Choi and J. M. Kim, *Nature Photonics* **3,** 341(2009).

[3] T.-H. Kim, K. S. Cho, E. K. Lee, S. J. Lee, J. Chae, J. W. Kim, D. H. Kim, J.-Y. Kwon, G. Amaratunga, S. Y. Lee, B. L. Choi, Y. Kuk, J. M. Kim and K. Kim, *Nature Photonics* **5,** 176 (2011).

[4] Q. Sun, et al., *Nature Photonics* **1,** 717 (2007).

[5] T.-H. Kim, D.-Y. Chung, J. Ku, I. Song, S. Sul, D.-H. Kim, K.-S. Cho, B. L. Choi, J. M. Kim, S. Hwang and K. Kim, *Nature Communicatios* **4,** Article number:2637(2011).

A16: Geometric Images of Quantum Mechanical Functions and Objects

Alexander P. Yefremov[1]

[1]*Physics Department, RUDN University, Moscow, Russian Federation*
E-mail:a.yefremov@rudn.ru,
alexander.p.yefremov@gmail.com

In this study we intend to demonstrate that conventional quantum mechanics:
(i)   admits "geometric" images,
(ii)   its basic (Schrodinger) equation can be strictly deduced within the most fundamental math medium,
(iii)   the Schrodinger equation turns out to be the base of equations of classical and relativistic mechanics.

The study is mostly linked with fundamental math structures [1] having clear images when written in matrix units. Thus, a novel geometric image of a complex number (in the matrix form) as a "conic gearing mechanism" is suggested [2], and a 2D cell is introduced, a local area of the fractal complex numbered surface, determined by the dyad vectors (it was called by Wheeler a "pre-geometry" [3]). It is shown that the single dyad may be regarded as a basic element for construction of all units of exclusive algebras of real, complex and quaternion numbers. Vector (imaginary) quaternion units in their turn are known to form a 3D frame initiating a Cartesian system of coordinates. These math structures help to formulate the sketched below "general theory of particle's mechanics" [4].

Two transformations of a 2D cell are considered, a phase flickering and the surface stretching; taken together they

violate the algebras multiplication. A condition saving the algebras "forever" in the form of a normalizing integral constant with respect to a free parameter is introduced; use of the Gauss theorem converts it into continuity type equation for dyad vectors as functions of coordinates of an abstract space. An arbitrary "propagation vector" emerges in the equation.

Choice of the propagation vector as gradient of the 2D cell phase leads to appearance of a simpler fractalized equation; written in the physical units (of Compton length) the equation precisely takes the form of the Schrodinger equation of quantum mechanics. Any of the 2D cell's dyad vectors can be treated as the "wave" or "state" function of the described particle. Separated into real and imaginary parts Schrodinger equation is represented as couple of the Bohm equations; one of them gives birth to the Hamilton-Jacoby equation of the classical mechanics, the 2D cell's flickering phase being the classical mechanical action.

Two different models of same particle are analyzed. One model is in fact being a flickering 2D cell loaded with a relative fractal mass localized in small area of the fractal space. This object principally is not observable. The other model is a mass distributed in a small 3D volume and rotating about one axis with frequency twice greater than that of the 2D cell's flickering; in the 3D space this particle is detected as a "material quasi-point", its rotation practically unobservable.

The "rotating material quasi-point" moving in the 3D space depicts a helix line by its any bordering point. Under condition restricting the value of velocity of this bordering point up to the speed of light, the expression for the helix line element gives precisely the Lagrangian of an inertial relativistic particle. In the non-relativistic approximation we automatically obtain the expression for the De Broglie wave and famous heuristic "momentum-wave vector" and "energy-frequency" links.

The possibility to find three mechanics normally considered quite different (even alien) in one consequent and logically consistent study seems hardy to be just a mathematical trick or an accidental coincidence.

References

[1] P. Lancaster and M. Tismenetsky. *The Theory of Matrices, Second Edition with Applications*. San Diego, USA, London, UK: Academic Press, 1985.

[2] A.P.Yefremov, "The conic-gearing image of a complex number and a spinor-born surface geometry". *Gravit. & Cosmol*. Vol.17, No 1, 2011, pp. 1-6.

[3] J. A. Wheeler, "Pregeometry: motivations and prospects." In: A. R. Marlov (ed.), *Quantum Theory and Gravitation*. New York: Academic Press, 1080, pp. 1–11.

[4] A.P.Yefremov, "General theory of a particle mechanics arising from a fractal

space" *Gravit. & Cosmol.* Vol.21, No 1, 2015, pp. 19-26.

A17: Harmonic Analysis of Quantum States and Observables

Artur Sowa[1]

[1]*Department of Mathematics and Statistics, University of Saskatchewan, Saskatoon, Saskatchewan, CANADA*
Email:sowa@math.usask.ca, web site: http://math.usask.ca/~sowa/

Harmonic analysis is a term broadly applied to a set of techniques for scrutinizing classical signals, as well as to the area of Mathematics that examines both the coherencies and limitations of these techniques, and frequently applies them inwardly toward the solution of other analytic problems. The central idea is that signals or functions can be decomposed into basic modes and catalogued according to their modal energy distribution profiles. Quantum Mechanics starts with a description of the basic modes (eigenstates) before addressing the more complex superpositions and tensor products. The resulting structures are high-dimensional, counter-intuitive, and seemingly recalcitrant to qualitative descriptions. A well-established remedial approach is the use of phase space methods predicated upon the Wigner function. However, while such methods are well adapted to the analysis of special types of states (Gaussian, coherent, or squeezed) they are less relevant in other situations. In the era of quantum technologies 2.0, as we embark to design quantum-state manipulating devices and quantum metamaterials, [1-2], and ask fundamental questions about the qualities of prevalent quantum states, [3], it is beneficial to have alternative analytic tools. The alternative proposed here is the Q-transform, [4], which provides a rigorous way of representing quantum observables in the form of doubly-periodic real functions and distributions. In particular, it furnishes a natural concept of Sobolev classes of observables and, through that, yields qualitative regularity-type results for a variety of quantum flows (both unitary and non-unitary). The choice of underlying fundamental modes furnishes various incarnations of the Q-transform, adapting it to any given problem of interest.

The Q-transform connects quantum theory to other phenomena of harmonic analysis, such as the broadband redundancy (BR), [5]. The BR results from an observation that there exist ensembles of spread spectrum waveforms which average to a pure tone, Fig. 1; as such it enables the construction of families of broadly diverse observables with a predesigned average. Among targeted applications of the BR is quantum tomography, where it is natural to look for optimal ensembles of measurements. The Q-transform should also prove useful in regard to the problem

of quantumness and speedup in quantum information processing. Where much progress has been achieved, e.g. [6-8], the Q-transform can yield additional insight into the possibility of efficient classical simulation of some quantum algorithms.
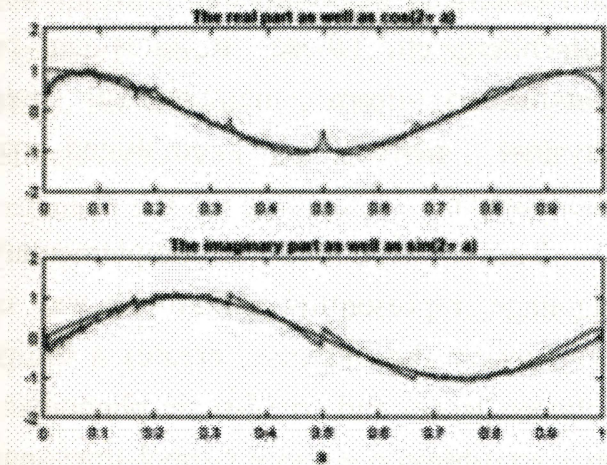

Fig1. The BR in brief: N different waveforms rich in high-frequency energy have an average (jagged lines) that in some sense converges to the pure tone as N tends to ∞. The rate of convergence depends on a parameter σ and competes against the energy of high-frequency modes in the individual waveforms. (Here σ = .7, N=237)

References

[1] A.L. Rakhmanov, A.M. Zagoskin, S. Savel'ev, and F. Nori, Phys. Rev. B **77**, 144507 (2008)

[2] A. M. Zagoskin, Quantum Engineering, Cambridge University Press (2011)

[3] W. H. Zurek, Nature Physics **5**, pp. 181-188 (2009)

[4] A. Sowa, arXiv:1609.01712 [quant-ph]

[5] A. Sowa, arXiv: 1603.03667 [math.GM]

[6] R.W. Spekkens, PRL **101,** 020401 (2008)

[7] A. Mari and J. Eisert, PRL **109,** 230503 (2012)

[8] L. Kocia, Y. Huang, and P. Love, arXiv: 1703.04630 [quant-ph]

A18: Stieltjes electrostatic model of quantum mechanics

K.V.S. Shiv Chaitanya

Department of Physics, BITS Pilani, Hyderabad Campus, India

In this talk, I will be presenting Stieltjes electrostatic model of quantuim mechanics. To show this first I will show Stieltjes electrostatic model is analogous to quantum Hamilton Jacobi formalism. This analogy allows, the bound state problem to mimics as n unit moving imaginary charges $i\hbar$, which are placed in between the two fixed imaginary charges arising due to the classical turning points of the potential. The interaction potential between n units moving imaginary charges $i\hbar$ is given by logarithm of the wave function. For an exactly solvable potential, this system attains stable equilibrium position at the zeros of the orthogonal polynomials depending upon the interval of the classical turning points. I will also show this problem is analogus to N point vortices in fluid dynamics. This analogy also helps us to resvolve wave particle duality N point charges or vortices, become imaginary, in a

constant background field will admit a wave solution under paraxial wave approximation. Therefore, in quantum mechanics as long as paraxial approximation is valid it behaves like a wave.

References

[1] K V S Shiv Chaitanya Pramana: 83, Issue 1 , 139, (2014)
[2] K V S Shiv Chaitanya and V Srinivasan, arxiv: 1609.06159.

A19: Twin physics - the concept of complementarity in the real world

Ir. Anna C.M. Backerra BMus

It is possible to tackle the principle of uncertainty from a mathematical perspective, which has been overlooked until now. A formalism is developed, based on the concept that determinate and indeterminate aspects of a phenomenon are mutually independent, and that they occur joined in nature in such a manner that one of both dominates an observation.

The basic item in the theory is the Heisenberg-unit, defined as a constant amount of potential energy. This mathematical item is the key to a better understanding of the universe, because it allows a fundamental division between potential and actual energy. The Heisenberg-unit is supplied with attributes of time, space and mark (a mathematical precursor of charge and electromagnetism). Time and space occur necessarily as two distinct qualities, although they are treated analogously, according to the advices of Einstein. Only by interaction with another Heisenberg unit, these attributes can be transformed from mathematical into physical items and combined to phenomena.

This so-called complementary language, representing a dualistic way of considering the universe, creates a bridge between large- and small-scale phenomena and so between quantum-mechanics and gravity. The quantization of Planck and the uncertainty relations of Heisenberg are incorporated from scratch. Moreover the laws of Maxwell emerge in an easy way. Important in the description is the conception of space as an independent entity, not as a lack of matter, having a potential equal to that of mass. The attributes of mark allow H-units to be neutral, positive or negative, which after interaction transform into neutral as well as charged particles without the necessity to divide the charge. By considering three types of Heisenberg-units as the basic elements of the universe, it is possible to show how their interaction generates elementary particles as neutron, proton, electron, neutrino, gluon and Higgs particle.

In this lecture we concentrate on gravitational attraction between two

elementary masses. Gravity appears as a consequence of the difference in spatial size between marked and unmarked Heisenberg-units, through which the range of gravity is larger than the range of electricity. This seems to be the reason for the apparent one-sidedness of gravity. The *repulsing* possibility of physical bodies stays out of the reach of electromagnetic effects and can be identified with the expansion of the universe.

A20: Quantized electrical conductance of thin metal nanowire

Yoshifumi Oshima

School of Materials Science, Japan Advanced Institute of Science and Technology, Nomi, Ishikawa, Japan
Email: oshima@jaist.ac.jp, web site: http://www.jaist.ac.jp/ms/labs/oshima-lab/en.html

Metal atomic contacts show interesting physical properties such as conductance quantization, large yield strength and reconstruction. Especially, conductance quantization has been studied energetically because of a key element of nanometer scale electronics. The geometry of metallic contact, which depends on the axis of the metal contact, has been considered to have an influence on electrical conductance behavior, but the structural observations have not been reported fully with measuring the electrical conductance. In this paper, the relationship between structural and conductance of gold [111], [001] and [110] contacts were studied.

Our developed STM holder can be installed in a UHV-TEM system (JEM-2000VF) kept below 1×10^{-7} Pa at room temperature [1]. A UHV condition is necessary to avoid contamination of the gold contacts. Gold contacts were fabricated by repeating an attaching-breaking cycle for the two electrodes using a piezo drive in the TEM system. The width of the gold contact gradually decreased from 7 to 1 nm and could be controlled by the piezo drive. During stretching of the contact, TEM images were recorded at 30 Hz, simultaneously with the conductance measurement. The conductance was measured at a sampling rate of 30 kHz when the bias voltage of 13 mV was applied between both electrodes in the STM holder. In our system, conductance evolution from tunneling to the contact regime is consecutively measurable. We confirmed that the incident electron beam had no influence on the conductance measurements.

The gold [111] contact was determined to be a short bottleneck, suspended between two truncated triangular pyramid electrodes surrounded by three {111} and three {100} facets [2]. It shows the typical conductance evolution of a gold [111] contact during stretching. Conductance

steps appear regularly and the conductance gradually decreases between two adjacent jumps. Between the jumps, the contact is stretched by 0.24 nm, which corresponds to the spacing of the (111) lattice.

On the other hand, the gold [110] contact became hexagonal prism shape (called gold [110] nanowires) (Fig. 1)[3]. It was surrounded by four {111} and two {001} facets and its cross-section was hexagonal. In the conductance histogram of Fig. 1, the conductance peaks were found to appear in steps close to the quantum unit. Below $10G_0$, the prominent conductance peaks corresponded to stable gold nanowires with a regular hexagonal cross-section, which value normalized by the quantum unit was equal to the number of conductance channels. It indicates that thin gold [110] nanowires are ballistic conductors below $10G_0$.
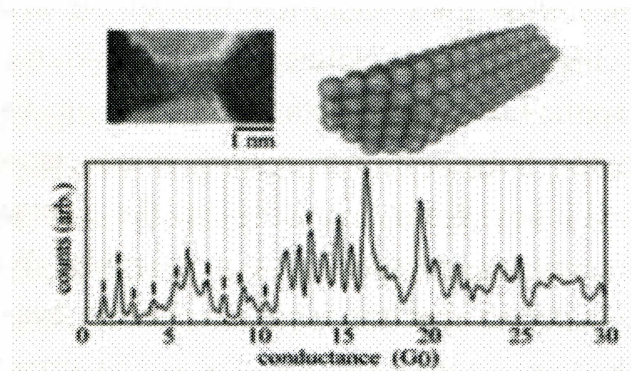
Figure 1　A TEM image of a gold [110] nanowire, the corresponding structure model and conductance histogram showing clear quantized conductance.

References

[1] Y. Oshima, et al., Surface Science 531, 209 (2003).
[2] Y. Oshima, et al., J. Phys. Soc. Jpn 79, 054702 (2010).
[3] Y. Kurui, Y. Oshima, et al., Phys. Rev. B79, 165414 (2009).

A21: Quantum wave mixing and resolving photonic classical and non-classical coherent states

V.N. Antonov[1,2], A.Yu. Dmitriev[2], R. Shaikhaidarov[1,2], T. Hönigl-Decrinis[1] and O.V. Astafiev[1,2]
[1]*Physics Department, Royal Holloway, University of London, Egham, Surrey TW20 0EX, United Kingdom*
Email:v.antonov@rhul.ac.uk
[2]*Moscow Institute of Physics and Technology, 141700 Dolgoprudny, Russia*

Superconducting quantum systems-artificial atoms are building blocks of novel on-chip quantum electronics, which utilize the quantum nature of electromagnetic waves [1, 2]. Particularly, single atoms can create and reveal quantized light states beyond classical statistics. In this work we demonstrate a novel fundamental physical phenomenon, the Quantum Wave Mixing (QWM), which attainable only in the systems where light-matter interaction is arranged between an individual photons and a single atom. QWM reveals itself as an elastic scattering of coherent classical and non-classical photonic states of

electromagnetic waves on a single artificial atom in a 1D space.

We demonstrate two regimes of QWM, comprising different degrees of "quantumness": The most spectacular one is QWM with non-classical coherent states, exhibiting spectra of a finite number of narrow coherent emission peaks. The spectrum is a fingerprint of interacting photon states, where the number of positive frequency peaks (due to stimulated emission) always exceeds by one the negative ones (due to absorption). We also study four- and higher-order wave mixing of classical coherent waves on the artificial atom. In this case the time dynamics of the peaks exhibits a series of Bessel-function quantum oscillations with orders determined by the number of interacting photons.

with the symmetric one $a_- a_+^* a_- b_{-3}^+$. In the mixing with non-classical states, the time symmetry is broken resulting in the asymmetric spectrum. c) Schematic representation of QWM with non-classical coherent states and sensing of the coherent quantum states. Two sequential pulses ω_- and then ω_+ are applied breaking time symmetry and, therefore, spectrum symmetry. Coherent photonic states are created in the atom by the first pulse at ω_- and then mixed with the second pulse of ω_+. Single-photon, $N_{ph} = 1$, state $|\beta\rangle_-$ can only create a peak at $\omega_3 = 2\omega_+ - \omega_-$ because only one photon at ω_- can be emitted from the atom. Two photon, $N_{ph} = 2$, coherent state $|\gamma\rangle_-$ results in creation of an additional peak at $3\omega_+ - 2\omega_-$, because not more than two photons can be emitted. Also one photon of ω_- can be absorbed, $N_{ph} - 1$, creating additional left-hand-side peak at $2\omega_- - \omega_+$ in this case.

Fig1. a) A false colored SEM image of the device: a superconducting loop with four Josephson junctions, behaving as an artificial atom, is embedded into a transmission line and strongly interacts with propagating electromagnetic waves. b) Four-wave mixing processes resulting in the single-photon field creation at $\omega_3 = 2\omega_+ - \omega_-$. In classical mixing, the process operators $a_+ a_-^* a_+ b_3^+$ comes in pair

References

[1] O. Astafiev et al., Nature, 449, 588-590 (2007).

[2] I.-C. Hoi, et al., New Journal of Physics, 15, 025011 (2013).

A22: Single carrier transport in graphene nanostructure

Takuya Iwasaki, Zhongwang Wang, Manoharan Muruganathan, Hiroshi Mizuta

School of Materials Science, Japan Advanced Institute of Science and Technology, Asahidai 1-1, Nomi, Ishikawa, JAPAN

Email: t.iwasaki@jaist.ac.jp, web site: http://www.jaist.ac.jp/ms/labs/mizuta-lab/

Spin of electron in graphene quantum dots (GQDs) is a promising candidate for the implementation of spin qubit in solid states.[1] Single carrier transport in geometrically-defined graphene quantum dots has been investigated so far. However, the Coulomb blockade phenomena through a single charging island at the inherent Dirac point has not been observed due to edge roughness and charge localization (doping) in graphene,[2,3] which leads to the formation of unintentional multiple charging islands in graphene nanostructures.[4,5] To obtain the reliable single carrier transport property in graphene, it is crucial to investigate and reduce their influence.

Here we report the transport characteristics in geometrically-defined GQD, and graphene single constriction devices. In the former devices, according to the Coulomb oscillation and diamond characteristics, multiple dots are formed even though the single dot is designed structurally. This indicates that unintentional dots are formed in the graphene channel comprising both the constriction and quantum dot structures. The quantum dot formation can be attributed to the strength of potential disorder originated from both edge roughness and doping. Then, we examine the graphene constriction devices with a short length and a narrow width, to minimize the influence of edge roughness. In addition, we carefully control the position of the charge neutrality point (i.e., doping concentration) by the annealing treatment.[6] Consequently, the periodic Coulomb oscillation and the regular Coulomb diamond characteristics are observed at 5 K in the certain gate voltage range, indicating the carrier transport occurs through a single charging island.

The formation of single charging island could be interpreted as the result of the electron confinement in the constriction region by quantum reflection leading to the localization of the wave function (i.e., quasi-bound state). This result importantly implies that single carrier transistors with the single charging island could be achieved in graphene by the combination of constriction structure patterning and CNP control.

(a) Geometrically-defined GQD
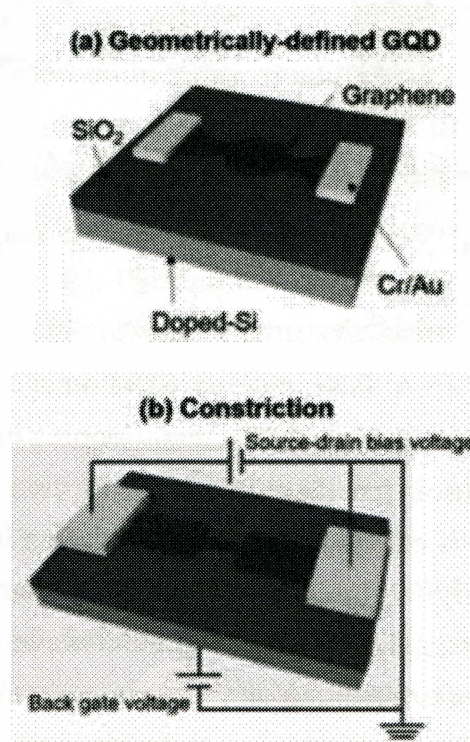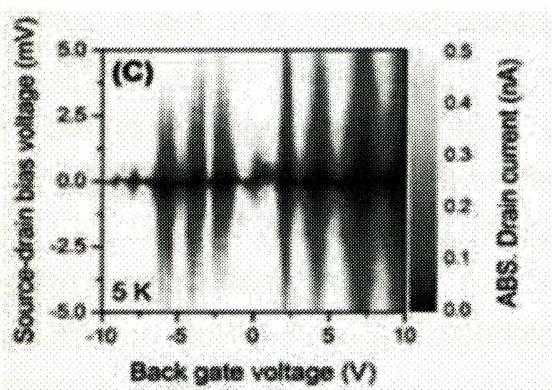
(b) Constriction

Fig1. (a) Schematic illustration of geometrically-defined graphene quantum dot device. (b) Schematic drawing of graphene single constriction device. Graphene is contacted with the metal electrodes made of Cr/Au. Doped Si substrate covered with SiO_2 is used as back gate. (c) Coulomb diamond characteristic of the graphene constriction device measured at 5 K.

References

[1] B. Trauzettel, D.V. Bulaev, D. Loss, and G. Burkard, *Nat. Phys.* **3**, 192 (2007).

[2] D. Bischoff *et al.*, *Appl. Phys. Rev.* **2**, 031301 (2015).

[3] J. Güttinger *et al.*, *Rep. Prog. Phys.* **75**, 126502 (2012).

[4] F. Sols, F. Guinea, and A.H. Castro Neto, *Phys. Rev. Lett.* **99**, 166803 (2007).

[5] K. Todd, H.-T. Chou, S. Amasha, and D. Goldhaber-Gordon, *Nano Lett.*, **9**, 416 (2009).

[6] T. Iwasaki, M. Muruganathan, M.E. Schmidt, and H. Mizuta, *Nanoscale* **9**, 1662 (2017).

A23: Novel Transient Nonlinear Optical Processes in Bulk Solids and Nanostructures

E. Yu. Perlin[1,2]

[1]*Research Center "Informational Optical Technologies", ITMO University, St. Petersburg, Russia*
Email: perlin.mail.ifmo.ru, web site http://www.ifmo.ru/viewperson/347/perlin_evgeniy_yurevich.htm
[2]*Department of Experimental Physics, Institute of Physics, Nanotechnologies, and Telecommunications, Peter the Great Polytechnic University, St. Petersburg, Russia*

Novel features of high-order nonlinear optical processes in solids under femtosecond powerful laser pulses will be considered. The following processes will be discussed:

a) Nonlinear absorption of femtosecond laser pulses under conditions of multiphoton resonances in direct-gap bulk solids and heterostructures with deep quantum wells, quantum wires, and quantum dots [1];

b) absorption of femtosecond light pulses due to indirect interband transitions in crystals [2];

c) nonlinear absorption of radiation pulses under the two-photon resonance in solids in the conditions of femtosecond pump-probe spectroscopy [3];

d) multiphoton absorption controlled by the resonance optical Stark effect in crystals [4-7];

e) transient interband optical double resonance in solids [8, 9]

Quantum-mechanical calculations of probabilities of elementary processes involved in above-mentioned phenomena were carried out within high-order perturbation theory. The results of these calculations were applied to analyze kinetics of non-equilibrium electron-hole pairs producing and optical switching the media between states with essentially different optical and electrical properties.

It was shown that in all cases under consideration a narrow region of laser intensities j appears where the populations of electron states dramatically change even at small change of j. Theoretical results are in a good agreement with experimental data if they are available. A number of crystals and heterostructures, whose electron band structure and geometric parameters allow the above-described transient nonlinear processes of photoexcitation and optical switching, are considered in detail.

References

[1] E.Yu. Perlin, K.A. Eliseev, E.G. Idrisov, and Ya.T. Khalilov, Opt. Spectrosc. **113**, 383 (2012).

[2] K.A. Eliseev and E.Yu. Perlin, Opt. Spectrosc. **119**, 911 (2015).

[3] E.G. Idrisov and E.Yu. Perlin, Opt. Spectrosc. **115**, 497 (2013).

[4] A.V. Ivanov and E.Yu. Perlin, **106**, (I) 677, (II) 685 (2009).

[5] E.Yu. Perlin and A.V. Fedorov, Opt. Spectrosc. **78**, 106 (2012).

[6] M.A. Bondarev, A.V. Ivanov, and E.Yu. Perlin, Opt. Spectrosc. **112**, 445 (1995).

[7] M.A. Bondarev and E.Yu. Perlin, J. Opt. Technol. **80**, 661 (2013).

[8] E.Yu. Perlin, JETP, **78**, 98 (1994).

[9] M.A. Bondarev and E.Yu. Perlin, Opt. Spectrosc. **122**, No. 4 (2017).

A24: Spintronic applications of mono-axial chiral helimagnet

Junichiro Kishine
Division of Natural and Environmental Sciences, the Open University of Japan, Chiba, Japan
Email:kishine@ouj.ac.jp

In a magnetic crystal belonging to chiral space group, competition of the relativistic spin-orbit Dzyaloshinskii-Moriya (DM) interaction and ferromagnetic exchange interaction causes a helical magnetic arrangement with definite vector chirality and a winding period of several tens of nanometers. The most intriguing property of chiral helimagnet is that there appears a nonlinear regular lattice of spin magnetic moments under weak magnetic field applied perpendicular to the helical axis. This state, called chiral soliton lattice (CSL), is an extremely robust topological ground state, where magnetic topological charges condense into regular lattice. The spatial

period of the CSL is controlled by magnetic field.

When itinerant electrons coexist such as in the case of CrNb3S6, the CSL acts on the itinerant electrons as magnetic superlattice potential. On the other hand, the itinerant electrons cause spin torque transfer into the CSL to cause collective translation of the CSL. Consequently, we anticipate that the CSL would exhibit a variety of interesting functions, including spin current induction, nontrivial soliton transport, new kind of elementary excitations, current-driven collective transport, anomalous magneto- resistance, soliton confinement and so on. These theoretical proposals are strongly supported by experimental demonstration that the CSL is formed in a single crystal of CrNb3S6.

It is an interesting topic to explore dynamical response of the CSL when it is weakly confined or pinned. In such a case, there arises an extrinsic energy scale in the CSL dynamics. We mean by "weak" that the confinement or pinning effects are treated in perturbative manner, i.e., we consider how the CSL sliding may be affected by these extrinsic effects. These effects will open up new perspectives in the field of spintronics. In this presentation, I will give a recent theoretical results with special emphasis on spintornic applications of mono-axial chiral helimagnets.
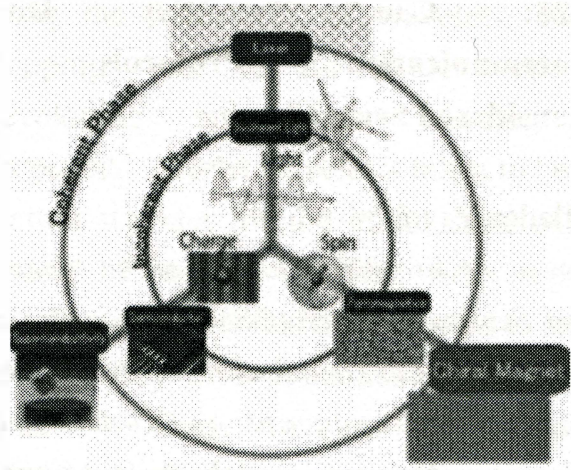
Fig1. Macroscopic cohenrece and materials functionality

References

[1] J. Kishine and A.S.Ovchinnikov, Solid State Physics Vol.66, Chapter 1 (Elsevier, Academic Press, 2015).

[2] Y. Togawa, Y. Kouska, K. Inoue and J. Kishine, J. Phys. Soc. Jpn., invited review paper (Oct. 2016).

[3] I. Proskurin, A.S. Ovchinnikov, P. Nosov, J. Kishine, to appear in New Journal of Physics (2017).

[4] Y.Togawa, T.Koyama, K.Takayanagi, S.Mori, Y.Kousaka, J.Akimitsu, S.Nishihara, K.Inoue, A.S.Ovchinnikov, and J.Kishine, Phys.Rev.Lett.108, 107202 (2012).

[5] J.Kishine, I.V.Proskurin and A.S.Ovchinnikov, Phys.Rev.Lett. 107, 017205 (2011)

[6] J.Kishine, I.G.Bostrem, A.S.Ovchinnikov, and Vl.E.Sinitsyn,Phys.Rev.B89, 014419 (2014)

A25: Can Two-Way Direct Communication Protocols Be Considered Secure?

Mladen Pavičić

Center of Excellence for Advanced Materials and Sensing Devices (CEMS), Photonics and Quantum Optics Unit, Ruđer Bošković Institute, Zagreb, Croatia and *Department of Physics, Nanooptics, Humboldt-University Berlin, Germany* Email: mpavicic@irb.hr, web site: http://www.irb.hr/users/mpavicic

We consider intercept-resend attacks on two kinds of direct two-way QKD protocols - ping-pong Bell state protocol with entangled photons [1] and LM05 with single photons [2] - in which an undetectable Eve can decode all the messages in the message mode (MM) and show that the mutual information between parties (Alice, Bob, and Eve) is not a function of disturbance but is always maximal and equal to unity as shown in Figure 1(b).
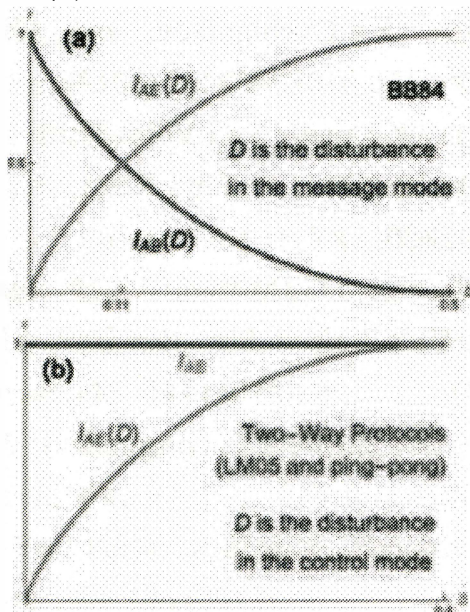
Fig. 1. Mutual information plots for (a) the one-way probabilistic protocol BB84 vs. (b) two- way deterministic protocols with either entangled Bell states or with LM05-like single photon states. Essential difference between them is that in (a) Eve causes polarization flips in the message mode, while in (b) Eve ideally does not cause any polarization flip in the message mode.

The disturbance (D) Eve induces is in the control mode (CM) and therefore the standard approach and protocols for estimating and calculating the security are not available since they all assume the presence of D in MM. As a result, a critical D cannot be determined, the standard error correction procedure might not applicable for eliminating Eve's information, the efficiency of the privacy amplification is curtailed, and the unconditional security as proposed in [3] and [4] cannot be considered proved without solving these issues. In a way, Alice's sending of the key is equivalent to sending an unencrypted plain text "secured" by an unreliable indicator of Eve's presence and the protocols cannot be considered for implementation before one proves or disproves that a novel kind of privacy amplification for such deterministic attacks can be designed.

of Croatia through the CEMS funding are acknowledged.

References

[1] Boström, K., T. Felbinger, Deterministic secure direct communication using entanglement, *Phys. Rev. Lett.* **89**, 187902–1–4 (2002).

[2] Lucamarini, M., S. Mancini, Secure deterministic communication without entanglement. *Phys. Rev. Lett.* **94**, 140501–1–4 (2005)

[3] Lu, H., C.H.F. Fung, X. Ma, Q. yu Cai, Unconditional security proof of a deterministic quantum key distribution with a two-way quantum channel. *Phys. Rev. A* **84**, 042344-1-5 (2011).

[4] Li, J., L. Li, H. Jin, R. Li, Security analysis of the "PingPong" quantum communication protocol in the presence of collective-rotation noise, *Phys. Lett. A* **377**, 2729–2734 (2013).

A26: Quantum Dynamics and Electronic Spectroscopy within the framework of Wavelets

Mohamad Toutounji

College of Science, Department of Chemistry, P. O. Box 17551, UAE University, Al-Ain, UAE

Important aspects of electronic spectroscopy and quantum dynamics in condensed harmonic systems are formulated using the framework of wavelets, and a stepping stone to our future work on developing anharmonic wavelets is proposed. Morlet wavelet is taken to be the mother wavelet for the initial state of the system of interest. This work reports daughter wavelets that may be used to study spectroscopy and dynamics of harmonic systems. These wavelets are shown to arise naturally upon optical electronic transition of the system of interest. Natural birth of basis (daughter) wavelets emerging on exciting an electronic two-level system coupled, both linearly and quadratically, to harmonic phonons is discussed. It is shown that this takes place through using the unitary dilation and translation operators, which they happen to be part of the time evolution operator of the final electronic state. The corresponding optical autocorrelation function and linear absorption spectra are calculated to test the applicability and correctness of the herein results. The link between basis wavelets and Liouville space generating function is established. An anharmonic mother wavelet is also proposed in case of anharmonic electron-phonon coupling. A brief description of deriving anharmonic wavelets and the corresponding anharmonic Liouville space generating function is explored. In the conclusion a mother wavelet (be it harmonic or anharmonic) which accounts for Duschinsky rotation is suggested.

A27: Quantum Vision in 3-D

Yehuda Roth

Oranim Academic College, Q.Tivon 36006, Israel Email: yudroth@gmail.com

Coherent states represent a single physical entity that stand for a concept. For example, if a **single** particle is located in two places $|x_1\rangle$ and $|x_2\rangle$ it is possible to define the symmetry-antisymmetry concepts through the states

$$|\pm\rangle\frac{1}{\sqrt{2}}\left(|x_1\rangle\pm|x_2\rangle\right)$$

Consider a 3-D body that emits photons. Those photons represents its characteristics such as its dimension shape and colors. Although the body usually emits incoherent photons, it is conceived and interpret as a single object. Identifying the object relates it to a concept.

Thus, we suggest that conceiving an object in our mind corresponds with a physical process of re-coherent that associate the incoherent photons with a single pure state.

Although most viewed 3-D bodies are composed of incoherent photons, with the appropriate superposition, it is possible to generate a single state (single photons) that represents the 3-D body. Thus, constructing a device that generates and emits such pure state photons will enable us to conceive and view a 3-D image.

A28: Bosonization of open quasi-1D systems: Theory and applications

Eugene Sukhorukov

University of Geneva, Switzerland

Between many prominent contributions of Markus Büttiker to mesoscopic physics, the scattering theory approach to the electron transport and noise [1,2] stands out for its elegance, simplicity, universality, and popularity between theorists working in this field. It offers an efficient way to theoretically investigate open electron systems far from equilibrium. However, this method is limited to situations where interactions between electrons can be ignored, or considered perturbatively. Fortunately, this is the case in a broad class of metallic systems, which are commonly described by the Fermi liquid theory. Yet, there exist another broad class of electron systems of reduced dimensionality, the so-called Tomonaga-Luttinger liquids [3,4], where interactions are effectively strong and cannot be neglected even at low energies. Nevertheless, strong interactions can be accounted exactly using the bosonization technique [5,6], which utilizes the free-bosonic character of collective excitations in these systems. In my talk, I will review the scattering theory approach to the bosonization of open quasi-one dimensional electron systems [7] and discuss some applications, such as Fermi edge singularity (FES) phenomenon far

from equilibrium [8], FES in multi-level quantum dots [9], and the thermal decay of Coulomb blockade oscillations [10].

References

[1] M. Büttiker, Phys. Rev. B **46**, 12485 (1992).

[2] For a review, see Y. M. Blanter, and M. Büttiker, Phys. Rep. **336**, 1 (1986).

[3] S.-I. Tomonaga, Prog. Theor. Phys. **5**, 544 (1950).

[4] J. M. Luttinger, J. Math. Phys. **4**, 1154 (1963).

[5] A. O. Gogolin, A. A. Nersesyan, and A. M. Tsvelik, *Bosonization in Strongly Correlated Systems* (University Press, Cambridge 1998).

[6] Th. Giamarchi, *Quantum Physics in One Dimension* (Ox- ford University Press, Oxford, 2003).

[7] E. Sukhorukov, Physica E **77**, 191 (2016).

[8] I. Chernii, I. P. Levkivskyi, E. V. Sukhorukov, Phys. Rev. B **90**, 245123 (2014).

[9] A. S. Goremykina, E. V. Sukhorukov, Phys. Rev. B **95**, 155419 (2017).

[10] S. Jezouin, *et al.*, Nature **536**, 38 (2016).

A29: How to make spin and lattice dynamical together?

J. Fransson

Department of physics and astronomy, Uppsala University, Sweden

Email:Jonas.Fransson@physics.uu.se

A coupled spin and lattice dynamics approach is developed which merges on the same footing the dynamics of these two degrees of freedom into a single set of coupled equations of motion. Our discussion begins with a microscopic model of a material in which the magnetic and lattice degrees of freedom are included. This description comprises local exchange interactions between the electron spin and magnetic moment as well as local couplings between the electronic charge and lattice vibrations. We construct an effective action for the spin and lattice variables in which the interactions between the spin and lattice components is determined by the underlying electronic structure. In this way, we obtain expressions for the electronic contribution to the inter-atomic force constant, the isotropic and anisotropic spin-spin exchanges, as well as the electronically mediated coupling spin-lattice exchange. The last of these exchanges is provides a novel description for coupled spin and lattice dynamics. It is important to notice that our theory is strictly bilinear in the spin and lattice variables and provides a minimal model for the coupled dynamics of these subsystems. Questions concerning time-reversal and inversion symmetry are rigorously addressed and it is shown how these aspects are absorbed in the tensor structure of the interaction fields. Using our novel results regarding the spin-lattice coupling, we can provide simple

explanations of ionic dimerization in double anti-ferromagnetic materials, as well as, charge density waves induced by a non-uniform spin structure. In the final parts, we construct a set of coupled equations of motion for the combined spin and lattice dynamics, reduced to a form which is analogous to the Landau-Lifshitz-Gilbert equations for spin dynamics and damped driven mechanical oscillator for the ionic motion, however, comprising contributions that couple these descriptions into one unified formulation. We provide Kubo-like expressions for the discussed exchanges in in terms of integrals over the electronic structure and, moreover, analogous expressions for the damping within and between the subsystems.

A30: Effect of magnetic impurity on electronic spin levels in quantum ring

P. Dahan

School of Engineering at Ruppin Academic Center Emek-Hefer 40250, Israel

p.dahan@ruppin.ac.il

A theory of magnetic impurities in quantum ring, QR, under magnetic field is formulated in terms of a Friedel-Anderson resonance scattering model. We consider transition metal, TM, ions substituting semiconductors QR and found that both short-range potential and resonance components of impurity scattering influence mainly the first QR energy level, near $k \approx 0$, $k = m + \Phi/\Phi_0$, m and Φ/Φ_0 are respectively the angular moment and flux. It is well-known that the short range term produces gaps in the energy levels $E_{n,m}(\phi)$ (the quantum number n introduced to enumerate the levels), which are periodic functions of flux $v = \Phi/\Phi_0$. However, the role of magnetic impurities in formation of the excitation spectrum in QR was not discussed thoroughly as yet. The differences obtained, compared with the case of bulk, are due primarily to lowering of its T_d symmetry to a D_{2d} symmetry in 2D QR, which lifts the symmetry bans for the hybridization integrals of V_d. As results, e-state (d-orbital) is strongly hybridized with QR states with $k \approx 0$ [1], thus bound states near $k \approx 0$ appeared.

The role of spin effects is more profound: the fact that the spin state of a TM ion is determined by the interatomic Coulomb and exchange interactions, makes the resonance scattering spin selective [1]. The QR states therefore are spin selective with zero-field spin splitting that causes strong spin polarization of the localized QR electron in the flux near $k \approx 0$. We consider the case of a strong scattering limit [1,2], in which the impurity e-level with spin up, $\mathcal{E}_{d\uparrow}$, is located very deep below the conduction band, and spin down, $\mathcal{E}_{d\downarrow}$, is located near the conduction band edge. Since the resonance scattering potential has a strong energy dependence characteristic, the spin up and spin down of the QR are

modified with different energy values, $\delta_{\uparrow}$ and $\delta_{\downarrow}$, respectively, Figure 1. The zero-field spin splitting in the QR states involves various electronic effects in particular, the polarized spin current can occur.
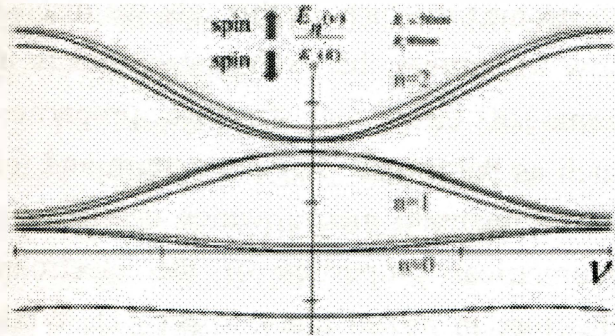
Fig1. Dimensionless QR levels for strong scattering limit where the impurity level $\mathcal{E}_{d\uparrow}$ pushes the QR levels with spin up upward and $\mathcal{E}_{d\downarrow}$ pushes the QR levels with the spin- down downward. The zero field spin splitting is significantly greater than that of a Zeeman splitting mainly for the level n=0. R_1 and R_2 are the inner and outer QR radii respectively.

References

[1] P. Dahan et al., *Phys. Rev. B* 65 1653131 (2002)

[2] P. Dahan, *Semiconductor Science and Technology*, 22, 1323, (2007).

A31: Emissive ultra-small Au nanocluster for highly-efficient organic photovoltaics

Dong Chan Lim[1]

[1]*Surface Technology Division, Korea Institute of Materials Science (KIMS), Changwon, R.O. Korea*
Email: dclim@kims.re.kr, web site: http://www.kims.re.kr

Organic photovoltaic (OPV) have intensively studied in recent years due to their advantages such as cost effectiveness and possibility of applications in flexible and transparent devices. One of the ideal deice set-up of OPVs, to achieve high efficiency and stability, is the inverted structured single and tandem OPVs which have greatest potential for achieving an improvement of device performances. Beside the device structure, various nanomaterials such as doped metal oxide interlayer, nanowire, plasmonic metal nanoparticles, carbon based materials (graphene, CNT, fullerene), and etc. are introduced, which show simultaneous enhancement of the efficiency and stability of OPVs. Among these, utilizing SPR effects with various metal nanoparticles (NPs) like Au or Ag NPs in a few tens of nm-meter size has been the most successful approach. However, we cannot expect the reproducibility using this NPs.

In this work, we have incorporated ultra-small (<1.6 nm) Au nanocluster on inverted BHJ solar cells, instead of tens of nm-sized metal NPs. Monolayer-protected metal clusters, especially those with a sub-nm-sized metal core, show unexpected various interesting optical, electrical, and magnetic properties. Figure 1 shows the

photoluminescence image of Au nanocluster solution. It cannot be expected in conventional Au nanoparticle with tens of nanometer size. Because of effective energy transfer, based on protoplasmonic fluorescence of Au nanocluster, the highest performing photovoltaics fabricated with the Au nanocluster yielded a PCE of 9.15%; this value represents an ~20% increase in the efficiency compared to solar cells without the Au nanocluster. [1]
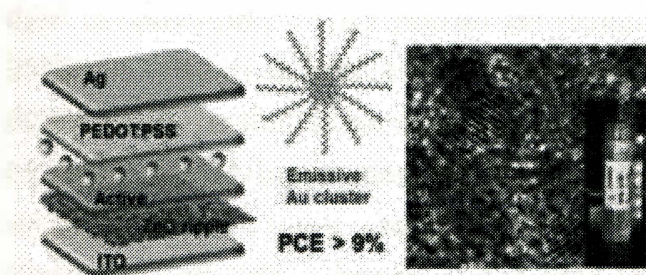
Fig1. Device structure of OPV and TEM, PL image of Au nanocluster

Reference

[1] Dong Chan Lim et. Al., *Advanced Energy Materials* **5**, 1600393 (2015).

A32: Geometrical contributions to the Exchange interactions: From Equilibrium to Nonequilibrium

Frank Freimuth[1]

[1]IAS-1, Forschungszentrum Jülich GmbH, Jülich, Germany

Email:f.freimuth@fz-juelich.de

While the spin-spiral approach is a powerful method to calculate the exchange constants of realistic materials within density functional theory, it has the drawback that it does not explicitly express the exchange constants in terms of the electronic structure. In this talk we discuss how to express the exchange constants in terms of electronic structure properties, such as the mixed Berry curvature and the mixed quantum metric, which describe the geometrical properties of the electronic structure in mixed phase space [1]. While the mixed Berry curvature [2,3,4] plays a central role in the Dzyaloshinskii-Moriya interaction the symmetric exchange interaction involves additionally the quantum metric in mixed phase space [1]. Our expressions for the exchange constants bear a strong formal resemblance to Fukuyama's theory [5] of the orbital magnetic susceptibility, which can be expressed in terms of geometrical quantities as well [6].

In contrast to the spin-spiral approach, our formalism expresses the exchange constants directly in terms of the electronic structure information, which allows us to study the relationship to other effects and phenomena important in spintronics. For example, spin-transfer torque and spin-orbit torque [7,8] can be interpreted as nonequilibrium exchange interaction and nonequilibrium magnetic anisotropy. Consequently, the spin-orbit torque is given by the mixed Berry curvature. In first order of the spin-orbit interaction the

Dzyaloshinskii-Moriya interaction is related to the ground-state spin current [9]. Thus, spin-currents excited by light are expected to lead to nonequilibrium DMI.

References

[1] F. Freimuth, S. Blügel and Y. Mokrousov, arXiv:1701.08872.

[2] F. Freimuth, R. Bamler, Y. Mokrousov and A. Rosch, *PRB* **88**, 214409 (2013).

[3] F. Freimuth, S. Blügel and Y. Mokrousov, *JPCM* **26**, 104202 (2014).

[4] F. Freimuth, S. Blügel and Y. Mokrousov, *JPCM* **28**, 316001 (2016).

[5] H. Fukuyama, Progress of Theoretical Physics **45**, 704 (1971).

[6] Y. Gao, S. A. Yang, and Q. Niu, Phys. Rev. B **91**, 214405 (2015).

[7] F. Freimuth, S. Blügel and Y. Mokrousov, *PRB* **92**, 064415 (2015).

[8] F. Freimuth, S. Blügel and Y. Mokrousov, *PRB* **90**, 174423 (2014).

[9] F. Freimuth, S. Blügel, and Y. Mokrousov, ArXiv eprints (2016), 1610.06541.

A33: Semiconductor Based Magnetoresistance and Magnetic Logic

Xiaozhong Zhang, Zhaochu Luo

School of Materials Science and Engineering, Tsinghua University, Beijing, 100084, China
Email:xzzhang@tsinghua.edu.cn

We developed a silicon based magnetoresistance (MR) device which combines the nonlinear property of diode and Hall Effect of semiconductor. The device can achieve a large MR at a few tens mT [1,2]. We further developed a silicon based magnetic logic device which can do four Boolean logic functions of AND, OR, NAND and NOR. [3]. As all these pure silicon devices have a disadvantage that they cannot work at low magnetic field of ~mT, we propose an alternative route to improve MR performance by coupling nonlinear transport effect of semiconductor and anomalous Hall effect of magnetic material of CoFeB in one device. This device has MR of >20000 % with ~1 mT, the largest MR value at low magnetic field of mT.

We further proposed a magnetic logic-memory device (Figure 1) by coupling anomalous Hall Effect in magnetic material and negative differential resistance phenomena in semiconductor [5]. All four basic Boolean logic operations could be programmed by magnetic bit at room temperature with high output ratio (> 1000 %) and low magnetic field (~5 mT). This device demonstrated that non-volatile information reading, processing and writing could be realized in one step and one device. Hence, logic and non-volatile memory could be closely integrated in one chip. The time and energy used in the processes of information transformation and transfer could be saved. Moreover, this device was comparable with the function of

neuron cell in brain that also combined memory and information process in one unit. A network with these highly parallel logic-memory devices could perform massively parallel non-volatile computing and might offer a possible route to approach brain-like artificial intelligence beyond traditional CMOS route.
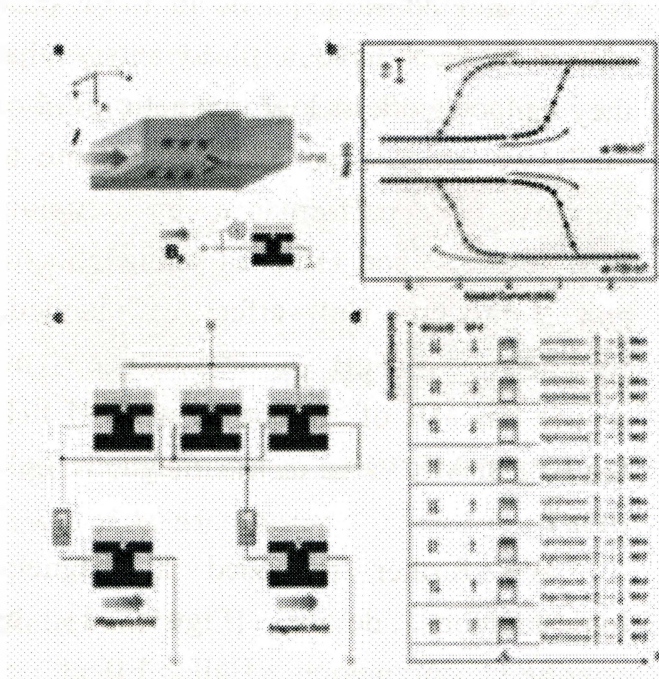
Fig1. Schematics of our magnetic logic-memory device.

References

[1] C.H. Wan, et al, *Nature* **477**, 304 (2011).

[2] Z.C. Luo et al. *Journal of Applied Physics* **117**, 17A302 (2015)

[3] Z.C. Luo et al. *Advanced Functional Materials* 25, 158 (2015).

[4] Z.C. Luo, et al., *Advanced Materials* **28**, 2760 (2016).

[5] Z.C. Luo, et al., *Advanced Materials* **29**, 1605027 (2017).

A34: Electrical Transport Properties of Two-dimensional Electrons in InGaAsN/GaAsSb Type II Quantum Well

Shuichi Kawamata [1,2]*, Akira Hibino [1], Sho Tanaka [1], Yuichi Kawamura [1,2]
[1] *Graduate School of Engineering, Osaka Prefecture University, Sakai, 599-8531, Japan*
[2] *Organization for Research Promotion, Osaka Prefecture University, Sakai, 599-8570, Japan*
Email: s-kawamata@riast.osakafu-u.ac.jp

The InP-based InGaAs/GaAsSb type II multiple quantum well is the system for developing optical devices for 2 – 3 m wavelength regions [1]. By doping nitrogen into InGaAs layers, the system becomes effective to fabricate the optical devices with longer wavelength [2]. In this report, electrical transport properties are reported on the InGaAsN/GaAsSb type II system. The epitaxial layers with the single hetero or multiple quantum well structure on InP substrates are grown by molecular beam epitaxy. The electrical resistance of samples with different nitrogen concentration has been measured as a function of the magnetic field up to 9 Tesla at several temperatures between 2 and 8 K. The effective mass of two-dimensional electrons is obtained from the temperature dependence of the amplitude of the Shubnikov-de Haas oscillations. Figure 1 shows the nitrogen concentration dependence of the effective mass m* normalized by the free electron

mass m_0. The effective mass increases as the nitrogen concentration increases from 0.0 to 1.5 % [3]. The mass enhancement occurs with corresponding to the reduction of the bandgap energy. These results are consistent with the band anti-crossing model [4,5].
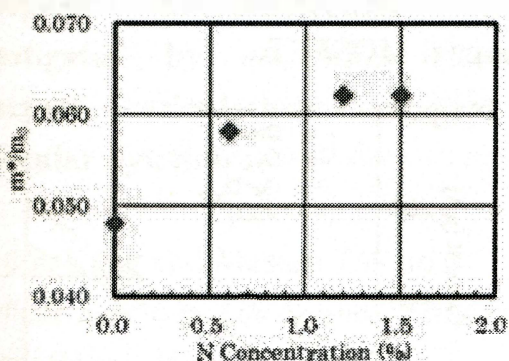
Fig1. Nitrogen concentration dependence of effective mass for InGaAsN/GaAsSb [3].

References

[1] Y. Yonezawa, R. Hiraike, K. Miura, Y. Iguchi and Y. Kawamura, Physica E, 42, 2781 (2010).

[2] Y. Kawamura and T. Sahashi, Jpn. J. Appl. Phys., 53, 028004 (2014).

[3] S. Kawamata, A. Hibino, S. Tanaka and Y. Kawamura, J. Appl. Phys. 120, 142109_1-3 (2016).

[4] W. Shan, W. Walukiewicz, J. W. Ager III, E. E. Haller, J. F. Geisz, D. J. Friedman, J. M. Olson, and S. R. Kurtz, Phys. Rev. Lett., **82**, 1221 (1999).

[5] C. Skierbiszewski, P. Perlin, P. Wisniewski, W. Knap, T. Suski, W. Walukiewicz, W. Shan, K. M. Yu, J. W. Ager, E. E. Haller, J. F. Geisz, and J. M. Olson, Appl. Phys. Lett., 76, 2409 (2000).

A35: Density functional theory calculation for interface electronic structure of SiC power electronic devices

Tomoya Ono

Center for Computational Sciences, University of Tsukuba, Tsukuba, Ibaraki, Japan Email:ono@ccs.tsukuba.ac.jp, web site: http://sip.ccs.tsukuba.ac.jp

SiC is attracted much attention due to its excellent physical properties, such as a high thermal conductivity, high breakdown strength, and large band gap. However, unlike Si metal-oxide-semiconductor field-effect transistors (MOSFETs), SiC-MOSFETs, primarily of the n-channel type, suffer from unacceptably low carrier mobility. Among various polytypes of SiC, 4H-SiC, in which Si and C atoms can occupy one of three positions along the [1-100] direction is the most widely used polytype for SiC-MOSFETs. Within these four bilayers, there are two inequivalent lattice sites, usually known as h (hexagonal) and k (quasi-cubic) based on the site occupied by the Si atoms in the neighboring bilayers. In our previous study, we found that interface type determines whether conduction band edge internal-space states at the interface are affected by the presence of O defects, as with h type, or not, as with k type.[1]

In this study, we perform first-principles calculation to investigate how the electron scattering property of the SiC/SiO_2 interface changes depending on the

interface, i.e. h and k types, and when O atoms, which are introduced during dry oxidation, are subsequently inserted.[2] Calculations are carried out using RSPACE.[3] To perform the transport calculation, we adopt the Green's function method and the Landauer-Büttiker formalism within the framework of density functional theory. We investigate three models, one O atom Oif, two O atoms Osub+Oif, and VCO_2, which appears after introducing three excess O atoms and removing a CO molecule to relieve the interface stress caused by lattice constant mismatch.[1]

The channel current with respect to the applied bias is shown in Fig. 1. We can observe a significant reduction of the current due to the existence of the O atoms for the h type while the amount of the current is unaffected for the k type. Two physical phenomena combine to prevent electron transmission in the h type. First, the internal-space states appear from the top of the interface in the h type. Second, the energy level of the internal-space states is shifted upward by the Coulomb interaction with inserted O atoms or defects.

For comparison, we also examine the transmissions through the h and k types with carbon-related defects. Similarly to the case of the oxygen-related structures, the transmission at the h type is markedly decreased. It is surprising that the oxygen-related structures, which are naturally generated at the SiC/SiO_2

interface during dry oxidation, cause the electron scattering because the oxygen-related structures considered here have been reported to be electrically inactive. According to the discussion about the local density of states at the interface, the internal-space states will play important role for the carrier scattering at the n-channel MOSFET.
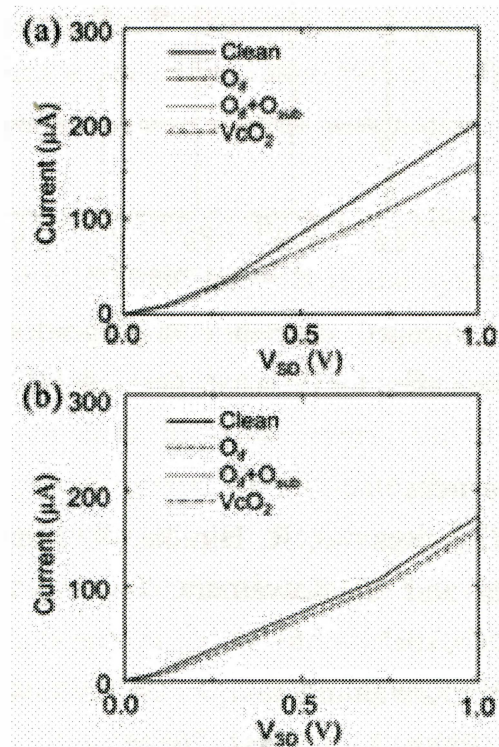
Fig1. Calculated channel current for (a) h type and (b) k type.

References

[1] C. J. Kirkham and T. Ono, J. Phys. Soc. Jpn. **85** 024701 (2016).

[2] K. Hirose, T. Ono, Y. Fujimoto, and S. Tsukamoto, *First Principles Calculations in Real-Space Formalism, Electronic Configurations and Transport Properties of Nanostructures* (Imperial College, London, 2005).

[3] S. Iwase, C. J. Kirkham and T. Ono, Phys. Rev. B **95** 041302 (2017).

A36: Dynamical mechanisms of biological macromolecular systems investigated by *ab initio* electronic structure calculations coupled to molecular dynamics

Jiyoung Kang and Masaru Tateno

Graduate School of Life Science, University of Hyogo, Hyogo, Japan

Email:jiyoungkang01@google.com, web site: http://biophys.web.fc2.com/index.html

In order to investigate mechanisms of structural changes that are responsible for electron and proton transfer in biological macromolecular systems, hybrid *ab initio* quantum mechanics (QM)/molecular mechanics (MM) molecular dynamics (MD) simulation has been conducted with respect to huge systems composed of enzymes, membrane, and solvent.

For such an aim, we have previously built a super-parallel *ab initio* QM/MM MD computation system by combining the gamess and amber engines, for which the interface is treated with our C program together with the modified games and amber programs in our hybrid *ab initio* QM and MM calculations [1-5].

In the present study, we investigated functional mechanisms of cytochrome c oxidase (CcO) from bovine, which is the terminal enzyme of the electron transport chain, catalyzing an O_2 molecule to two water molecules to pump the protons. This reaction occurs in the binuclear center (BNC), which is composed of the Cu_B and heme a_3 sites.

To explore mechanisms of the ligand recognition (CO and O_2) in the BNC, we performed full *ab initio* QM and hybrid *ab initio* QM/MM MD calculations. Here, our structural model included the enzyme, lipid bilayer, and solvent water molecules (~420,000 atoms), which realized a realistic calculation study of this biological macromolecular system.

As a result of the analysis, we observed the translocation of CO (ligand) in the BNC, from Cu_B to Fe of heme a_3, and thereby revealed that the simultaneous and dynamical sliding motion of heme a_3 occurred together with the translocation of the ligand, in a concerted manner. This displacement of heme a_3 took place within the heme plane, and the resultant stable structure was well consistent with the crystallographic structures of CcO in the presence of the CO ligand bound to Fe of heme a_3.

In the session, we discuss the detailed mechanisms to induce the sliding motion of heme a_3 and the conformational changes of a nearby helix (Helix X), including the positional shifts of -helical sites that are found within Helix X, which elucidated that the dynamical properties found in the interactions of the ligand with the enzyme

provided the driving force for the structural changes.

Thus, our analysis shows that hybrid *ab initio* QM/MM MD simulation is a powerful and essential methodology to investigate functional mechanisms of biological macromolecular systems, based on their dynamical 3D and electronic structures. In the session, other biological applications are also discussed.

References

[1] J. Kang, T. Ohta, Y. Hagiwara, K. Nishikawa, T. Yamamoto, H. Nagao, and M. Tateno, *J. Phys. Cond. Matt.*, **21** (2009) 064235.

[2] Y. Hagiwara, M. J. Field, O. Nureki, and Masaru Tateno, *J. Am. Chem. Soc.*, **132** (2010), 2751.

[3] J. Kang, H. Kino, and M. Tateno, *Biochim. Biophys. Acta Bioenerg.*, **1807** (2011) 1314.

[4] J. Kang, Y. Hagiwara, and M. Tateno M., *J. Biomed. Biotech.*, **2012** (2012), 236157.

[5] J. Kang, H. Kino, M. J. Field, and M. Tateno, *J. Phys. Soc. Jpn.*, **86** (2017), 044801.

A37: Experimental determination of the electronic structure of CH$_3$NH$_3$PbI$_3$ hybrid organic-inorganic perovskite

M. Lee[1], A. Barragán[1], M.N. Nair[1,2], V. Jacques[1], D. Le Bolloc'h[1], P. Fertey[2], K. Jemli[3], F. Lédée[3], G. Trippé-Allard[3], E. Deleporte[3], A. Taleb-Ibrahimi[2], and A. Tejeda[1]

[1]Laboratoire de Physique des Solides, CNRS, U. Paris-Sud, U. Paris-Saclay, Bat. 510, 91405 Orsay, France

Email: antonio.tejeda@u-psud.fr, web site: https://www.equipes.lps.u-psud.fr/tejeda/

[2]Synchrotron SOLEIL, Saint-Aubin, 91192 Gif-sur-Yvette,

[3]Laboratoire Aimé Cotton, ENS Cachan, CNRS, U. Paris-Sud, U. Paris-Saclay, Bat. 505, 91405 Orsay, France

Organic-inorganic hybrid perovskites are promising absorber materials for low-cost photovoltaic solar cells or optoelectronic devices [1-5]. Among these perovskites, methylammonium triiodideplumbate (CH$_3$NH$_3$PbI$_3$, MAPbI$_3$ or MAPI) exhibits currently the highest efficiency. Here we have analyzed the structural transition in MAPI by X-ray diffraction at the β phase and we have correlated it to its electronic properties. Despite all the extensive work on hybrid organic-inorganic halide perovskites, their experimental band structure measured with k-resolution has remained elusive. Such an experimental determination is a necessary requirement for an accurate theoretical description and understanding of the system. The impact of the structural phase transitions on the band structure in the operation temperature range of solar cells needed also to be elucidated. Herein, we present the experimental determination of the band structure of MAPI with k resolution by angle-resolved photoemission at 170 K [6].

Our results show that the spectral weight is strongly affected by the cubic symmetry although traces of the tetragonal band structure are appreciated.

Some deviations with respect to theoretical calculations are observed, which may help to reach a more precise description of this paradigmatic system of the hybrid perovskite family. The project leading to this application has received funding from the European Union's Horizon 2020 research and innovation programme under grant agreement No 687008 (GOTSolar).

References

[1] S.D. Stranks and H.J. Snaith, Nature Nanotech 10, 391 (2015).

[2] M. Grätzel, Nature Materials 13, 838 (2014).

[3] J. Even et al., J. Phys. Chem. C 119, 10161 (2015).

[4] Y. Wei et al., J. Phys. D: Appl. Phys. 46, 135105 (2013).

[5] H. Diab et al., J. Phys. Chem. Lett. 7, 5093 (2016).

[6] M. Lee et al., (submitted).

B01: A novel exchange spring magnet with an insulating nano-sized soft magnetic oxide exchange-coupled with micron-sized hard magnetic nitride

N. Imaoka[1,2]

[1]*National Institute of Advanced Industrial Science and Technology (AIST), Aichi, Japan*

Email:n-imaoka@aist.go.jp, web site: http://www.aist.go.jp/

[2]*Asahi Kasei Corporation, Shizuoka, Japan*

A novel high-electrical-resistance composite magnet [1-3] was fabricated by compacting or consolidating micron-sized ferromagnetic $Sm_2Fe_{17}N_3$ powder particles [4] coated with a continuous nano-sized soft magnetic ferrite layer, which suppresses inter-grain conductivity but sustains magnetic exchange interactions among grains (see Fig.1(A)-(C)). $Sm_2Fe_{17}N_3$ powder particles with a size of 2 μm were coated with an "iron ferrite" layer having a grain size of ~10 nm using ferrite plating, an aqueous process [3]. The samples were compacted at < 1 GPa to form a ferrite/$Sm_2Fe_{17}N_3$ composite magnet followed by consolidating to 92–94 vol% using the explosive consolidation (EC) technique. Coercivity and rectangularity of the compacting composite magnet decreased slightly, by 2.0 % and 1.4 %, respectively, as compared to those of the $Sm_2Fe_{17}N_3$ powder compact. The fully dense ferrite/$Sm_2Fe_{17}N_3$ magnet exhibited a resistivity of ~4000 μΩ cm, which was ten times higher than that of a fully dense $Sm_2Fe_{17}N_3$ magnet. Thus, the soft magnetic ferrite layer in our composite magnet retains magnetic exchange coupling among ferromagnetic $Sm_2Fe_{17}N_3$ grains, simultaneously suppressing inter-grain electrical coupling to increase resistivity. This decreases eddy current loss and improves the high-frequency characteristics

of composite magnets. Therefore, our composites are good candidates for magnets that are operated at high frequencies for advanced applications, such as electrical vehicles magnets. Moreover, the occurrence of exchange-coupling in the ferrite/$Sm_2Fe_{17}N_3$ composites was confirmed by recoil permeability estimation, microstructure analysis (Fig.1(D)), and calculation of the reduction in remanence due to the introduction of the ferrite layer in $Sm_2Fe_{17}N_3$ magnets [2]. Finally, we discuss methods for consolidating micron-sized $Sm_2Fe_{17}N_3$ powders while maintaining their high coercivity, on the basis of our study results and the soft magnetic behavior [5] of thermodynamically unstable nanostructures on the surface of $Sm_2Fe_{17}N_3$ powders.
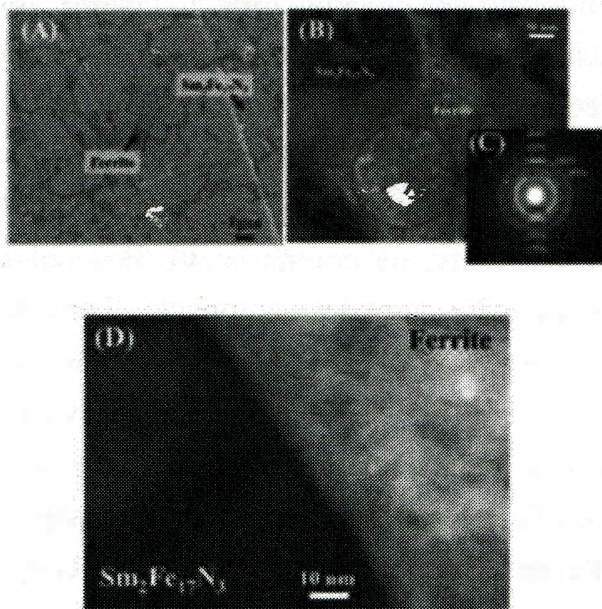
Fig1. (A) SEM image and (B) TEM image of ferrite/$Sm_2Fe_{17}N_3$ EC magnets and (C) electron diffraction pattern for the circled area in (B). The ferrite (black boundaries) layer almost surrounds the entire surface of the $Sm_2Fe_{17}N_3$ (gray grains) powders as shown in (A). Miller indices indicate the cubic spinel structure. (D) TEM image of the interface between $Sm_2Fe_{17}N_3$ main phase and ferrite boundary phase in ferrite/$Sm_2Fe_{17}N_3$ EC magnets. There is no phase between the main phase and the boundary phase.

References

[1] N. Imaoka, Y. Koyama, T. Nakao, S. Nakaoka, T. Yamaguchi, E. Kakimoto, M. Tada, T. Nakagawa and
M. Abe, *J. Appl. Phys.* **103**, 07E129 (2008).
[2] N. Imaoka, E. Kakimoto, K. Takagi, K. Ozaki, M. Tada, T. Nakagawa and M. Abe, *AIP advances* **6**, 056022 (2016).
[3] N. Imaoka, M. Abe, T. Nakagawa and M. Tada, *European patent application* 2 228 808 B1 (4 January 2017).
[4] T. Iriyama, K. Kobayashi, N. Imaoka, T. Fukuda, H. Kato and Y. Nakagawa, *IEEE Trans. Magn.* **28**, 2326 (1992).
[5] N. Imaoka, K. Takagi, K. Ozaki, T. Iriyama and H. Kato, *J. Phys. Conf. Ser.* accepted (2017).

B02: Tuning hysteresis in metamagnetic shape memory alloys for refrigeration applications

Daniel Salazar Jaramillo

BCMaterials, Bizkaia Science & Technology Park, Derio 48160, Spain
Email:daniel.salazar@bcmaterials.net, web site:

One of the challenges of modern societies consists in to increase the equipment energy efficiency, with the aim of reducing the energy consumption. In this sense, the magnetic refrigeration, a solid-state technology based in the magnetocaloric effect (MCE), attracts large interest because it is considered a feasible substitute of the conventional air-compressed refrigerant systems due to, among other advantages, its superior efficiency (of up to 60% of Carnot's cycle). However, to be commercially engaging, this technology still needs cheap materials with enhanced refrigerant properties. Among the studied materials, metamagnetic shape memory alloys-MSMA (mainly, Heusler-type Ni-Mn-based alloys) represent a new kind of multifunctional (smart) materials which develop exotic properties as magneto-deformation effect, giant magnetoresistance and inverse magnetocaloric effect as a consequence of a magneto-structural transformation [1]. These technologically relevant properties are strongly related to magnetic and structural instabilities and are due to a decrease of ferromagnetism induced by martensitic transformation (MT).

Recent results of the magnetic properties and the direct measurement of the MCE obtained in MSMA are presented in this work. In order to have a wide view

of the mechanisms that affect the MCE response, several NiMnIn-based MSMA were studied in bulk and in ribbon shape, analysing the magnetocaloric response associated to the MT and the magnetic phase transition in the austenite phase by estimating the magnetic entropy change, ΔS_M, from magnetization measurements, and measuring directly the adiabatic temperature change, ΔT_{ad}. [2].

References

[1] P. Álvarez-Alonso, C.O. Aguilar-Ortiz, J.P. Camarillo, D. Salazar, H. Flores-Zuñiga,, V.A. Chernenko, App. Phys. Lett. **109** (2016) 212402.

[2] P. Álvarez-Alonso, J. López-García, G. Daniel-Perez, D. Salazar, P. Lázpita, J.P. Camarillo, H. Flores-Zuñiga, D. Rios-Jara, J.L. Sánchez-Llamazares, and V.A. Chernenko, Key Eng. Mater. **644** (2015) 215.

B03: Abnormal growth of Goss grains in grain oriented silicon steel driven by distribution characteristics of VC nano-particles

I. Petryshynets, F. Kovac, M. Sebek, V. Puchy, L. Falat
Institute of Materials Research, Slovak Academy of Sciences, Watsonova 47, 04001, Košice, Slovakia
Email:ipetryshynets@saske.sk

Despite of a long history of continuously improved magnetic properties, the further development of grain oriented (GO) electrical steel is still an exciting field for industrial and joint fundamental research. The grain oriented steels with 3% Si are an excellent soft magnetic materials produced today and mainly used as core materials of transformers. The final properties of these steels such as anisotropy of magnetic field and low power losses are provided by strong crystallographic orientation {110}<001> in the sheet plane (Goss texture). Strong Goss texture is a result of technological rout proposed in 1934 by Goss [1], which has been not significantly changed from those times. In order to obtain the Goss texture, the inhibitors such as MnS, AlN and MnS+AlN play an important role in controlling the grain growth of the first and the secondary recrystallizations that take place during the long time final box annealing.

In the present work we have used the novel approach for the abnormal growth of Goss grains. This approach employs the system of VC nano-precipitates in the combination with the dynamic continuous annealing during the secondary recrystallization. The laboratory slab of grain oriented steel was subjected to hot rolling with reduction of the thickness of sheet to 2.2 mm, and subsequently, the influence of coiling temperatures on the distribution characteristics of VC particles was analyzed by TEM. The obtained results have confirmed the presence of VC nanoparticles with a typical size of $20 - 30$ nm located preferentially in the vicinity of grain boundaries. Later, the hot rolled strips were subjected to the cold rolling with the reduction $\varepsilon \sim 84\%$, followed by primary recrystallization, temper rolling and final annealing in dynamic conditions in the temperature range $850^{\circ}C$ - $1150^{\circ}C$. This procedure led to evolution of the sufficiently strong {110}<001> Goss texture, which is comparable to that obtained in the conventionally treated GO steels. Moreover, the steels treated by this new method showed the comparable magnetic properties as the materials passed the conventional long – time heat treatment (e.g. the coercivity of our steels reached $\sim$ 11 A/m). The proposed approach allowed to reach the equal material's quality at significantly shortened time in comparison to the conventional process of GO steel fabrication.

Reference

[1] Goss, N.P. Electrical sheet and apparatus for its manufacture and test. *U.S. Patent 1*, 965, 559, (1934).

B04: High frequency magnetoimpedance and magnetoelastic resonance in magnetic microwires for biological and tagging applications

P. Marín, A. Hernando

Instituto de Magnetismo Aplicado. Departamento de Física de Materiales (Universidad Complutense de Madrid) Nacional VI Km 22.5 28230 (Las Rozas) Madrid (SPAIN)

Email:mpmarin@fis.ucm.es, web site: http://www.ucm.es/ima

The development of wireless sensors and biosensors is a topic of great current interest. Amorphous magnetoelastic microwires are perfect candidates to be used as sensing elements based on two important properties ie.: magnetoelastic resonance and high frequency giant magnetoimpedance. It was observed that such microwires present the key feature of performing magnetoelastic resonance, at the KHz range of frequency, in the absence of applied field. This fact, in addition to their small size, gives the microwires unique advantages over the widespreaded ribbons, currently in use as magnetoelastic sensors. The frequency, amplitude, and damping of the vibration gives information of the sensor environment. On the other side the microwire reflectivity in the microwaves range can be modulated by means of magnetoimpedance effect. The maximum induced electric current, as well as the maximum ac modulation, occurs for frequencies determined by the microwire length. The modulation also varies as a function of the dc-applied field and applied stress.

References

[1] P. Marín, D. Cortina, and A. Hernando. *IEEE Trans. on Magn* **44(11)**, 3939 (2008)

[2] A. Hernando, V. Lopez-Dominguez, E. Ricciardi, K. Osiak, P. Marin, *IEEE Trans. on Ant. And Propagations* **64 (3)**, 1112 (2016)

[3] C. Herrero-Gómez, A.M. Aragón, M. Hernando-Rydings, P. Marín, A. Hernando, *Applied Physics Letters* **105**, 092505 (2014)

B05: The behaviour of soft magnetic composite cores for Electrical Machines both in standard environmental conditions and in cryogenics

Fabrizio Marignetti

Department of Electrical and Information Engineering, University of Cassino and South Lazio, Cassino, ITALY

email: marignetti@unicas.it, web site: www.ledasolutions.it

Modern electromagnetic and electromechanical devices have complex flux paths, often developing in three dimensions. Moreover, the supply

frequency of electrical machines and transformers is increasing in order to reduce their dimensions. For these applications, the use of soft magnetic composite materials is advantageous. Soft magnetic composite cores may help reducing the eddy current loss in electric machines with complex MMF content. However, their performances must be carefully modelled and evaluated.

A comparative study is made at room temperature and at cryogenic temperature. The torque density of axial flux machines with different soft magnetic composite cores is compared. Also, a linear tubular machine was specially built to assess the behavior of soft magnetic composite cores at cryogenic temperature.

The increase of core loss of soft magnetic composite materials at cryogenic temperatures is limited as shown in Fig.1. Therefore they are suitable for use in cryogenic machines, like the HTS cold core transformers.

Although many magnetic materials are used in key fields of applications, e.g. in special machines, superconducting machines, magnetic shields, particle accelerators in fusion energy, MRI magnets and other, a database of their characteristics is missing, as well as their modelling at a microscopic level. This presentation represents the starting point for a systematic study on the subject from the point of view of an application designer.
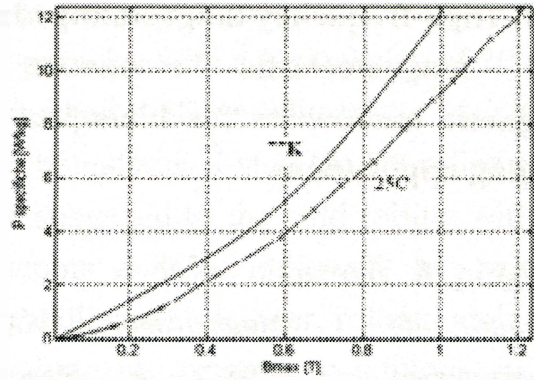
Fig1. Comparison of core loss density of the ATOMET-EM1 composite at 50Hz, at temperatures of 25C and 77K.

References

[1] F. Marignetti, "On Liquid-Nitrogen-Cooled Copper-Wound Machines With Soft Magnetic Composite Core," in *IEEE Transactions on Industry Applications*, vol. 46, no. 3, pp. 984-992, May-june 2010.

[2] F. Marignetti, V. D. Colli and S. Carbone, "Comparison of Axial Flux PM Synchronous Machines With Different Rotor Back Cores," in *IEEE Transactions on Magnetics*, vol. 46, no. 2, pp. 598-601, Feb. 2010.

[3] Mutze, A., Jack, A.G., Mecrow, B.C.: "Alternate designs of low cost brushless-DC motors using soft magnetic composites". International Conference on Electrical Machines (ICEM). Brugge, August 2002

[4] Jérôme Cros and Philippe Viarouge, "New Structures of Polyphase Claw-Pole Machines" IEEE Trans. on Industry Applications, vol. 40, no. 1, January/February 2004

B06: Single dopants as stepping stones for inter-band tunneling in silicon tunnel diodes

Manoharan Muruganathan[1*], Daniel Moraru[2], Michiharu Tabe[2], Hiroshi Mizuta[1]

[1]School of Materials Science, Japan Advanced Institute of Science and Technology, Japan

[2]Research Institute of Electronics, Shizuoka University, Japan

*Email: mano@jaist.ac.jp

As the Tunnel Field Effect Transistor (TFET) overcomes the subthreshold slope thermal limitation of MOSFETs, they are a potential successor of MOSFETs [1]. Moreover, silicon-based TFETs are the most attractive because of the well-established silicon technology. However, band-to-band tunneling (BTBT) in Si requires assistance of phonons for momentum conservation due to its indirect bandgap characteristics. Recently, isoelectronic traps (IETs) showed the increase in the inter-band tunneling current without phonon assistance [2]. In this research work, we report the role of co-dopants at the p-to-n interface of the tunnel diode in the tunneling current enhancement without any phonon assistance. These results are based on the first-principles simulations in comparison with our experimental results for nano-pn tunnel diodes [3].

To carry out realistic device simulation, atomistic structure of the simulated device is constructed with p- and n-type regions with the doping concentration of 5×10^{19} cm^{-3} (Fig. 1(a)). In the thin central intrinsic Si region, single P and B dopants are placed. The uniform bulk doping in the regions away from the depletion region was realized by using the atomic compensation technique [4-5]. These devices exhibit typical Esaki-diode negative differential conductance (NDC) behaviors. Moreover, we noticed a remarkable tunnelling current increase for (100) Si channel with a P-B pair placed 1.3 nm apart as compared to no discrete dopants in the depletion region (Fig. 1(b)). When the single dopants were placed at optimized distance from the uniformly doped bulk regions then energy states are created in the depletion region of the tunnel diode. This leads to an increase in the inter-band tunnelling current. These results illustrate the impact of individual dopants in the depletion region and provide pathways to increase the inter-band tunnelling in nano-pn tunnel diodes. Detailed discussion of nano-pn diode with different crystal orientation, dopant positions and I-V characteristics will be given in the conference presentation.

(a)
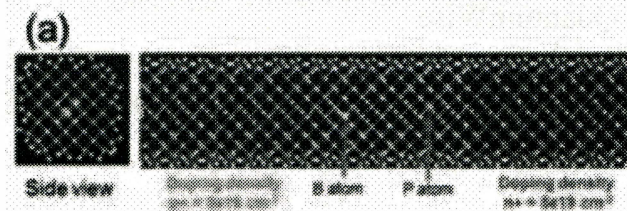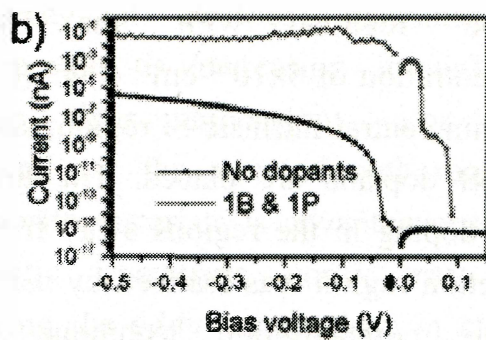
Fig. 1 (a) Atomistic structure of simulated pn diode configuration with co-dopants at the centre of the channel (right) and side view of the nano-pn diode. (b) I-V characteristics of nano-pn diode with and with-out co-dopants at the device central region.

References

[1] A. M. Ionescu et.al., Nature 479.7373 (2011): 329-337.

[2] T. Mori et al., Appl. Phys. Lett. 106, 083501 (2015).

[3] M. Tabe et.al., Applied Physics Letters 108.9 (2016): 093502.

[4] M. Brandbyge et.al., Physical Review B 65.16 (2002): 165401. [5] Atomistix ToolKit QuantumWise

B07: Multi-scaled Simulations on Molecular-based Flash Memory

Vihar P. Georgiev[1], Laia Vila-Nadal[2], Leroy Cronin[2] and Asen Asenov[1]

[1]*Device Modelling Group, School of Engineering, University of Glasgow, Glasgow, G12 8LT, UK.*

Email: vihar.georgiev@glasgow.ac.uk, web site: http://web.eng.gla.ac.uk/groups/devmod/

[2]*Scholl of Chemistry and WestCHEM, University of Glasgow, Glasgow, G12 8QQ, UK*

Recently interest in electronic, magnetic and optical materials based on inorganic, organic, hybrid and nano-materials has increased significantly. Such new materials have a potential to bring the technology and the research into the more than Moore and beyond Moore era. In this work, we present an exciting research in the field of molecular electronics based on hybrid nano-materials. The main aim is to establish a link between the variability, scalability and reliability of a non-volatile flash memory cell, in which the charge-storing components constitute of a layer of polyoxometalates molecular clusters (POMs).

Moreover, modelling and simulations of flash cell transistors with a POM-based floating gate play a pivotal role for the sustainability of any further experiment effort in this direction [1]. For the purpose of this study, we develop a fast, accurate and reliable simulation tool based on detailed physical models spanning from quantum mechanics all the way up to continuous physics and various devices

architectures - see Fig. 1. The quantum chemical calculations are based on the Kohn-Sham approach to density functional theory (DFT). The 3D numerical simulations of the full flash cell deploy the drift-diffusion transport formalism and include density-gradient quantum-corrections. The motivation for using this plethora of modelling techniques is the complexity of the system. Accurate description of the molecules requires quantum chemical calculations on an atomic level, while the description of the current flow through the flash cell demands continuous modelling. Fig. 2 reveals the 3D electrostatic potential in the oxide and the substrate obtained from our numerical simulations. Fig. 2 also presents the position of molecules in the oxide and of random dopants in the source and the drain of the device [2].

Our ultimate goal is to provide an informed guidance for both chemical synthesis and device design and fabrication thanks to the knowledge derived from device modelling and simulation and from computational chemistry calculations.
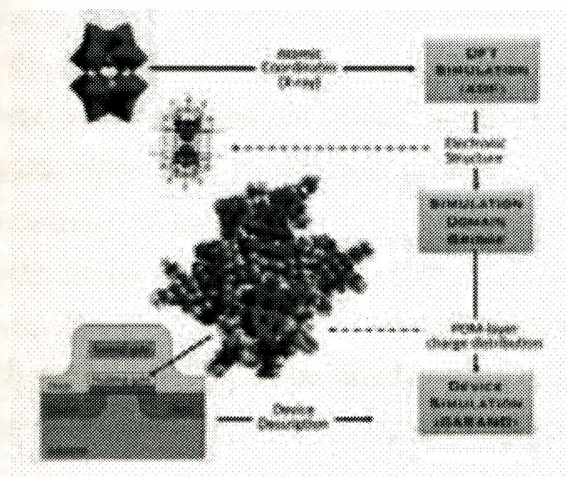
Figure 1. Simplified block diagram of the simulation methodology, linking density functional theory (DFT) and continuous flash-cell modelling.
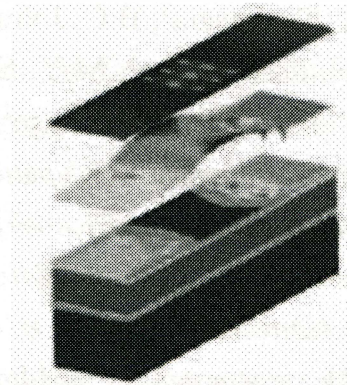
Figure 2. 3D electrostatic potential in the oxide and the substrate. Fingerprint of the 3x3 POMs in the gate and the random dopant in the source and the drain is clearly visible.

References

[1] C. Busche, L. Vila-Nadal, J. Yan, H. N. Miras, D. L. Long, V. P. Georgiev, et al., "Design and fabrication of memory devices based on nanoscale polyoxometalate clusters," Nature, vol. 515, pp. 545-549, Nov 27 2014.

[2] V. P. Georgiev, S. Markov, L. Vila-Nadal, C. Busche, L. Cronin, and A. Asenov, "Optimization and Evaluation of Variabilit in the Programming Window of a Flash Cell With Molecular Metal-Oxide Storage," IEEE Transactions on Electron Devices, vol. 61, pp. 2019-2026, Jun 2014.

B08: Quantum tunneling microscope of an atomic scale device in silicon

B. Voisin[1*], J. Salfi[1], J. Bocquel[1], M. Usman[2], A. Tankasala[3], B.C. Johnson[2], J.C. McCallum[2], R. Rahman[3], M.Y. Simmons[1], L.C.L. Hollenberg[2] and S. Rogge[1]

[1]Centre for Quantum Computation and Communication Technology, School of Physics, The University of New South Wales, Sydney, NSW 2052, Australia

[2]Centre for Quantum Computation and Communication Technology, School of Physics, University of Melbourne, Parkville, VIC 3010, Australia

[3]Purdue University, West Lafayette, Indiana 47906, USA

Email:benoit.voisin@unsw.edu.au

Simulating many-body quantum physics represents a formidable challenge for engineered spin systems in the solid-state that will help our understanding of nature. This requires the ability to engineer interactions between sites, local measurements of their quantum states and preferably dynamic control of the Hamiltonian [1]. Such an experimental platform has been sought after, as instance in the cold-atom community [2], but has not yet been established. Here we show the possibility of combining those capabilities by probing and manipulating the quantum states of the active element of a nanoelectronic device.

Silicon enables placing single donors with atomic precision [3], imaging their wavefunction [4, 5] using a scanning tunneling microscope (STM), and their spin interactions can be tuned in the quantum regime [6]. We have designed an atomically precise device using STM lithography (Fig.1a) and probed its wavefunction in real space in the Coulomb blockade regime within the same quantum tunneling microscope [7]. We address this device with atomically precise electrodes made of a combination of top-down and bottom-up approaches to tune the chemical potential and the occupation number in-situ, and to ensure full control on the tunnel rates (Fig.1b).

Enabling dynamic local and global measurements of atomic precision devices will benefit to a broad range of quantum systems, from the understanding of qubit coupling in quantum computation to topological properties of large scale complex arrays of spins.
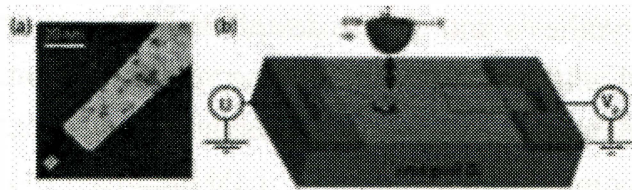
Fig1. (a) Example of STM lithography. (b) A STM tip measures in real space the spatial charge distribution of an atomically precise device.

References

[1] K. Kantian et al., Phys Rev Lett. **115**. 165301(2015).

[2] P. Jurcevic *et al.*, Nature **511**, 202-205 (2014).

[3] M. Fuechsle *et al.*, Nature Nanotechnology **7**, 242-246 (2012).

[4] J. Salfi *et al.*, Nature Materials **13**, 605-610 (2014).

[5] M. Usman *et al.*, Nature Nanotechnology **11**, 763-768 (2016).

[6] J. Salfi *et al.*, Nature Communications **7**, 11342 (2016)

[7] B. Voisin *et al.*, in prep (2017).

B09: Heavy-hole states in Ge hut wires

Hannes Watzinger[1], Christoph Kloeffel[2], Lada Vukušić[1], Marta D. Rossell[3,4], Violetta Sessi[5], **Josip Kukučka**[1], Raimund Kirchschlager[1], Elisabeth Lausecker[1], Alisha Truhlar[1], Martin Glaser[6], Friedrich Schäffler[6], Armando Rastelli[6], Andreas Fuhrer[4], Daniel Loss[2], Georgios Katsaros[1]

[1]Institute of Science and Technology Austria, Am Campus 1, 3400 Klosterneuburg, Austria

[2]Department of Physics, University of Basel, Klingelbergstr. 82, 4056 Basel, Switzerland

[3]Electron Microscopy Center, Empa, Swiss Federal Laboratories for Materials Science and Technology, Überlandstrasse 129, 8600 Dübendorf, Switzerland

[4]IBM Research Zürich, CH-8803 Rüschlikon, Switzerland

[5]Chair for Nanoelectronic Materials, Technical University Dresden, 01062 Dresden, Germany

[6]Institute of Semiconductor and Solid State Physics, Johannes Kepler University, Altenbergestr. 69, 4040 Linz, Austria

e-mail: hannes.watzinger@ist.ac.at

Holes confined in quantum dots are promising candidates for the realization of spin qubits due to the combination of a strong spin orbit coupling and a weak hyperfine interaction. In our group we study holes which are confined in SiGe self-assembled nanostructures [1], realized by direct growth of Ge on Si substrates via the Stranski-Krastanow growth mode. Here we focus on transport measurements through so called Ge hut wires [2], nanostructures with well-defined surfaces and growth orientations, with heights of about 2 nm and lengths exceeding one micrometer.

The g-factors, obtained from magnetotransport spectroscopy, show a high in-plane and out-of-plane anisotropy of up to 18. Numerical simulations which are in very good agreement with our experimental findings reveal a heavy-hole character of the low energy states [3]; such is important for achieving long dephasing times [4].

Keywords: SiGe, quantum dot, heavy hole, hole g-factor

References

[1] Katsaros, G. et al. Nature Nanotechnology **5**, 458-464 (2010);

Katsaros, G. et al. Phys. Rev. Lett. **107**, 246601 (2011);

Ares, N. et. al. Phys. Rev. Lett. **110**, 046602 (2013)

[2] Zhang, J. J. et al. Phys. Rev. Lett. **109**, 085502 (2012);

Watzinger, H. et al. APL Mater. **2**, 076102 (2014)

[3] Watzinger, H. et al. Nano Letters **16**, 6879-6885 (2016)

[4] Fischer, J. et al. PRB **78**, 155329 (2008)

B10: Highly robust and low frictional double network ion gel

Takaya Sato[1], Hiroyuki Arafune[1], Toshio Kamijo, Takashi Morinaga

[1]*Department of Creative Technology, National Institute of Technology, Tsuruoka College, Tsuruoka, Yamagata 997-8511, JAPAN*
Email:takayasa@tsuruoka-nct.ac.jp, web site: http://ts.tsuruoka-nct.ac.jp/en/category/aboutus

Gels are familiar material used as a soft contact lens, a water absorbing material and food. It can be defined that they are wet and soft materials that have the three dimensional polymer reticulation structure containing a large amount of solvent molecule. Physical characteristics of the gel such as a physical strength, the elongation rate, the coefficient of liquid absorption and the sol-gel transition temperature can be controlled by the molecular design of the polymer constituting the reticulation. However, most of the synthetic gels suffered from a lack of mechanical strength and a robustness, presently the application of gels were hardly put the industrial field.

However, a hydrogels made by a double network (DN) technique have excellent mechanical properties such as a high strength and a super toughness. Figure 1 showed the concept of DN-gel. The first network has hard and brittle feature by high cross-linking density and the second network has soft and high elastic feature by low cross-linking and high molecular weight. The DN-gel structure was that the second soft reticulation entangled to the first rigid framework prepared by two step sequential free radical polymerization process. This double network composite has high strength and high elasticity features despite it containing the solvent of 90% or more.
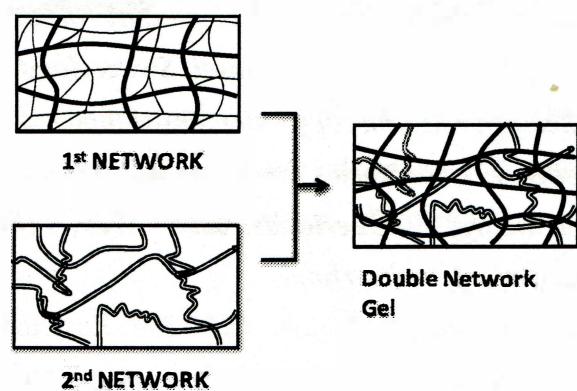
Fig. 1. Schematic illustration of the formation of Double network gel (DN-gel)

In some cases, because the DN-gel also exhibits low friction resistance, it attracts attention as a next generation's energy conservation material [1]. However, one big issue of the hydrogel using in the industrial fields is the instability of physical properties due to the evaporation of water. We attempt to prepare the newly DN-ionic gel (DN-ion gel) containing non-volatile ionic liquid as a swelling agent. The first network has constructed by using the ionic liquid type polymer that has high affinity for the ionic liquid used as a swelling agent. It was prepared from ionic liquid type monomer, *N*,*N*-diethyl-*N*-methyl-*N*-(2-ethylmethacrylate) ammonium bis(trifluoromethanesulfonyl)imide (DEMM-TFSI). In order to make the second network, we used a poly(methylmethacrylate) network with relatively high molecular weight.

Our tough gel not only showed the highest compression strength among previously reported gel materials including ionic liquids, but also indicated an extremely low coefficient of dynamic friction during 1000 times of the friction examination in vacuum and high temperature condition. These results would show high potential as a low friction material of the DN-ion gel [2].

References

[1] J. P. Gong, Y. Katsuyama, T. Kurokawa, Y. Osada, *Adv. Mater.*, **2003**, *14*, 1155-1158.

[2] H. Arafune, S. Honma, T. Morinaga, T. Kamijo, M. Miura, H. Furukawa, T. Sato, Adv. Mat. Interfaces, in press.

B11: Recent advances in unusual optical coatings for flexible optoelectronic device applications

Young Min Song[1]

[1]*School of Electrical Engineering and Computer Science, Gwangju Institute of Science and Technology, Gwangju 61005, Korea Email:ymsong@gist.ac.kr, web site: http://www.gist-foel.net*

Optical coatings on the basis of thin-film interference have been widely used as key elements in various optical components and optoelectronic devices. For example, anti-reflection or high-reflection is observed under conditions of constructive or destructive interference achieved by multi-layer stacks of dielectric materials. On the other hand, unusual optical coatings in terms of their geometry and functions have recently been studied for new type of optical devices. In this presentation, we show three different types of optical coatings, i.e., 1) ultra-thin films with highly absorbent media for coloration[1], 2) flexible and transparent electrodes based on epoxy-copper-ITO[2], and 3) tapered nanostructures for super-antireflection[3].
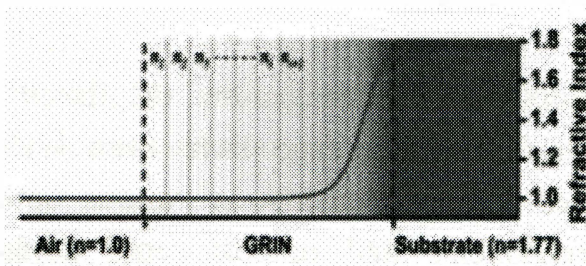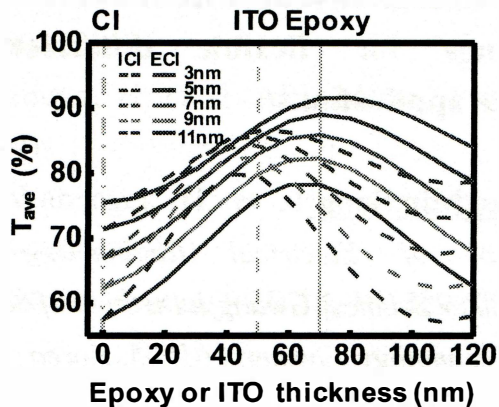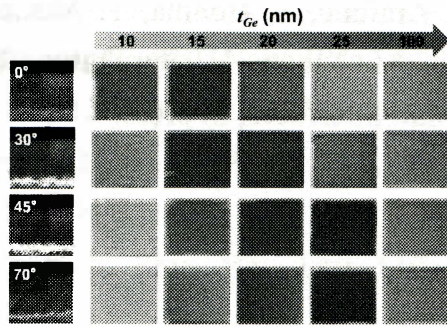
Fig1. (left) Representative images for ultra-thin films with highly absorbent media, (center) Average transmittance curves for transparent electrodes with epoxy-copper-ITO (solid curve) and with ITO-copper-ITO (dashed curve), (right) Effective refractive index profile for broadband and omnidirectional antireflection

References

[1] Y. J. Yoo, J. H. Lim, G. J. Lee, K.-I. Jang, and Y. M. Song, *Nanoscale* **9**, 2986 (2017)

[2] J.-K. Song, D. H. Son, J. M. Kim, Y. J. Yoo, G. J. Lee, L. Wang, M. K. Choi, J. W. Yang, M. C. Lee, K. S. Do, J. H. Koo, N. Lu, J. H. Kim, T. H. Hyeon, Y. M. Song, and D.-H. Kim, *Adv. Funct. Mater.* **27**, 1605286 (2017)

[3] K. W. Choi, Y. W. Yoon, J. H. Jung, C. W. Ahn, G. J. Lee, Y. M .Song, M. J. Ko, H. S. Lee, B. S. Kim, and I.-S. Kang, *Adv. Opt. Mater.* **5**, 1600616 (2017)

B12: Characterization of Wavelength Effect on Photovoltaic Property of poly-Si Solar Cell by Using Photoconductive Atomic Force Microscopy(PC-AFM)

Jinhee Heo

[1]*Advanced Characterization & Analysis Research Group, Korea Institute of Materials Science (KIMS), Changwon 641-010, Republic of Korea*

Email:pidellis@kims.re.kr, web site: http://www.kims.re.kr

We have investigated the effect of light intensity and wavelength of the solar cell device by using the photoconductive atomic force microscopy(PC-AFM). The POCl3 diffusion doping process was used to produce a p-n junction solar cell device based on a Poly-Si wafer and the electrical properties of prepared solar cells were measured by using a solar cell simulator system. The measured open circuit voltage(Voc) is 0.59 V and the short circuit current(Isc) is 48.5 mA. Also, the values of the fill factors and efficiencies of the

devices are 0.7 and approximately 13.6%, respectively. Besides, PC-AFM, a recent noteworthy method for nano-scale characterization of photovoltaic elements, was used for direct measurements of photoelectric characteristics in local instead of large areas.[1,2] The effects of changes in the intensity and wavelength of light shone on the element on photoelectric characteristics were observed. Results gained through PC-AFM were compared with the electric/optical characteristics data gained through a solar simulator. The voltage(VPC-AFM) at which the current was 0A in the I-V characteristic curves increased sharply until $1.8mW/cm^2$, peaking and slowly falling as light intensity increased. Here, VPC-AFM at $1.8mW/cm^2$ was 0.29V, which corresponds to 59% of the average Voc value as measured with the solar simulator. Also, while light wavelength was increased from 300nm to 1100nm, the external quantum efficiency (EQE) and results from PC-AFM showed similar trends on the macro scale, but returned different results in several sections, indicating the need for detailed analysis and improvement in the future.
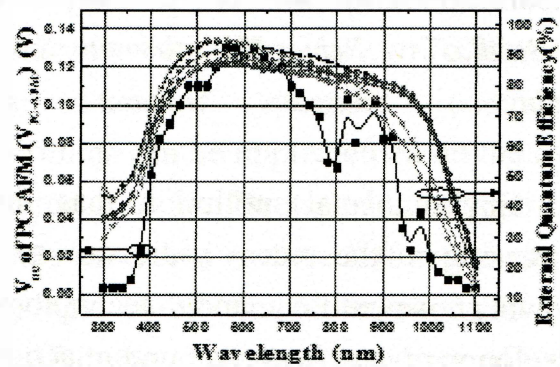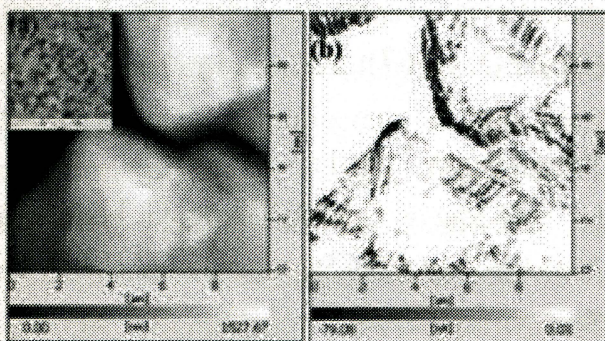
Fig1. (a) Topographic and (b) current mapping images of surface of solar cell devices which were attained by conductive- AFM. Inset in (a) shows a 150 x 150 μm scanned topography image. And external quantum efficiency (EQE) curves and VPC-AFM value with light wavelength of poly-Si solar cell devices.

References

[1] C. Groves, O. G. Reid and D. S. Ginger, Acc. Chem. Res., 43, 612 (2010)
[2] Jinhee Heo and Youngmok Rhyim, J. Korean Phys. Soc., 60, 9, 1322~1326 (2012)

B13: Organoclay nanocomposites for sustainable management of toxic waste compounds

Esperanza Pavón[1,2], Mauricio Escudey[2], Fernanda Albornoz[2], Agustín Cota[3], Francisco J. Osuna[1], María D. Alba[1],
[1]Instituto Ciencia de Materiales de Sevilla (CSIC-US). Sevilla, Spain
Email:esperanza.pavon@gmail.com
[2]Center for the Development of Nanoscience and Nanotechnology, Santiago, Chili

³*Laboratorio de Rayos X. CITIUS. Universidad de Sevilla. Av. Reina Mercedes s/n, Sevilla, Spain*

Environmental pollution has been increasing in the recent years due to the growing scientific and technological development, and hence, an urgent action is demanding to tackle it. Regarding pollution control, many efforts have been done to find an effective management of radioactive waste, heavy metals and organic pollutants using clay minerals [1]. However, the research devoted to the use of natural layered aluminosilicates foresees different drawbacks caused by inherent limitations of these materials, such as their low loading capacity, relatively small metal ion binding constants, and low selectivity. Synthetic organic-inorganic hybrid nanocomposites are advanced materials that combine the functionality of an organic molecule or polymer, with the structural properties of the inorganic component. Consequently, they are promising materials for the immobilization of organic and inorganic toxic compounds.

In this work, we analyze the remediation capabilities of a family of organoclays based on synthetic swelling high charge mica exchanged with organic molecules with variable chain length (figure 1) [2]. Their effectiveness in the adsorption of heavy metals (Pb, Hg, As), toxic ions (I⁻) and aromatic hydrocarbons is explored and compared to natural clays. The results demonstrated that these organoclays nanocomposites are better adsorbents compared to natural clays and bentonites.
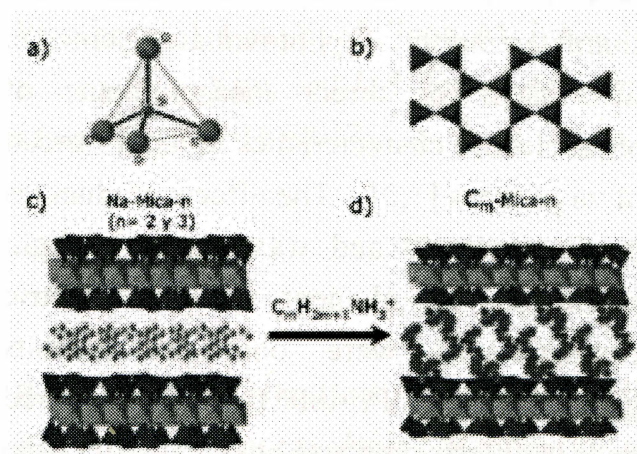
Fig1. Schematic representation of the organofuncionalization of swelling high charge mica: (a, b) clay structure unit, (c) Na-n-Mica, and, (d) organoclay nanocomposite

References
[1] F. Bergaya, B.K.G. Theng, G. Lagaly, *Handbook of Clay Science, Vol. 1* (Elsevier Science), 1 (2006)

[2] C. Pazos, M. A. Castro, M. Mar Orta, E. Pavón, J. Valencia Rios, M. D. Alba, *Langmuir* 28, 7325 (2012)

B14: Quantum Analogue Computing with Phi-Bits

Keith Runge[1], Pierre A. Deymier[1]

[1]*Materials Science and Engineering, University of Arizona, AZ, USA*

Email:krunge@email.arizona.edu,deymier@email.arizona.edu

Web site: http://www.newfos.org

Simple model systems are used to illustrate the emergence of a new science of sound that accounts not only for spectral and refractive characteristics of waves but also addresses the amplitude and phase of these waves. A harmonic crystal with side springs attached to a rigid substrate leads to an elastic wave equation that can be written in the form of the relativistic Klein-Gordon equation. [1. 2] This relativistic Klein-Gordon equation is subsequently factored into the Dirac equations whose solutions impose a restriction on the amplitude of forward and backward going waves that is reminiscent of the Pauli exclusion principle. Using forward and backward going wave amplitudes as pseudospins, we define an analogue of the quantum computing bit (qubit) for vibrational motion, the φ-bit.

Figure 1 shows prototype φ-bits produced in our laboratories. To illustrate how standard quantum computing algorithms can be implemented on the φ-bit architecture, the Deutsch-Josza algorithm will be described in three different contexts. A single φ-bit implementation of the algorithm demonstrates the power of using quantum computing analogues for these algorithms. The two φ-bit Deutsch-Josza algorithm are investigated when the φ-bits are in parallel operations. For the parallel two φ-bit algorithm, non-separability of the superposition of states of the system is demonstrated and used for achieving exponential complexity.

Fig1. Image of prototype φ-bits produced at the University of Arizona.

References

[1] P. A. Deymier, K. Runge, N. Swinteck, and K. Muralidharan, Comptes Rendus Mécanique, **343**, 700 (2015).

[2] P. A. Deymier and K. Runge, Crystals **6**, 44 (2016).

B15: Quantum Computation: From Laboratory Demonstrations to state-of-the-art Algorithms for Quantum image Processing

Abdullah M. Iliyasu[1,2]

[1]*Electrical Engineering Department, College of Engineering, Prince Sattam Bin Abdulaziz University, Al-Kharj, Kingdom of Saudi Arabia*
[2]*School of Computing, Tokyo Institute of Technology, Yokohama, Japan*
Email:a.iliyasu@psau.edu.sa

Beyond the promise of improved limits for miniaturisation, massive performance speed-up for certain tasks, new and unrivalled levels of protection in secure communication; astounding applications in information processing; and ultra-precise measurements [1], the theoretical discoveries and propitious conjectures emanating from quantum computing have positioned it as a key element in modern science. Motivated by these important potentials, a lot of effort has been devoted to the physical realisation of hardware to execute quantum computing algorithms and applications. Physical embodiments of the qubit, the information carrier on the quantum-mechanical framework, and operations to manipulate it are available from many approaches. Among these are implementations based on nuclear magnetic resonance; ion, atom and cavity electrodynamics; solid state, and superconducting systems. Other technologies being considered for realising physical quantum hardware includes those based on quantum dot and optical or photonic systems [1].

While tremendous progress has been recorded in general areas of quantum computation and quantum information processing, an open question that is only receiving attention recently is that related to the palpable uses and applications for quantum computing hardware beyond the laboratory.

In this talk, we present an overview of recent advances in quantum image processing (QIP), which is an emerging sub-discipline that is focused on extending conventional image processing tasks and operations to the quantum computing framework. It is primarily devoted to utilising quantum computing technologies to capture, manipulate, and recover quantum images in different formats and for different purposes [2]. Due to some of the astounding properties inherent to quantum computation, notably entanglement and parallelism, it is anticipated that QIP technologies will offer capabilities and performances that are, as yet, unrivalled by their traditional equivalents. These improvements could be in terms of computing speed, guaranteed security, minimal storage requirements, etc. [2,3]. The talk will dwell on the innovative representations proposed to encode images based on the quantum mechanical composition of the information carrier, the operations realisable on these representations, as well as likely protocols

and algorithms for their applications [2]. In particular, we focus on recent progresses on QIP-based security technologies including quantum watermarking, quantum image encryption, and quantum image steganography. This review is aimed at providing the audience with a succinct, yet adequate compendium of the progresses made in the QIP sub-area [1-3], which is intended to stimulate further interest aimed at the pursuit of more advanced algorithms and experimental validations for available technologies and extensions to other domains [2,3].

References

[1] A. M. Iliyasu, *Entropy* **15**(8), 2874-2974; doi:10.3390/e15082874 (2013)

[2] F. Yan, A. M. Iliyasu and P. Q. Le, *International Journal of Quantum Information* **15**(3), 1730001 doi:10.1142/S0219749917300017 (2017)

[3] F. Yan, A. M. Iliyasu and P. Q. Le, *Quantum Information Processing* **15**(1), doi:10.1007/s11128-015-1195-6 (2016).

B16: The foundation of Biothermology from the point of view of nano/microscale thermophysical properties of biopolymers

Noriko Hiroi[1], Takayuki Nakamura[1], Takaya Saito[1], Akira Funahashi[1]

[1]*Department of Biosciences and Informatics, Keio University, Yokohama, Kanagawa, Japan Email:hiroi@bio.keio.ac.jp, web site: http://fun.bio.keio.ac.jp/~hiroi*

Biothermology has started during these years based on technological development for detecting temperature of intracellular sub-compartments, which is thermology to be adapted for the phenomena of nano- to sub-micrometer scale. Those technologies and techniques stand on various different principles; on one hand, the fact may be a supportive evidence for the arguments about existence of temperature distribution in intracellular environment. On the other hand, we need to consider if all the detected values mean the same phenomenon.

In this talk, I will introduce the various detection methods of intracellular temperature with the principles behind the methods including our research results [1]. At the same time, I will indicate the requirements to perform successful experiments additionally to the principles detecting temperature. For example, proper maintenance of cell culturing and image processing are both necessary when we aim to detect intracellular temperature of living cells, not only the correct knowledge of physics.

Finally, the desired technological development for live thermal diffusion imaging will be exhibited at the end of the talk [2].

Key Principle	Ref
Miniaturization of detector	Biophys. J. 106 (2014) 2458–2464, Cell Res. 21 (2011) 1517–1519, Appl. Phys. Lett. 102 (2013) 193705, Biophys. J. 92 (2007) L46–8
Molecular conformation change dependent on temperature	J. Am. Chem. Soc. 131 (2009) 2766–2767, Nat. Commun. 3 (2012) 705, Nat. Methods 10 (2013) 1232–1238
Characteristics of semiconductor	ACS Nano 5 (2011) 5067–5071, Nano Lett. 10 (2010) 5109–5115, Sci. Rep. 6 (2016) 22071, Biochem. Biophys. Res. Commun. 302 (2003) 496–501
Characteristics of photon dependent on thermal energy	OPTICS EXPRESS Vol. 17, No. 5 (2009) 3298, Nano Lett. 2012, 12, 2107–2111

Table 1. Examples of various detection methods of intracellular temperature of living cells.

References

[1] R Tanimoto, T Hiraiwa, Y Nakai, Y Shindo, K Oka, N Hiroi, A Funahashi. "Detection of temperature difference in neuronal cells." *Scientific reports* **6** (2016)

[2] N Hiroi, R Tanimoto, K Ii, M Ozeki, K Mashimo, A Funahashi. "Requirement of spatiotemporal resolution for imaging intracellular temperature distribution." *SPIE Technologies and Applications of Structured Light*, **102510Q**-102510Q-4. (2017)

B17: Dynamics of quantum mechanical systems in the area of quark physics

Shashank Bhatnagar

Department of Physics, Chandigarh University, Mohali-140413, India

Bethe-Salpeter Equation (BSE) [1] describes the bound state of two or more fermions in a relativistically covariant manner. It is an equation that is firmly rooted in Quantum Field Theory. BSE is quite general and has applicability in many branches of theoretical physics. BSE was first applied to positronium (electron-positron)[1]. It is now actively being applied to mesons (quark-anti-quark systems) in particle physics, and recently to excitons (electron-hole pairs) in condensed matter physics. In some systems like in solids of rare gases, the electron or hole interact so strongly that they can form bound states located inside the gap (excitons). To describe electron- hole interactions (excitonic effects), one has to resort to a two-particle formalism by solving the BSE

for two-particle correlation function. The first ab-initio application [2] of BSE in condensed matter physics was to calculation of optical absorption spectrum of a cluster: Na_4. Subsequent works have shown its capability to correctly reproduce excitons and excitonic effects. The whole idea behind the BSE approach is: when two particles form a bound state, they interact quite often, and we can not describe this situation by summation over a few Feynman diagrams. Bethe-Salpeter Equation is a relativistic n (n> 1) body bound state equation. This equation is fully covariant and is firmly rooted in Quantum Field Theory. We can expand any general interaction as an iteration of one-quantum exchange diagrams ("Moller interactions") in ladder approximation.
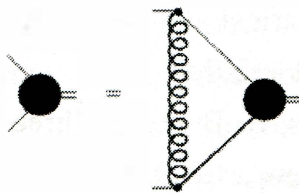
Fig.1: Feynman diagrammatic form of Bethe-Salpeter Equation

For any general two-particle interaction, the propagator K under Ladder approximation (iteration of one-quantum exchange) satisfies the equation, $K=K_0+K_0 VK$, where, K is any general two-particle interaction . For particles forming a bound state, K looks like an s-channel pole, and the bound state propagator factorizes at the bound state s-channel pole, leading to Bethe-Salpeter Equation (BSE), which in covariant form can be expressed as [3-7]:

$$i \; (2\pi)^4 S_F^{-1}(p1)\psi(P,q)S_F^{-1}(-p2) = \int d^4 q' K(q,q')\psi(P,q'),$$

where $\psi(P,q)$ is the full 4D BS wave function that is made up of hadron-quark vertex sandwiched by the propagators of the quark and the anti-quark. The hadron-quark vertex gives effective coupling of a hadron to all its constituents. The framework of BSE rests on Lorentz and gauge invariance, due to which it has a very wide applicability all the way from low energy spectroscopy to high energy transition amplitudes, and can be used to study both light and heavy quark systems in an integrated manner. We have been involved in a programme on hadron dynamics at the quark level with use of a 4x4 representation of Bethe-Salpeter equation. We have recently applied it to the study of mass spectra of ground and excited states of scalar (0^{++}), pseudoscalar (0^{-+}), vector (1^{--}) and axial vector (1^{++}) and (1^{+-}) charmonium and bottomonium, and also studied the weak decay constants of P and V quarkonia, two-photon and two-gluon decay widths of P-quarkonia, single photon radiative decay widths of V-quarkonia, and two-photon decays of scalar quarkonia [3-7]. The results are in good agreement with data and other models.

References

[1] H.A.Bethe, E.E.Salpeter, Phys. Rev. 84, 1232 (1951)

[2] G.Onida et al., Phys. Rev. Lett. 75, 818 (1995)

[3] S.Bhatnagar, J.Mahecha, Y. Mengesha, Phys. Rev. D 90, 014034 (2014)

[4] H.Negash, S.Bhatnagar, Intl. J. Mod. Phys. E25, 1650059 (2016)

[5] S.Patel, P.C.Vinodkumar, S.Bhatnagar, Chinese Phys. C40, 053102 (2016)

[6] S.Bhatnagar. L. Alemu, arxiv:1601.03234v3[hep-ph] (2017)

[7] H. Negash, S.Bhatnagar, arxiv:1703.06082 [hep-ph] (2017).

A38: Hybrid Quantum Systems: Spin qubits coupled to electromagnetic fields

Guido Burkard[1]

[1]*Department of Physics, University of Konstanz, Germany*

Email:guido.burkard@uni-konstanz.de;web site: https://theorie.physik.uni-konstanz.de/burkard

Electron spins in coupled semiconductor quantum dots can be endowed with a controllable electric dipole via the Pauli Exclusion Principle. We show how this effect enables electric control of spin qubits, while also causing deleterious spin decoherence [1-3]. We find that decoherence can be avoided to a large extent at so-called "sweet spots". Electric-dipole spin control was also achieved optically for defects in diamond [4]. We highlight two hybrid quantum systems consisting of spins in a solid and photons in an electromagnetic cavity [1,5].
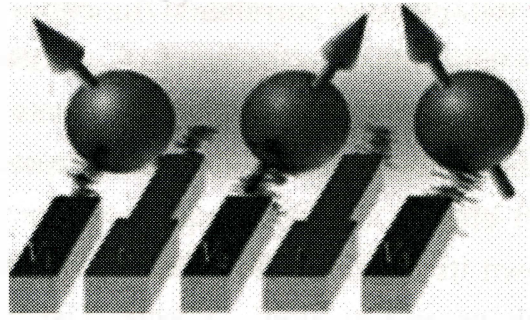
Fig1. Three-spin qubit in a triple quantum dot under the influence of electrical noise appearing at the electrostatic gates V_1, V_2, and V_3, and through the tunnel barriers t_l and t_r.

References

[1] M. Russ, F. Ginzel, G. Burkard, Coupling of three-spin qubits to their electric environment, Phys. Rev. B 94, 165411 (2016).

[2] M. Russ, G. Burkard, Asymmetric resonant exchange qubit under the influence of electrical noise, Phys. Rev. B 91, 235411 (2015).

[3] M. Russ, G. Burkard, Three-electron spin qubits (review article), aXiv:1611.09106.

[4] B.B. Zhou, A. Baksic, H. Ribeiro, C.G. Yale, J.F. Heremans, P.C. Jerger, A. Auer, G. Burkard, A.A. Clerk, D.D. Awschalom, Accelerated quantum control using superadiabatic dynamics in a solid-state lambda system, Nature Physics 13, 330 (2017).

[5] G. Burkard, V.O. Shkolnikov, D.D. Awschalom, A cavity-mediated quantum CPHASE gate between NV spin qubits in diamond, accepted for Phys. Rev. B [arXiv:1402.6351].

A39: Electronic structure of zigzag nanoribbons in an uniform magnetic field

Jan Smotlacha [1], R. Pincak [2]

[1]*Bogoliubov Laboratory of Theoretical Physics, Joint Institute for Nuclear Research, 141980 Dubna, Russia*

Email:smota@centrum.cz,   web   site: http://theor.jinr.ru/disorder/smotlacha.html

[2]*Institute of Experimental Physics, Slovak Academy of Sciences,*

Watsonova 47, 040 01 Košice, Slovak Republic

The electronic spectra of the nanostructures show an interesting behaviour under the influence of the uniform magnetic field: the dependence of the energy levels on the magnetic field show a fractal structure. This feature follows from the procedure of the calculation in which the matrix form of the Schrödinger equation is replaced by the system of the Harper equations, where the exponentials with the magnetic factors are supplied to all of the terms [1]. We studied the spectra of the phosphorene and the graphene zigzag nanoribbons with the atomic vacancies [2] and we investigated an interesting feature of these spectra – for a concrete kind of the placement of the vacancies, the dependence of the number and the size of the gaps on the magnetic field is characteristic (Fig. 1). Moreover, new edge states appear. Next, we calculated the density of states for different concentrations of the Gaussian distribution of the vacancies and in this way, we verified the metallic properties.
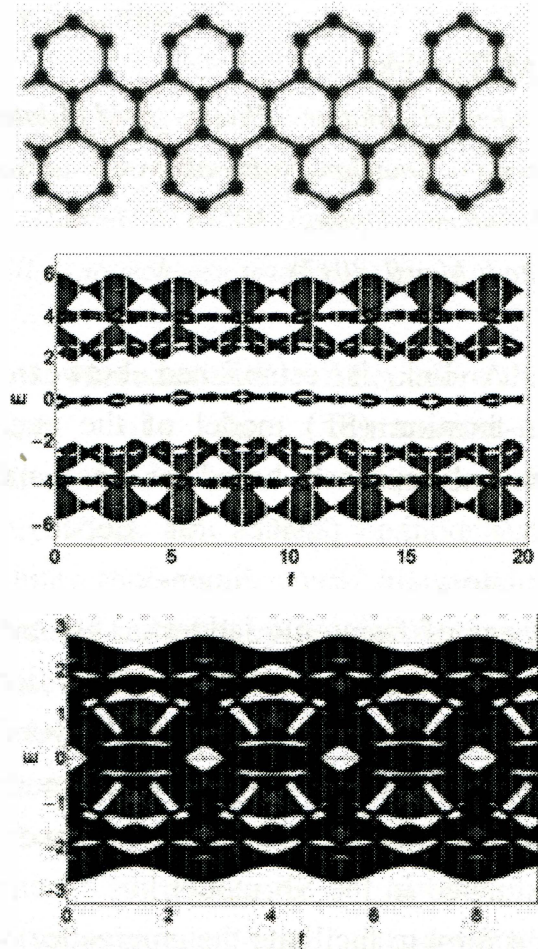
Fig1. Electronic spectra of phosphorene and graphene zigzag nanoribbons depending on magnetic field.

References

[1] K. Wakabayashi, M. Fujita, H. Ajiki, and M. Sigrist, *Phys. Rev. B* **59**, 8271 (1999).

[2] J. Smotlacha and R. Pincak, Electronic Properties of Phosphorene and Graphene Nanoribbons in Magnetic Field, submitted for publication in *Phys. Rev. B*, (2017).

A40: The ladder physics in the Spin Fermion model (Keynote)

A. M. Tsvelik[1]

[1]*Condensed Matter Physics and Materials Science Division, Brookhaven National Laboratory, Upton, NY 11973-5000, USA*
(Dated: May 9, 2017)

A link is established between the spin-fermion (SF) model of the cuprates and the approach based on the analogy between the physics of doped Mott insulators in two dimensions and the physics of fermionic ladders. This enables one to use nonperturbative results derived for fermionic ladders to move beyond the large-N approximation in the SF model. It is shown that the paramagnon exchange postulated in the SF model has exactly the right form to facilitate the emergence of the fully gapped d-Mott state in the region of the Brillouin zone at the hot spots of the Fermi surface. Hence the SF model provides an adequate description of the pseudogap.

A41: Strange metal state near a heavy-fermion quantum critical point

Yung-Yeh Chang[1], Silke Paschen[2], Chung-Hou Chung[1,3]

[1]*Department of Electrohysics, National Chiao-Tung University, HsinChu, Taiwan, R.O.C.*
[2]*Institute of Solid State Physics, TU Vienna, Vienna, Austria*
[3]*Physics Division, National Center for Theoretical Sciences, HsinChu, Taiwan, R.O.C. Email:chung@mail.nctu.edu.tw, web site: http://gate.ep.nctu.edu.tw/~chchung/*

Recent experiments [1][2] on quantum criticality in the Ge-substituted heavy-electron material YbRh2Si2 under magnetic fields have revealed a possible non-Fermi-Liquid (NFL) strange metal (SM) state [2] over a finite range of fields at low temperatures, which still remains a puzzle. In the SM region, the zero-field antiferromagnetism (AF) is suppressed. Above a critical field, it gives way to a heavy Fermi liquid with Kondo correlation. The T (temperature)-linear resistivity and the T-logarithmic followed by a power-law singularity in the specific heat coefficient at low T, salient NFL behaviours in the SM region, are un-explained. We offer a mechanism to address these open issues theoretically based on the competition between a quasi-2d fluctuating short-ranged resonant- valence-bonds (RVB) spin-liquid (FL* phase) and the Kondo correlation (LFL phase) near criticality [3]. Via a field-theoretical renormalization group (RG) analysis on an effective field theory beyond a large-N (Sp(N)) approach to an anti-ferromagnetic Kondo-Heisenberg lattice model, we identify the critical point, and explain remarkably well both the crossovers and

the SM behaviour. The strange metal state can be interpreted as the extended quantum critical region to T $\to$ 0 due to its proximity to Kondo breakdown at criticality.

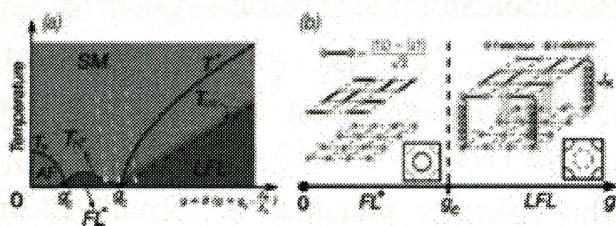Fig1. (a). Schematic phase diagram of Ge-substituted YbRh2Si2.The parameter g refers to the magnetic field B. Dashed arrows refer to the direction of RG flows. T*, T_{LFL}, T_N, T_{FL*} are crossover scales. (b). Schematic plot describing the competition between the RVB spin-liquid FL* phase induced by AF RKKY coupling Jϕ and the Kondo LFL phase via Kondo hybrizidation strength J_K near gc at zero temperature. A jump from a small (at g<gc) to a large (at g>gc) Fermi surface occurs at the quantum critical point gc [3].

References

[1] J. Custers, P. Gegenwart, H. Wilhelm, K. Neumaier, Y. Tokiwa, O. Trovarelli, C. Geibel, F. Steglich, C. Ppin, and P. Coleman, Nature (London) 424, 524527 (2003).

[2] J. Custers, P. Gegenwart, C. Geibel, F. Steglich, P. Coleman, and S. Paschen, Phys. Rev. Lett. 104, 186402 (2010).

[3]. Yung-Yeh Chang, Silke Paschen, Chung-Hou Chung, arXiv:1701.04599.

A42: An effective potential theory for time-dependent multi-configuration wave function

Tsuyoshi Kato

Department of Chemistry, School of Science, the University of Tokyo, Japan

Email:tkato@chem.s.u-tokyo.ac.jp

1. Introduction After more than a decade of the formulation of multi-configuration time-dependent Hartree-Fock (MCTDHF) method to treat electronic dynamics in atoms and molecules induced by the interaction with intense ultrafast laser pulses from first principles [1], the theoretical efforts exerted on the developments of the method has been changed their aspects from the basic formulations and the proof-of-principle type calculations to practical calculations in order to elucidate the many electron dynamics by comparisons with experimental results [2]. Recently, efforts have been made to improve the numerical performance of the MCTDHF method aiming to reduce the size of the configuration space by restricting the orbital excitation schemes [3,4], although a different approximation of factorized configuration interaction coefficients [5] as well as the multi-layer formulation of MCTDHF [6] have been introduced recently.

In the present study, we propose an alternative formulation for the time propagation of a time-dependent

multi-configuration wave function in which the spin-orbitals follow a single-particle time-dependent Schrödinger equation (TDSE) specified by a *multiplicative time-dependent local effective potential* $v_{\text{eff}}(\boldsymbol{r}, t)$.

2. Theory We consider an N-electron time-dependent wave function $\Psi(1, 2, \cdots, N, t)$ perturbed by a time-dependent external field. The wave function is assumed to be represented by

$$\Psi(1,2,3,\cdots,N,t)$$
$$= \sum_{K=1} C_K(t) \Phi_K(1,2,3,\cdots,N,t), \quad 1)$$

where $\{C_K(t)\}$ represent time-dependent configuration interaction coefficients and $\{\Phi_K(t)\}$ time-dependent Slater determinants. The time-dependence of each Slater determinant is due to the time dependence of the constituent spin-orbitals. The total Hamiltonian of the system is represented by $\hat{H}(t) = \hat{T} + \hat{V}_{\text{ext}}(t) + \hat{V}_{\text{ee}}$, where $\hat{T}$, $\hat{V}_{\text{ext}}(t) = \sum_{j=1}^{N} v_{\text{ext}}(\boldsymbol{r}_j, t)$, and $\hat{V}_{\text{ee}}$ represent the kinetic energy operator, the sum of nuclear attraction potential and the time-dependent external perturbation, and the electron-electron repulsion potential, respectively. The spin-orbitals are assumed to obey a single-particle TDSE expressed by

$$\left[i\hbar \frac{\partial}{\partial t} - \left(-\frac{\hbar^2}{2m_e} \frac{\partial^2}{\partial r^2} + v_{\text{eff}}(r,t) \right) \right] \phi_k(x,t) = 0 \quad (k = 1,2,\cdots,N,\cdots), \quad 2)$$

where $x = (\boldsymbol{r}, \sigma)$ denotes the spatial and spin-coordinates of an electron, and $v_{\text{eff}}(\boldsymbol{r}, t)$ is the effective potential to be calculated. We define an effective Hamiltonian for the relevant system as

$$\hat{H}_{\text{eff}}(t) = \hat{T} + \sum_{j=1}^{N} v_{\text{eff}}(\boldsymbol{r}_j, t)$$
$$= \hat{T} + \hat{V}_{\text{eff}}(t). \quad 3)$$

The effective potential is formulated by using McLachlan's minimization principle in which the difference of the time-evolution of the wave function $\Psi(1,2,\cdots,N,t)$ is minimized between the TDSEs specified by $\hat{H}(t)$ and $\hat{H}_{\text{eff}}(t)$.

3. Discussion We report the detailed theoretical analysis of the properties of the effective potential associated with an exact wave function. Furthermore, as an elementary application of the present formalism, we propose a direct method to calculate the so-called Brueckner orbitals [7] as a special solution of a set of spin-orbitals calculated as eigenfunctions for a single-particle Schrödinger equation specified by a time-independent effective potential $v_{\text{eff}}(\boldsymbol{r})$ that is associated with an exact ground-state wave function.

References

[1] For example, T. Kato and H. Kono, *Chem. Phys. Lett.* **392** (2004) 533-540.

[2] K.L. Ishikawa and T. Sato, IEEE *J. Sel. Topics Quantum Electron.* **21** (2015) 8700916-1-16.

[3] H. Miyagi and L.B. Madsen, *Phys. Rev. A* **87** (2013) 062511-1-12.

[4] T. Sato and K. L. Ishikawa, *Phys. Rev.* A **91** (2015) 023417-1-15.

[5] E. Lötstedt, T. Kato, and Y. Yamanouchi, *J. Chem. Phys.* **144** (2016) 154116-1-13.

[6] H. Wang and M. Thoss, *J. Chem. Phys.* **131** (2009) 024114-1-14.

[7] R.K. Nesbet, *Phys. Rev.* **109** (1958) 1632-1638.

A43: Typical and untypical states for non-equilibrium quantum dynamics

Robin Steinigeweg[1],[*]

[1]*University Osnabrück, Physics Department, D-49076 Osnabrück, Germany*

[*]*Email: rsteinig@uos.de*

The real-time broadening of density profiles starting from non-equilibrium states is at the center of transport in condensed-matter systems and dynamics in ultracold atomic gases. Initial profiles close to equilibrium are expected to evolve according to linear response, e.g., as given by the current correlator evaluated exactly at equilibrium. Significantly off equilibrium, linear response is expected to break down and even a description in terms of canonical ensembles is questionable.

In my talk, I show that single pure states with density profiles of maximum local amplitude yield a broadening in perfect agreement with linear response, if the structure of these states involves

randomness in terms of decoherent off-diagonal density-matrix elements. While these states allow for spin diffusion in the XXZ spin-1/2 chain at large exchange anisotropies, coherences yield entirely different behavior [1]. In contrast, charge diffusion in the strongly interacting Hubbard chain turns out to be stable against varying such details of the initial conditions [2].

References

[1] R. Steinigeweg, F. Jin, D. Schmidtke, H. De Raedt, K. Michielsen, J. Gemmer, *Phys. Rev. B* **95**, 035155 (2017).

[2] R. Steinigeweg, F. Jin, H. De Raedt, K. Michielsen, J. Gemmer, arXiv:1702.00421 (2017).

A44: Dynamics of a Mobile Impurity in a One-Dimensional Bose Liquid

A. Petkovic and Z. Ristivojevic

Laboratoire de Physique Théorique, Université de Toulouse, CNRS, UPS, 31062 Toulouse

Email: petkovic@irsamc.ups-tlse.fr

In this talk we consider a quantum impurity propagating in a one-dimensional Bose liquid. As a result of scattering off thermally excited quasiparticles, the impurity experiences the friction. We provide a microscopic theory and find that, at low temperatures, the resulting force

scales either as the fourth or the eighth power of temperature, depending on the system parameters. For temperatures higher than the chemical potential of the Bose liquid, the friction force is a linear function of temperature. Our approach enables us to find the friction force also in the crossover region between the two limiting cases. In the integrable case, corresponding to the Yang-Gaudin model, the impurity becomes transparent for quasiparticles and thus the friction force is absent. Our results could be further generalized to study other kinetic phenomena.

A45: The upper security bound for subcarrier wave quantum key distribution

A.V. Kozubov[1], A.A. Gaidash[1], G.P. Miroshnichenko[1], A.V. Gleim[1,2]

[1]*ITMO University, Department for Photonics and Optical Information Technology,*
199034 Kadetskaya Line 3b, Saint Petersburg, Russia
Email:avkozubov@corp.ifmo.ru
[2]*Kazan National Research Technical University KAI, 420111, Karl Marx str. 10, Kazan, Russia*

In order to ensure secure operation of a QKD system for real-life applications, one needs to consider possible eavesdropping strategies and define optimal parameters for the experimental setup. In this work we perform security analysis for SCW QKD [1] against one of the most powerful collective attacks on phase protocols: a collective beam splitting attack [2].

To solve this task, we perform realistic description of different SCW QKD system components. It requires a coordinated solution of several problems using methods of quantum optics. First of all, we describe the process of photonic quantum state preparation and binary information encoding. For correct quantum bit error rate (QBER) estimation we construct a theory for photonic quantum state decoherence process during propagation in optical fibers. We also provide mathematical description of detection process and processing of classical binary bit strings.

It strongly should be mentioned that such security analyse has never been done for SCW QKD systems. The main results of this work are the following. Using data from [3] we obtained equations for input coherent state transformation by an electro-optical modulator, with using more accurate model and taking into account all possible sidebands and geometric sizes of the modulator. We then constructed formulas for sidebands detection probability using Markov's approximation, which take into consideration detection efficiency and a parameter defining dark count rate. We also obtained equations for Holevo information bound in Alice-Eve channel [4] and made estimations for both

for pure and mixed states. Moreover, the capacity of the SCW QKD channel (modelled as binary symmetric erasure channel) was investigated, taking phase errors into account. Error and uncertain results probabilities were calculated depending on channel length. Finally, using the equations from [1, 5], we estimated secure key rate for different system parameters.

Using the obtained equations, we studied the dependence of secret key rate in SCW QKD setup depending on the device parameters and channel length. Fig. 1 shows that with protocol parameters optimized using the updated model our system we is capable of operating in channels with losses up to 67 dB (including Bob losses), compared to 42 dB reported previously in. Notably, the results were achieved despite a relatively low phase change frequency of 100 MHz. As can be seen from the figure, detector dark count rate f remains the main limiting factor for the maximum QKD distance. The values used in calculations (f = 0.01, 10, 10^3 Hz with quantum efficiency (QE) 20%) imply using modern superconducting nanowire single photon detectors, which are available on the market.

These results are important for constructing long-distance QKD links and multiuser quantum networks using SCW QKD instrumentation: an ultra-high bandwidth approach to QKD compatible with existing optical fiber infrastructure.

References

[1] A. V. Gleim, V. I. Egorov, Yu. V. Nazarov, S. V. Smirnov, V. V. Chistyakov, O. I. Bannik, A. A. Anisimov, S. M. Kynev, A. E. Ivanova, R. J. Collins, S. A. Kozlov, and G. S. Buller. Secure polarization-independent subcarrier quantum key distribution in optical fiber channel using BB84 protocol with a strong reference. Opt. Express, Vol. 24, No. 3, p.2619-2633, (2016)

[2] Valerio Scarani, Helle Bechmann-Pasquinucci, Nicolas J. Cerf, Miloslav Dušek, Norbert Lütkenhaus, Momtchil Peev. The security of practical quantum key distribution. Rev. Mod. Phys, V. 81, №3, p.1301-1350, (2009)

[3] Miroshnichenko G P, Kiselev A D, Trifanov A I, Gleim A V 2016 arXiv:1605.05770v1

[4] Holevo A. S. Bounds for the quantity of information transmitted by a quantum communication channel //Problemy Peredachi Informatsii. – 1973. – T. 9. – №. 3. – C. 3-11.

[5] B. Korzh, N. Walenta, R. Houlmann, H. Zbinden. A high-speed multiprotocol quantum key distribution transmitter based on a dual-drive modulator. Optics Express, Vol. 21, Issue 17, pp. 19579-19592, (2013)

A46: New insights from mesoscopic simulations of electrolyte transport under confinement

Vincent Dahirel[1], M. Jardat, X. Zhao, L. P. Ocampo

[1]Chemistry Department, Sorbonne Universités, UPMC Paris 06, Paris, France

Email:Vincent.dahirel@upmc.fr

Dynamic Light Scattering, Laser Zetametry, or conductimetry are easily available techniques to characterize solutions through their dynamical properties. However, the theories used for data analysis often neglect key phenomena, such as hydrodynamic interactions between individual ions. Unfortunately, hydrodynamic interactions cannot be analytically evaluated for most systems of interest, like highly concentrated electrolytes, or confined electrolytes. In the case of ions at interfaces, Poisson-Nernst-Planck (PNP) or analogous equations might not necessarily be reliable when direct correlations between individual ions are strong. Evaluating such failure of widely used theories is of paramount importance for the understanding of transport properties in industrial, geological or biological systems.

In recent years, mesoscopic simulation techniques were developed that can include all hydrodynamic and coulombic interactions of electrolytes in the presence of interfaces. We used such mesoscopic simulation techniques to quantify the deviations of ion transport coefficients from their ideal values for bulk ions and confined ions.

We started with unconfined electrolytes and assessed the limitations of an advanced electrolyte transport theory developed in our group [1], using Brownian Dynamics (BD) with hydrodynamic interactions [2], and hybrid molecular dynamics / Stochastic Rotation Dynamics (SRD) [3,4]. In a second part, we investigated the role of ionic correlations in electroosmotic transport in nanoporous media [5]. We compare the SRD mesoscopic simulation technique with PNP, and find regimes for which deviations from PNP arise either because of the strength of the electrostatic interactions, or because the size of solutes begins to play a role. We also managed to decrease ion-ion hydrodynamic interaction while keeping the viscous dissipation on the ions constant, and could quantify the contributions of the mean field hydrodynamics and ion-ion correlations to the mass and charge flows.

Our results show that in many cases, usual theories should not be used to analyse experimental data. However, alternative simulation tools are always difficult to use, and can be very expensive in term of computation time. In a last part, we studied several strategies to reduce to computational cost of mesoscopic simulations [5].

References

[1] R. Pusset, S. Gourdin-Bertin, E. Dubois, J. Chevalet, G. Mériguet, O. Bernard, V. Dahirel, M. Jardat and D. Jacob, *Phys. Chem. Chem. Phys.* **17**, 11779 (2015).

[2] V. Dahirel, B. Ancian, M. Jardat, G. Mériguet, P. Turq and O. Lequin, *Soft Matter* **6**, 517 (2010).

[3] G. Batôt, V. Dahirel, G. Mériguet, A. A. Louis, and M. Jardat, *Phys. Rev. E* **88**, 043304 (2013).

[4] V. Dahirel, X. Zhao, and M. Jardat, *Phys. Rev. E* **94**, 023317 (2016).

[5] D. Cerratti, A. Obliger, M. Jardat, B. Rotenberg, and V. Dahirel, *Mol. Phys.* **113**, 2476 (2015).

A47: Magnetization Reversal Process in Thin Amorphous Ferromagnetic Film with Surface Anisotropy

N. A. Usov[1,2], O. N. Serebryakova[1,2]

[1]*National University of Science and Technology «MISiS», 119049, Moscow, Russia*
Email: usov@obninsk.ru
[2]*Pushkov Institute of Terrestrial Magnetism, Ionosphere and Radio Wave Propagation, Russian Academy of Sciences, IZMIRAN, 108480, Troitsk, Moscow, Russia*

Amorphous ferromagnetic materials with perpendicular magnetic anisotropy are promising for creation of new generation of high-density data storage devices and spin-transfer torque magnetic random access memory [1]. It is well known [2] that it is surface anisotropy which is responsible for the high perpendicular magnetic anisotropy observed in very thin ferromagnetic films and multilayers. In this report three-dimensional numerical simulation is used to study equilibrium micromagnetic configurations and magnetization reversal process in thin amorphous ferromagnetic films with surface anisotropy. The numerical results are obtained in the simplest Néel approximation for surface anisotropy energy, a surface anisotropy constant K_s being a single phenomenological parameter. It is found that for negative values of the surface anisotropy constant the film is perpendicular magnetized for sufficiently small thickness, $L_z < L_{z,min}(|K_s|)$. The critical thickness depends on the absolute value of the surface anisotropy constant. For thickness $L_z > L_{z,min}$ the spin canted state has the lowest total energy as compared to various multi-domain configurations. As an example of the calculations performed, Fig. 1 shows the perpendicular hysteresis loops of thin amorphous CoSiB film with in plane sizes 120×360 nm, saturation magnetization M_s = 500 emu/cm^3, exchange constant A = 10^{-6} erg/cm, and in-plane induced volume anisotropy constant K_V = 10^4 erg/cm^3. The hysteresis loops 1), 2) correspond to the spin canted state. For the perpendicular magnetized state the hysteresis loop 3) is nearly rectangular, the magnetization reversal starts by means of the nucleation of the

buckling mode at the nucleation field H_n = -450 Oe. However, within the interval -570 Oe < H < H_n a nonlinear stabilization of the buckling mode is observed. The nucleation field of the buckling mode is investigated as a function of the CoSiB film sizes and in-plane aspect ratio.
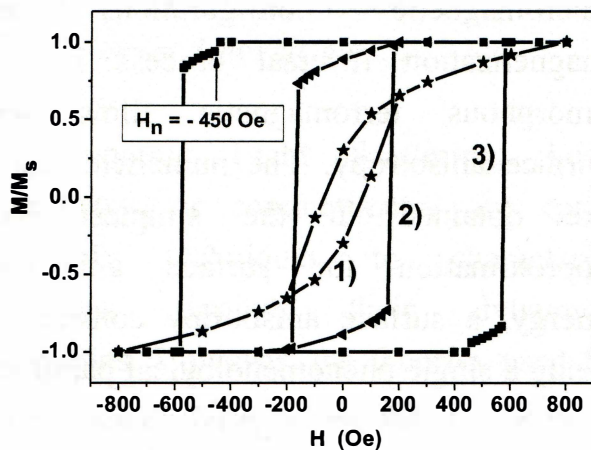

Fig1. Perpendicular hysteresis loops of CoSiB amorphous film of thickness L_z = 6 nm with various values of surface anisotropy constant: 1) K_s = -0.8 erg/cm^2, 2) K_s = -0.9 erg/cm^2, 3) K_s = -1.0 erg/cm^2.

References

[1] J. Yoon, S. Jung, Y. Choi, J. Cho, C.-Y. You, M.H. Jung, and H.I. Yim, *J. Appl. Phys.* **113**, 17A342 (2013).

[2] M.T. Johnson, P.J.H. Bloemen, F.J.A. den Broeder, and J.J. de Vries, *Rep. Prog. Phys.* **59**, 1409 (1996).

A48: Granular Matter in Extraterrestrial Environments – Modeling and Simulation of Regolith in Planetary Exploration

Roy Lichtenheldt[1]
[1]*Insitute of System Dynamics and Control, German Aerospace Center (DLR),Weßling, Bavaria, Germany*
Email:Roy.Lichtenheldt@dlr.de, web site: http://www.dlr.de/sr

In everydays life, moving on soft, sandy soils is a well-known task for everyone us. Regardless, the interaction physics of and with granular matter is still not fully understood. Whilst in terrestrial applications a direct recovery of locomotion gear is possible by external means, planetary exploration are fend for themselves.The talk will introduce enhanced but yet efficient simulation methods that are used in development of locomotion gear. Validated application models allow for in-depth analysis of the interaction, even beyond the possibilities given by measurements: As shown in figure 1 flows of granular matter may be tracked in any part of the medium, forces and locomotion behaviour can be predicted and mutual influences of locomotion gear and sand can by analyzed. Given the possibilities of the models, particle simulation poses a great chance to further improve future locomotion gear. Thus the focus will be on improvements of the

particle-based Discrete Element Method (DEM).

One of the tasks for modeling the correct shear strength of granular matter is efficient coverage of grain rolling and interlocking. To allow for efficient simulations the complex shapes of real grains need to be simplified. Covering certain features like angularity or rounded edges is crucial. In the proposed approach two dimensional rolling geometries are attached to the spherical grains and superimposed to 3D equivalent bodies [1]. Resulting in an improved non-linear torque behaviour, it becomes possible to cover behaviour like tilting or rotational interlocking. Details on the method will be presented alongside torque-laws for different shapes, including edge rounding.

A second challenge in particle simulations is parameter identification. Real-world sand grains are too small to directly identify inter-grain contact parameters. The state of the art treats this problem with multi-parameter calibration to measured data, leading to non-unique solutions in long lasting processes [2]. A method to identify a parameter set without the need of preliminary simulations or calibration has been developed [3] and will be explained throughout the talk.

Additionally methods to improve efficiency, e.g. dynamic boundaries, will be shown. The presented methods will be presented alongside their applications in current planetary exoploration mission. These range from "the Mole", a self-impelling nail for NASA's InSight Mission to Mars, over MASCOT, DLR's asteroid hopping currently on its way to asteroid Ryugu, to Wheels of planetary exploration rovers (Figure 1).

Fig1. Particle Flow beneath a planetary Rover Wheel (ExoMars Rover).

References

[1] R. Lichtenheldt, B. Schäfer, *Planetary Rover Locomotion on soft granular Soils - Efficient Adaption of the rolling Behaviour of nonspherical Grains for Discrete Element Simulations, In: Particle-based Methods III (ISBN 978-84-941531-8-1)*, pp. 807-818 (2013).

[2] R. Lichtenheldt, *Lokomotorische Interaktion planetarer Explorationssysteme mit weichen Sandböden – Modellbildung und Simulation* (Dr. Hut München), 301 (2016).

[3] R. Lichtenheldt, *A novel systematic method to estimate the contact parameters of particles in discrete element simulations of soil, In: Particle-based Methods IV (ISBN 978-84-944244-7-2)*, pp. 430-441 (2015)

A49: Experimental and modelling studies of interaction of e- beam (10-345 MeV) with materials designed for radiation shielding for the MCP detector on JUICE mission to Jupiter

M. Tulej[1], D. Lasi[1], S. Meyer[1], M. Lüthi[1], A. Galli[1], D. Piazza[1], P. Wurz[1], L. Desorgher[2], D. Reggiani[2], H. Xiao[2], W. Hajdas[2], A. Cervelli[3], S. Karlsson[4], L. Kalla[4], and S. Barabash[4]

[1]Space Research and Planetary Sciences, Physics Institute, University of Bern, CH-3012, Bern, Switzerland.

Email: marek.tulej@space.unibe.ch, website: http://www.space.unibe.ch

[2]Laboratory of Particle Physics, Paul Scherrer Institute, CH-5232, Villigen, Switzerland

[3]Laboratory for High Energy Physics, Sidlerstrasse 5, CH-3012 Bern, Switzerland

[4]Swedish Institute of Space Physics, Space Kampus 1, Kiruna, Sweden

Experiments with high-energy electrons (17.5–345 MeV/c) and GEANT4 modelling are applied to size and shape an effective layered shielding suppressing the radiation-induced noise on the MCP detector. The MCP detector is planned to be used in the time-of-flight mass spectrometer (NIM) on the JUpiter ICy moons Explorer (JUICE), a large-class mission of the European Space Agency slated to launch in May 2022, to study Jupiter and its three icy moons: Europa, Ganymede, and Callisto [1, 2].

The radiation environment at Europa is the most critical and is characterized by electron and proton fluxes of the order of 10^7 and 10^6 $\# \cdot cm^{-2} \cdot sr^{-1} \cdot s^{-2}$ (integral fluxes for a reference energy of > 1 MeV), respectively. Of these two major components of the radiation spectrum, electrons are the most difficult to shield. The spectrum of electrons at Jupiter extends to energies as high as several hundreds of MeV with fluxes as high as $10^2 - 10^1$ $\# \cdot cm^{-2} \cdot sr^{-1} \cdot s^{-2}$, whereas the proton flux is about two orders of magnitude lower. Fluxes of electrons in the energy range of ~10 – ~100 MeV represent the most critical fraction of the radiation spectrum at Jupiter for NIM, because of both their high abundance and their long range in shielding materials [3, 4].

Our experimental studies were conducted at the secondary proton beam line piM1 at the Paul Scherrer Institute in Villigen (Switzerland). During the first phase of the experiments, MCP detection efficiency in the function of electron beam energy was investigated following detailed beam calibrations. In the same test campaign, we have investigated also the effects of the interaction between the electron beam and a layered shielding composed of 2 mm Al – (1-10) mm Ta – 1 mm Al, that was indicated in our earlier studies as optimal for NIM [4]. The modeling studies could be verified by experimental findings. Building on the results obtained during this first test campaign, we have calculated a new

optimized shielding with GEANT4 simulation (i.e., most effective against radiation with minimum mass) and conducted a new series of experiments with a more sophisticated test setup and a flight-like MCP detector assembly (fig.1). The results of this second test campaign allowed to conclude on the final shape of the MCP shielding and, more in general, for the shielding of other detectors against highly-energetic electrons [5-8].
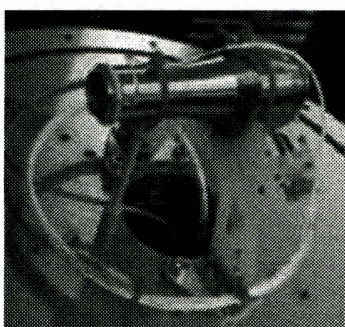

Fig 1. (left) The shielded detector inside the vacuum chamber. The outer material is Ta (10 mm in the line of sight of the MCP. Part of the internal aluminum layer is visible to the left, where ions enter the detector. (right) Graphical output of GEANT4 run with 201 MeV/c beam on the shielded detector.

References

[1] S. Barabash, et al., EPSC vol. 8, (2013), 8–13 Sept., London, UK.
[2] P. Wurz, et al., *Planet. Sp. Science* 74 (2012) 264-269.
[3] JS-14-09 v5.4, JUICE Environment Specification, European Space Agency (2015).
[4] JGO-PEP-TN-0901-I1R0 v1.0, Radiation analysis of PEP NU, L. Desorgher (2010).
[5] W. Hajdas et al., *J. Appl. Math. Phys.*, 2 910 (2014).
[6] M. Tulej et al., *Rev Sci. Instrum.* **86**, 083310 (2015).
[7] M. Tulej et al., *Nucl. Instrum. Methods Phys. Res. B*, **383**, 21 (2016).
[8] D. Lasi et al., *IEEE Transactions on Nuclear Science,* **64**, 605 (2017).

A50: Emittance Reduction by increasing the ion source extraction field: comparing data with simulations

Martin P. Stockli, and Baoxi Han
Spallation Neutron Source, Oak Ridge National Laboratory, Oak Ridge, TN 37830, USA Email:stockli@ornl.gov, web site: http://neutrons.ornl.gov/sis

The Spallation Neutron Source has been operating near 1 MW for the last 7 years with peak powers up to 1.4 MW. This requires ~35 mA H- beam current at a 6% duty factor in the linear accelerator (LINAC). Experiments have shown the maximum LINAC beam current is achieved when the electron dump electrode is kept at a voltage that forms a uniform extraction field [1]. Unfortunately, about

five years ago the transmission of the first RF accelerator, the RFQ, significantly degraded and since then 55-60 mA need to be injected into the RFQ rather than the previous ~40 mA. There is a strong correlation between the beam current injected into the RFQ and the measured transmission [2].

Recent experiments have shown that increasing the extraction field by applying a positive +5 kV voltage to the extractor and scaling the electron dump voltage accordingly increases the RFQ input current by ~1 mA (top trace in Fig. 1a). Raising the extractor voltage beyond 5 kV does not further increase the RFQ input current, which is consistent with an ion-density limited extraction. However, when the two lenses of the electrostatic low-energy beam transport (LEBT) are retuned, the RFQ output current increases by up to ~3 mA for up to +15 kV extractor voltage, as seen in the bottom trace of Fig. 1a. The 3 mA increase may not sound impressive, but it yields an additional 120 kW after being accelerated to 1 GeV, which can increase the neutron yield by ~10%.

To better understand the process, our LEBT was modeled with PBGUNS. Figure 1b shows the optimal beam transport for a grounded extractor, where the beam barely passes through the extractor, then rapidly expands into lens 1. Lens 1 requires a high voltage to squeeze the beam into lens 2, which squeezes the beam into the RFQ. Figure 1c shows the beam transport

modeled with +20 kV on the extractor; the smaller beam clears the extractor and does not expand as much into lens 1. Lens 1 provides less focusing, which allows for a higher lens 2 Voltage to focus the beam into the RFQ with less convergence.

The reduced space charge between the meniscus and lens 1 likely causes the smaller beam diameter, which in turn reduces aberrations, leads to a smaller emittance, and in turn appears to increase the transmission through the RFQ.

The model calculations will be discussed and compared to experimental data.
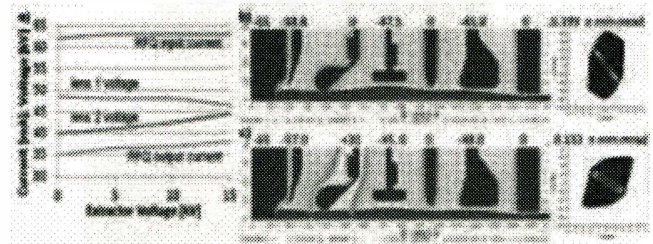
Fig1. a) The enhanced RFQ transmission suggests a reduced input emittance; PBGUNS model of the electrostatic low energy beam transport a) with the nominal extraction and b) with an extraction field enhanced by a +20 kV extractor.

References

[1] M.P. Stockli, B. Han, S.N. Murray, T.R. Pennisi, C. Piller, M. Santana, R.F. Welton, *Rev. Sci. Instrum.* **81,** 02A729 (2010).

[2] M.P. Stockli, B. Han, S.N. Murray, T.R. Pennisi, C. Piller, M. Santana, R.F. Welton, *Rev. Sci. Instrum.* **87,** 02B140 (2016).

A51: Tuning optical and catalytical properties of ligated metallic nanoclusters for bio-imaging application and hydrogen storage

Vlasta Bonačić-Koutecký [a,b]

[a]Department of Chemistry, Humboldt Universitat zu Berlin, Brook-Taylor-Strasse 2, 12489 Berlin, Germany. E-mail: vbk@cms.hu-berlin.de

[b]Center of excellence for Science and Technology-Integration of Mediterranean region (STIM) at Interdisciplinary Center for Advanced Sciences and Technology (ICAST), University of Split, Meštrovićevo šetaliste 45, HR-21000 Split, Croatia

Nonlinear two-photon apsorption (TPA) is defined as electronic excitation of a molecular system induced by the simultaneous absorption of pair of photons and is accessible with femtosecond pulses delivered with standard femtosecond oscilators with wavelengths tunability in 700-1300nm range. This is therefore advantageous to access deeper penetration into the biological tissue media, important for bio-imaging. We report theoretical and experimental results on TPA cross sections of ligated silver clusters exhibiting extraordinary large TPA with aim to design new ligand-core nonlinear optical flourophores with considerably improved spacial resolution. Our findings provide the responsible mechanism and allow proposing new classes of nanoclusters with large TPAs which are promising for numerous applications.

Nature uses a number of design principles to create different classes of enzyme catalysts capable of a wide range of chemical transformations of substrates. Embedding the metal center within a ligated nanocluster also facilitates reactivity, which can be further tuned by the choice of ligand. We examined theoretically and experimentally how the binuclear silver hydride cation, $[Ag_2(H)]^+$, can be structurally manipulated by the appropriate choice of phosphine ligands to switch on the protonation of the hydride by formic acid to liberate hydrogen, which is a key step in the selective, catalysed decomposition of formic acid that does not occur in absence of ligands. The selective, catalysed decomposition of formic acid has potentially important applications in areas ranging from hydrogen storage to the generation of in situ hydrogenation sources for reduction of organic substrates. Implementation of found gas phase reactions into zeolites opens the avenue to propose new catalysts for the decomposition of formic acid.

A52: Nonlinear Plasmonics and Extremely Accurate Sensing

Sergey A. Ponomarenko[1], Franklin Che[1] and Michael Cada[1]

[1]Department of Electrical and Computer Engineering,Dalhousie University, Halifax, NS, B3H 4R2 Canada Email: serpo@dal.ca website: http://www.top.ece.dal.ca

The past decade or so has seen rapid development in the field of plasmonics which studies the collective electromagnetic oscillations of conduction electrons in metals [1]. These oscillations are also known as surface plasmon resonance (SPR), with the position and intensity of the SPR strongly determined by the type of conductor and dielectric properties of the surrounding environment [2]. This has led to the development of a variety of sensors with applications in biochemical and environmental sensing [3].

Most of the plasmonic sensors mentioned above are based on linear plasmonics, where there is no frequency mixing of the incident light source. On the other hand, most of the research carried out in the field of nonlinear plasmonics, is geared towards the fundamental understanding of the generation, modification and enhancement of harmonic frequencies [4,5]. However, there has been some progress made in the development of nonlinear plasmonic sensors based on the processes of second harmonic generation (SHG) [6,7] and third harmonic generation [8], with most of these sensors based on LSP resonance of nanoparticles.

We have recently demonstrated the potential of using the nonlinear processes of sum-frequency generation (SFG) and difference-frequency generation (DFG) to develop highly sensitive plasmonic sensors using the simple Kretschmann configuration [9,10]. We are proposing a robust, simple and highly sensitive nonlinear surface plasmon sensor operating at visible and mid-infrared (MIR) wavelengths based on the Kretschmann geometry. We demonstrate ultra high wavelength sensitivities for the proposed sensor compared to that of traditional Kretschmann plasmonic sensors [11], especially at mid-infrared wavelengths, where many metals experience huge losses [12]. We also estimate the signal strength and figure of merit of the proposed sensor.

References

[1] H. Raether, *Surface plasmons on smooth surfaces*. (Springer, 1988).

[2] S. A. Maier, *Plasmonics: Fundamentals and Applications*. (Springer, 2007).

[3] J. Homola, "Surface plasmon resonance sensors for detection of chemical and biological species," Chemical reviews, **108,** 462 (2008).

[4] M. Lippitz, M. A. van Dijk, and M. Orrit, "Third-harmonic generation from single gold nanoparticles," Nano letters, **5,** 799 (2005).

[5] M. Kauranen and A. V. Zayats, "Nonlinear plasmonics," Nat. Photon., **6,**. 737 (2012).

[6] A. K. Singh, D. Senapati, S. Wang, J. Griffin, A. Neely, P. Candice, K. M. Naylor, B. Varisli, J. R. Kalluri, and P. C. Ray, "Gold nanorod based selective identification of escherichia coli bacteria using two-photon

rayleigh scattering spectroscopy," ACS Nano, **3**, 1906 (2009).

[7] A. Neely, C. Perry, B. Varisli, A. K. Singh, T. Arbneshi, D. Senapati, J. R. Kalluri, and P. C. Ray, "Ultrasensitive and highly selective detection of alzheimers disease biomarker using two-photon rayleigh scattering properties of gold nanoparticle," ACS Nano, **3**, 2834 (2009).

[8] M. Mesch, B. Metzger, M. Hentschel, and H. Giessen, "Nonlinear plasmonic sensing," Nano letters, 16, 3155 (2016).

[9] L. Wang, F. Che, S. A. Ponomarenko, and Z. D. Chen, "Plasmon-enhanced spectral changes in surface sum-frequency generation with polychromatic light," Optics express, **21**, 14159 (2013).

[10] F. Che, S. A. Ponomarenko, and M. Cada, "Giant spectral transformations in plasmon-enhanced difference-frequency generation with polychromatic light," Journal of Optics, vol. 18, no. 12, p. 125503, 2016.

[11] S. Roh, T. Chung, and B. Lee, "Overview of the characteristics of micro-and nano-structured surface plasmon resonance sensors," Sensors, 11, 1565, (2011).

[12] Q.-H. Phan, N. Nguyen-Huu, and Y.-L. Lo, "Optimized double-layered grating structures for chem/biosensing in midinfrared range," IEEE Sensors Journal **14**, 2938 (2014).

A53: To be presented

<u>Hardy Schloer</u>
Schloer Consulting Group, Germany

P01: Construction of diabatic states and evaluation of non-adiabatic coupling terms by using adiabatic potential energies only

<u>Kyoung Koo Baeck</u>, Heesun An
Department of Chemistry and Advanced Materials, Gangneung-Wonju National University, Gangneung 25457 Korea Email:baeck@gwnu.ac.kr, web site: http://knusun.gwnu.ac.kr/~qclab

The effect of nonadiabatic coupling terms (NACTs) between adiabatic electronic states is one of the most important factors that have to be included properly in any quantum mechanical study of polyatomic systems, especially for processes initiated by the absorption of a photon.[1] One direction for the study is to solve the time-dependent Schrödinger equation by using the wave-packet propagation method, which demands the construction of reliable semidiabatic states. Among several approaches generating diabatic states, the construction schemes on the basis of NACTs are most reliable and systematic. The other direction to handle the effect of NACT is to adopt one of many

different versions of, trajectory-based, semi-classical methods. In any of the two directions, the availability of reliable NACTs is very crucial, but the actual computation of NACTs by using either wave-functional-theory (WFT) of density-functional-theory (DFT) methods is still one of the most difficult and time-consuming parts in quantum mechanical studies of polyatomic systems.

To overcome the difficulty, we have recently developed a new scheme that minimizes the demands for the actual computation of NACTs by combined use of a Lorentz function and a Laplace function, simultaneously.[2] An interesting equation, $\alpha \times \beta = 1.397$, between the α and β parameters of the Lorentz and Laplace functions was also found. It was shown that a few (just four or five per each degree of freedoms) values of NACTs calculated at around guessed interstate crossing point are enough for the construction of reliable semidiabatic surfaces.[2] We then analyzed the relationship between our new scheme [2] and the previous "regularized diabatization" method [3], and finally found a new approximation scheme that provide us reliable magnitudes of NACTs by using adiabatic potential energy surfaces (PESs) only.[4] The new scheme can be used with any ab initio method. Our new methods were applied on several archetypical molecular systems, and their performance and limitations will be discussed.
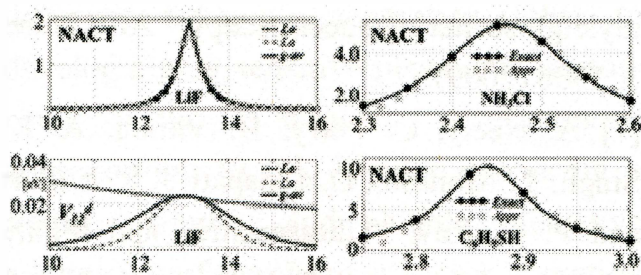
Fig1. Left and right columns show some typical results of the first [2] and the second [4] methods, respectively.

References

[1] K. K. Baeck, Int. J. Quantum Chem. 116, 634 (2016).

[2] H. An and K. K. Baeck, J. Chem. Phys. 143, 194102 (2015).

[3] H. Koeppel, J. Gronki, and S. Mahapatra, *J. Chem. Phys.* **115**, 2377 (2001).

[4] K. K. Baeck and H. An, J. Chem. Phys. 146, 064107 (2017).

P02: Microstructural Evolution of Electroless Ni deposited Electrospun Hollow Metal Nanotube for Electrolytic Cell SOEC and Bio-Sensing Applications

Yinhua Cui, Hojae Shim, Areum Kim, Eunmi Choi, Hansoo Park and Sung Gyu Pyo*

School of Integrative Engineering, Chung-Ang University, Korea

Email: sgpyo@cau.ac.kr, web site: http://impdl.cau.ac.kr

Electrospinning and electroless plating process were required to make hollow Ni nanofiber composites. Electrospun polymer nanofibers were used as a template of Ni nanofibers and about 50 nm electroless plated Ni was deposited on the polymer nanofibers by our newly method, following sintering process. The main objective of this study is to produce and analyze the microstructural evolution of hollow Ni nanofiber composites. The electrospinning method can form long fibers with diameters varying from tens of nm to several μm by applying electrostatic forces to a polymer solution. Viscosity of solution, applied voltage and needle radius have a decisive effect on the morphology of nanostructures. Nanobeads or inter-beads nanofibers were formed when viscosity is too low. As needle radius is increased, radius of electrospun nanofibers is also enlarged. 374±50 nm radius of nanofibers was applied to Ni deposition. After surface cleaning of PR nanofibers, Pd was deposited to improve adhesion properties of Ni. Continuous and uniform Ni film was deposited in the thickness of 10nm. It is expected that our nanocomposites are economical due to reducing absolute amount of catalysts as well as increasing reaction rate with maximized triple phase boundary. Electrospun PR nanofibers were used in the template of Ni nanofibers. In order to know decomposition temperature of SU-8 photoresist, thermal property was analyzed by TG-DTA. PR was perfectly decomposed when 631.2℃. Ni nanofibers

with template were sintered at 1200℃ in one hour. As a result, Ni nanofibers shrink by 22nm, disappearing the nanofibers template.

It is expected that our nanocomposites are economical because of increasing reaction rate with maximized TPB as well as reducing absolute amount of catalysts. In addition, hollow structures can be utilized as additional channels to pass through gas fuel. Mechanical strength, electrochemical properties, and chemical and thermal stability were evaluated to prove these effectiveness when our new materials were applied to hydrogen electrode for oxide electrolytic cell (SOEC) and Bio-sensing applications.
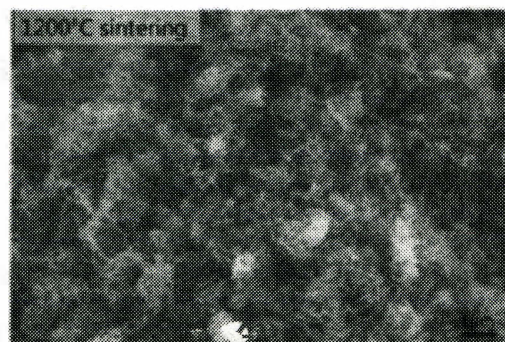
Fig 1. Microstructure of electroless deposited Ni nanofibers

References

[1] Lee, Cameron C., et al. "Preparation and characterization of helical self-assembled nanofibers" Chemical Society Reviews 38.3 (2009): 671-683.

[2] C. S. Sharma, R. Vasita, D. K. Upadhyay, A. Sharma, D. S. Katti, and R. Venkataraghavan, "Photoresist Derived Electrospun Carbon Nanofibers with Tunable

Morphology and Surface Properties" Ind. Eng. Chem. Res. 49, 2731 (2010)

P03: Theoretical identification of frontier orbitals that are possibly responsible for electron transfer in hydrogenases with oxygen-tolerance

Jaehyun Kim[1], Jiyoung Kang[1], and Masaru Tateno

Graduate school of life science, University of Hyogo, Ako, Hyogo, Japan

Email:jaehyunkim000@gmail.com

Hydrogenases are metalloenzymes that are involved in catalysis of the reversible redox reactions of hydrogen in microorganism. Most hydrogenases are readily inactivated by the presence of oxygen molecule, whereas membrane bound hydrogenases (MBHs) can be rapidly reactivated, which is known as O_2-tolerance hydrogenase. The proximal cluster, which is the transition metal-involved cluster that is located closest from the catalytic site, includes four Fe and three ions, and has been known to play a pivotal role in the oxygen tolerance. The crystal structures of MBH from *Ralstonia eutropha* where a hydroxide (OH⁻) ligand is bound in the proximal cluster have been determined, although the role of the OH⁻ is still left to be unknown. To reveal the role of the proposed OH⁻, we conducted *ab initio* quantum mechanics (QM) electronic structure calculations, employing our three distinct structural models (the atoms/functional groups included were different in the models to evaluate the effects of those species) in the presence/absence of the OH⁻ ion, where various distinct spin states were also imposed in terms of the superoxidized redox state.

As a consequence of the analysis, we revealed that in the absence of the OH⁻ ion, the frontier or the near-frontier orbitals were localized on Fe ions in the proximal cluster, while in the presence of the OH⁻ ion, the frontier orbitals were delocalized on the ligands, i.e., the S atoms of Cys19 and Cys17 residues and the hydroxide O atom, as well as Fe atoms. These features were common in all of our structural models, thus suggesting that the OH⁻ ion should enhance the electron transfer, as an intermediator, between the catalytic site and the proximal cluster by forming the route for the electron transfer. In fact, a previous biochemical mutagenesis study suggested that Cys19 (and His229) play a crucial role in the oxygen tolerance of MBH. Thus, the present analysis may provide a solid and general basis on the mechanisms of the proton/electron transfer between the proximal cluster and catalytic site in the reaction cycle of the hydrogenase.

AUTHOR INDEX

Program / Abstract (page)